1992

Transonic computation using Euler equations in stream function coordinate system.

Chang-Fa. An
University of Windsor

National Library
of Canada

Acquisitions and
Bibliographic Services Branch

395 Wellington Street
Ottawa, Ontario
K1A 0N4

Bibliothèque nationale
du Canada

Direction des acquisitions et
des services bibliographiques

395, rue Wellington
Ottawa (Ontario)
K1A 0N4

Your file Votre référence

Our file Notre référence

NOTICE

The quality of this microform is heavily dependent upon the quality of the original thesis submitted for microfilming. Every effort has been made to ensure the highest quality of reproduction possible.

If pages are missing, contact the university which granted the degree.

Some pages may have indistinct print especially if the original pages were typed with a poor typewriter ribbon or if the university sent us an inferior photocopy.

AVIS

La qualité de cette microforme dépend grandement de la qualité de la thèse soumise au microfilmage. Nous avons tout fait pour assurer une qualité supérieure de reproduction.

S'il manque des pages, veuillez communiquer avec l'université qui a conféré le grade.

La qualité d'impression de certaines pages peut laisser à désirer, surtout si les pages originales ont été dactylographiées à l'aide d'un ruban usé ou si l'université nous a fait parvenir une photocopie de qualité inférieure.

Canada

TRANSONIC COMPUTATION USING EULER EQUATIONS IN STREAM FUNCTION COORDINATE SYSTEM

by

Chang-Fa An

A Dissertation
Submitted to the Faculty of Graduate Studies and Research
through the Department of Mathematics and Statistics
in Partial Fulfillment of the Requirements for the
Degree of Doctor of Philosophy
at the University of Windsor

Windsor, Ontario, Canada
1992

ISBN 0-315-78866-6

Name _____

Dissertation Abstracts International is arranged by broad, general subject categories. Please select the one subject which most nearly describes the content of your dissertation. Enter the corresponding four-digit code in the spaces provided.

_____ 0759 U·M·I

SUBJECT TERM SUBJECT CODE

Subject Categories

THE HUMANITIES AND SOCIAL SCIENCES

COMMUNICATIONS AND THE ARTS

Architecture 0729
Art History 0377
Cinema 0900
Dance 0378
Fine Arts 0357
Information Science 0723
Journalism 0391
Library Science 0399
Mass Communications 0708
Music 0413
Speech Communication 0459
Theater 0465

EDUCATION

General 0515
Administration 0514
Adult and Continuing 0516
Agricultural 0517
Art 0273
Bilingual and Multicultural 0282
Business 0688
Community College 0275
Curriculum and Instruction 0727
Early Childhood 0518
Elementary 0524
Finance 0277
Guidance and Counseling 0519
Health 0680
Higher 0745
History of 0520
Home Economics 0278
Industrial 0521
Language and Literature 0279
Mathematics 0280
Music 0522
Philosophy of 0998
Physical 0523
Psychology 0525
Reading 0535
Religious 0527
Sciences 0714
Secondary 0533
Social Sciences 0534
Sociology of 0340
Special 0529
Teacher Training 0530
Technology 0710
Tests and Measurements 0288
Vocational 0747

LANGUAGE, LITERATURE AND LINGUISTICS

Language
- General 0679
- Ancient 0289
- Linguistics 0290
- Modern 0291

Literature
- General 0401
- Classical 0294
- Comparative 0295
- Medieval 0297
- Modern 0298
- African 0316
- American 0591
- Asian 0305
- Canadian (English) 0352
- Canadian (French) 0355
- English 0593
- Germanic 0311
- Latin American 0312
- Middle Eastern 0315
- Romance 0313
- Slavic and East European 0314

PHILOSOPHY, RELIGION AND THEOLOGY

Philosophy 0422
Religion
- General 0318
- Biblical Studies 0321
- Clergy 0319
- History of 0320
- Philosophy of 0322

Theology 0469

SOCIAL SCIENCES

American Studies 0323
Anthropology
- Archaeology 0324
- Cultural 0326
- Physical 0327

Business Administration
- General 0310
- Accounting 0272
- Banking 0770
- Management 0454
- Marketing 0338

Canadian Studies 0385
Economics
- General 0501
- Agricultural 0503
- Commerce-Business 0505
- Finance 0508
- History 0509
- Labor 0510
- Theory 0511

Folklore 0358
Geography 0366
Gerontology 0351
History
- General 0578
- Ancient 0579
- Medieval 0581
- Modern 0582
- Black 0328
- African 0331
- Asia, Australia and Oceania 0332
- Canadian 0334
- European 0335
- Latin American 0336
- Middle Eastern 0333
- United States 0337

History of Science 0585
Law 0398
Political Science
- General 0615
- International Law and Relations 0616
- Public Administration 0617

Recreation 0814
Social Work 0452
Sociology
- General 0626
- Criminology and Penology 0627
- Demography 0938
- Ethnic and Racial Studies 0631
- Individual and Family Studies 0628
- Industrial and Labor Relations 0629
- Public and Social Welfare 0630
- Social Structure and Development 0700
- Theory and Methods 0344

Transportation 0709
Urban and Regional Planning 0999
Women's Studies 0453

THE SCIENCES AND ENGINEERING

BIOLOGICAL SCIENCES

Agriculture
- General 0473
- Agronomy 0285
- Animal Culture and Nutrition 0475
- Animal Pathology 0476
- Food Science and Technology 0359
- Forestry and Wildlife 0478
- Plant Culture 0479
- Plant Pathology 0480
- Plant Physiology 0817
- Range Management 0777
- Wood Technology 0746

Biology
- General 0306
- Anatomy 0287
- Biostatistics 0308
- Botany 0309
- Cell 0379
- Ecology 0329
- Entomology 0353
- Genetics 0369
- Limnology 0793
- Microbiology 0410
- Molecular 0307
- Neuroscience 0317
- Oceanography 0416
- Physiology 0433
- Radiation 0821
- Veterinary Science 0778
- Zoology 0472

Biophysics
- General 0786
- Medical 0760

EARTH SCIENCES

Biogeochemistry 0425
Geochemistry 0996
Geodesy 0370
Geology 0372
Geophysics 0373
Hydrology 0388
Mineralogy 0411
Paleobotany 0345
Paleoecology 0426
Paleontology 0418
Paleozoology 0985
Palynology 0427
Physical Geography 0368
Physical Oceanography 0415

HEALTH AND ENVIRONMENTAL SCIENCES

Environmental Sciences 0768
Health Sciences
- General 0566
- Audiology 0300
- Chemotherapy 0992
- Dentistry 0567
- Education 0350
- Hospital Management 0769
- Human Development 0758
- Immunology 0982
- Medicine and Surgery 0564
- Mental Health 0347
- Nursing 0569
- Nutrition 0570
- Obstetrics and Gynecology 0380
- Occupational Health and Therapy 0354
- Ophthalmology 0381
- Pathology 0571
- Pharmacology 0419
- Pharmacy 0572
- Physical Therapy 0382
- Public Health 0573
- Radiology 0574
- Recreation 0575
- Speech Pathology 0460
- Toxicology 0383

Home Economics 0386

PHYSICAL SCIENCES

Pure Sciences

Chemistry
- General 0485
- Agricultural 0749
- Analytical 0486
- Biochemistry 0487
- Inorganic 0488
- Nuclear 0738
- Organic 0490
- Pharmaceutical 0491
- Physical 0494
- Polymer 0495
- Radiation 0754

Mathematics 0405
Physics
- General 0605
- Acoustics 0986
- Astronomy and Astrophysics 0606
- Atmospheric Science 0608
- Atomic 0748
- Electronics and Electricity 0607
- Elementary Particles and High Energy 0798
- Fluid and Plasma 0759
- Molecular 0609
- Nuclear 0610
- Optics 0752
- Radiation 0756
- Solid State 0611

Statistics 0463

Applied Sciences

Applied Mechanics 0346
Computer Science 0984
Engineering
- General 0537
- Aerospace 0538
- Agricultural 0539
- Automotive 0540
- Biomedical 0541
- Chemical 0542
- Civil 0543
- Electronics and Electrical 0544
- Heat and Thermodynamics 0348
- Hydraulic 0545
- Industrial 0546
- Marine 0547
- Materials Science 0794
- Mechanical 0548
- Metallurgy 0743
- Mining 0551
- Nuclear 0552
- Packaging 0549
- Petroleum 0765
- Sanitary and Municipal 0554
- System Science 0790

Geotechnology 0428
Operations Research 0796
Plastics Technology 0795
Textile Technology 0994

PSYCHOLOGY

General 0621
Behavioral 0384
Clinical 0622
Developmental 0620
Experimental 0623
Industrial 0624
Personality 0625
Physiological 0989
Psychobiology 0349
Psychometrics 0632
Social 0451

ABSTRACT

In this dissertation, a new approach has been developed to calculate the two dimensional steady transonic flow past airfoils using the Euler equations in a stream function coordinate system. Due to the importance of the transonic flow phenomenon in aeronautical practice, transonic flow computation has been an upsurging topic for the past two decades. Most existing transonic computation codes require the use of a grid generator to determine a suitable distribution of grid points. Although simple in concept, the grid generation takes a significant proportion of the CPU time and storage requirements. However, this time-consuming step can be completely avoided by introducing the von Mises transformation and the corresponding stream function coordinate system because this particular transformation combines the flow physics and flow geometry and produces a formulation in streamwise and body-fitting coordinates, without performing any conventional grid generation. In the present work, a set of the Euler equivalent equations in stream function coordinates is formulated. It consists of three equations with three unknowns. One unknown is a geometric variable, the streamline ordinate y, and the other two are physical quantities, density ρ and vorticity ω. For irrotational fluid flow, the Euler formulation is simplified to the full potential formulation in which only two unknowns are solved — y and R, the generalized density. To solve these equations, several numerical techniques are applied: type-dependent differencing, shock point operator, marching from a non-characteristic boundary and successive line overrelaxation, etc. Particular attention has been paid to the supercritical case where a careful treatment of the shock is essential. It is shown that the shock point operator is crucial to accurately capture shock waves. The computed results for both analysis and design problems show good agreement with existing experimental data. The limitations of the approach and further investigations have been discussed.

To my wife and my children, without their understanding, encouragement and love, this dissertation would not have been possible.

ACKNOWLEDGEMENTS

I wish to express my sincere appreciation to my supervisor, Dr. R. M. Barron, for his instructive advice. Without his help and encouragements, this dissertation could not have been completed. I greatly appreciate Dr. R. Camarero from Ecole Polytechnique de Montreal for his valuable comments and suggestions. I am particularly grateful to D. J. Jones from the Institute for Aerospace Research, National Research Council of Canada, for his numerical technique which I have used in this work. I also wish to thank Dr. N. Zamani for his assistance in aspects of numerical analysis skills. Special thanks are due to my colleagues, Mr. S. Zhang and Mr. H. Ye, for their constructive discussions.

TABLE OF CONTENTS

LIST OF FIGURES

NOMENCLATURE

$A_1, A_2, A_3, \ldots$ coefficients in 2nd order partial differential equations
A, B, C coefficients in difference equations corresponding to 2nd order PDE's
A, B, D constants of Jones' transformation define in (6-1)
$\widetilde{A}, \widetilde{B}, \widetilde{C}$ coefficients in difference equations corresponding to 1st order PDE's
a speed of sound
B_1, B_2, B_3 coefficients in 1st order partial differential equations
C_p pressure coefficient
E, F, G transformation metrics defined in (9-43)
F, G vectors defined in (2-12)
$\widetilde{F}, \widetilde{G}$ vectors defined in (2-11)
H total enthalpy
H_∞ total enthalpy in free stream
J Jacobian of a transformation
K $= 1/tan\beta$, defined in (5-1)
L elliptic differential operator defined in (9-54)
M Mach number
M_∞ Mach number in free stream
p pressure
R $= \rho^{\gamma+1}$, generalized density defined in (3-23)
$\widetilde{R}$ $= \rho^2$, defined in (3-5)
Re Reynolds number
RHS right hand side term corresponding to A, B, C
$\widetilde{RHS}$ right hand side term corresponding to $\widetilde{A}, \widetilde{B}, \widetilde{C}$
$\widetilde{r}$ $= r^2/2 - \psi$, defined in (9-19)
S arc length along any curve
s arc length along a streamline
(s, ψ) arc length/stream function coordinates
t time
u, v velocity components in x, y or x, r directions
V speed
(x, r) axial and radial coordinates
(x, y) Cartesian coordinates
(x, ψ) stream function coordinates
(x, ζ) coordinates defined in (9-53)
Y $= y - \psi$, defined in (6-2)
Z_1, Z_2, Z_3, Z_4 defined in (2-24), (2-27) and (2-29)
$\widetilde{Z_1}$ defined in (3-6)

α angle of attack
β shock wave angle or $= \Delta x/\Delta\psi$ or $\Delta\xi/\Delta\eta$
β_0 relaxation parameter for Γ
Γ circulation
γ ratio of specific heats
Δ equation discriminant
Δ, ∇, δ forward, backward and central difference quotient operators
μ density jump factor defined in (5-6)
ν switch parameter defined in (4-6)
(ξ, η) stretched coordinates in Jones' transformation
ρ density
σ density reciprocal $1/\rho$
(τ, ψ) transformed coordinates in unsteady flows
ϕ arbitrary curvilinear coordinate
ψ stream function
ω vorticity
∇^2 Laplace operator

Subscripts:
$x, y, \phi, \psi, \xi, \eta, \zeta$ partial derivatives
i, j, k grid points
LE, TE leading and trailing edges, respectively

Subscripts or superscripts:
$+, -$ upper/lower surfaces or downstream/upstream of shock waves

Chapter 1. Introduction

1.1 Transonic Flow Computation

Transonic flow is a widely encountered phenomenon in aeronautics and astronautics, occuring in flows past airfoils, wings, through nozzle throats, cascade blades or around blunt bodies, etc. Transonic flows are not easy to handle because the flow field is mixed supersonic/subsonic type with shock waves and, accordingly, its governing equations are nonlinear and of mixed hyperbolic/elliptic type with discontinuities. Therefore, transonic flow computation had little progress until Murman and Cole (1971) developed a type-dependent difference scheme and successfully solved the transonic small disturbance (TSD) equation twenty years ago. From then on, the numerical simulation of transonic flows has been one of the most upsurging topics for computational fluid dynamicists working in applied mathematics and aeronautical/aerospace engineering. The development of transonic computation may be divided into the following three stages:

1) TSD Stage: Following Murman and Cole's landmark work, Murman (1974) and Murman and Krupp (1974) analyzed the shock structure and jump conditions and proposed the concept of shock point operator for shock capturing. Hafez and Cheng (1977) proposed the shock fitting technique and utilized it to treat the discontinuities in the transonic flow field. On the other hand, Chan et al. (1975) developed a finite element method with Galerkin and least squares residuals to calculate transonic flows around airfoils. The research work on the solution of the TSD equation continued for about a decade (Ballhaus et al. 1978, Jones and Dickenson 1980, Engquist and Osher 1980, ...).

2) F. P. Stage: Jameson (1974, 1976) extended Murman and Cole's technique by constructing the rotated difference scheme and solved the full potential (F.P.) equation in the transonic range. In order to avoid the non-physical expansion shock, Hafez, South and Murman (1979) proposed the artificial density concept and solved the F. P. equation without upwind differencing. Holst and Ballhaus (1979)

also solved the F. P. equation using an implicit approximate factorization method. Transonic full potential calculations have attracted many researchers' attention and now have become widespread, for instance, Steger and Lomax (1972), Habashi and Hafez (1982a), Osher et al.(1985), Hafez et al. (1987), Dulikravich (1988), Hafez and Lovell (1988), etc.

3) Euler Stage: The full potential calculation is not accurate enough in some cases due to the neglect of entropy variation and vorticity production associated with shock waves. In this case, the Euler equations should be applied. A variety of numerical algorithms and computer codes to solve the Euler equations in the transonic regime have been developed, for example, Steger's (1978) application of Beam and Warming's (1976) implicit finite difference scheme to transonic flows, Pulliam and Chaussee's (1981) implicit approximate factorization algorithm, Jameson, Schmidt and Turkel's (1981) finite volume method with the explicit Runge-Kutta time stepping scheme, Steger and Warming's (1981) flux vector splitting method, Osher and Chakravarthy's (1983) upwind shock capturing scheme, Harten's (1983) total variation diminishing scheme, Ni's (1982) multigrid scheme for Euler equations, Moretti's (1985) nonconservative λ scheme, Jameson and Yoon's (1987) LU decomposition implicit scheme, Ecer and Akay's (1983) finite element methods and so forth. At an Euler solvers workshop in Monterey, CA, USA, researchers reported and discussed the recent progress in Euler solver investigations (see, for example, Pulliam 1987). The common features of most Euler schemes are:

i) The basic structure of the schemes is central differencing plus some form of artificial dissipation/viscosity/density;

ii) A favorable property of the Euler equations is that the nonlinear flux vectors are homogeneous functions of degree one of the primitive variable vector. This is a basic property which is exploited in most Euler schemes;

iii) Most schemes fall in the category of the time-dependent technique in which the steady Euler equations are solved by seeking the time-asymptotic solution to the unsteady Euler equations. Iterative relaxation algorithms are also considered

in this category.

Alternatively, quite a few researchers have attacked the transonic flow problem from another side, using the stream function/vorticity formulation, e.g. Habashi and Hafez (1982b), Hafez and Lovell (1983), Habashi et al.(1985), Atkins and Hassan (1985), Wang (1985), Hafez and Ahmad (1988), Sherif and Hafez (1988), Hafez et al.(1989) and so on.

1.2 Stream Function Coordinate System (SFC)

In most CFD problems, grid generation is usually the first step of the computation to provide a body-fitting mesh system. The degree to which a numerical method can reduce the grid generation portion of CPU time is an important index of its efficiency and applicability. However, this step can be completely avoided by introducing the von Mises transformation (Ames 1965) and the corresponding stream function coordinate (SFC) system. The von Mises transformation is a streamline-based coordinate transformation which produces a body-fitting coordinate system without performing any conventional grid generation. This is because the transformation has an excellent property that allows a single set of equations to play a double role, i.e. simultaneously serving as governing equations (flow physics) and grid generation equations (flow geometry). In recent years, the stream function (or streamline) coordinate system has been used in fluid flow computations. Some of them are reviewed below.

For incompressible potential flow, Jeppson (1970) solved an axisymmetric flow from a large reservoir through a circular orifice using a streamline coordinate system in which the velocity potential and Stokes stream function are independent variables and the radial and axial dimensions are unknowns. Yang and Nelson (1979) employed a similar method to solve a 2D incompressible potential flow through the Griffith diffuser. Breeze-Stringfellow and Burggraf (1983) treated the interference flow of a propeller and a nacelle by solving the axisymmetric potential flow in stream tube coordinates where the stream function and axial distance are co-

ordinates. Using the same coordinates, Greywall (1985) solved 2D incompressible potential flows.

For incompressible viscous fluid flows, Duda and Vrentas (1967) developed a so-called Protean coordinate system, whose fundamental feature is the use of stream function as an independent variable in the radial direction of an axisymmetric flow. Essentially, this coordinate transformation is an extension of the method employed by von Mises (1927) to transform the boundary layer equations into a tractable form. Clermont and Lande (1986) and Andre et al. (1989) proposed a stream tube method in which the flow field is solved in a mapped domain where the transformed streamlines are rectilinear or circular. Their method is used to investigate axisymmetric viscous flows including the flow through a convergent duct and a jet flow at the exit of a cylindrical tube. To handle hydraulic power machinery problems, Takahashi (1982) derived the governing equations for 2D and axisymmetric laminar flows in an orthogonal curvilinear coordinate system where one coordinate is a streamline and the other is perpendicular to the streamline. The metrics are to be solved as unknowns. Using this method, Takahashi solved the 2D liquid jet flow from a channel with parallel walls into the atmosphere, Takahashi and Tsukiji (1985) solved a 2D laminar jet issuing from a skewed-symmetrical orifice in the spool valve mechanism generally used in hydraulic power systems and Tsukiji and Takahashi (1989) solved an axisymmetric laminar jet leaving a Poiseuille tube.

For compressible fluid flows, on the other hand, Pearson (1981) proposed a 3D streamline coordinate method in which the streamline geometry is expressed in terms of two parameters (for 2D flow only one parameter is needed) and is corrected iteratively by the transformed governing equations in the streamline coordinates. In fact, this approach is the same as that in the von Mises transformation if the two parameters are taken as two stream functions. Using this method, he calculated a 2D jet flow from an orifice into the air. Owen and Pearson (1988) extended the method to solve an axisymmetric actuator disc flow in a turbomachine and 3D flows through ducts with various cross sections and the flow past a 3D corner. In the case

of unsteady flow, Srinivasan and Spalding (1986) solved the shock tube flow using 1D unsteady gas dynamics equations for primitive variables in stream function coordinates. In turbomachinery analysis and design, since Wu (1952) proposed the general theory of the stream surfaces to solve cascade problems, the applications of this theory have been extensive. A typical work of this kind is the image-plane method used in the inverse problems of cascade flows by Liu and Tao (1989) and Chen et al.(1989). Their method leads to a problem of solving an integro-differential equation for the meridian angle in cylindrical coordinates in the von Mises coordinates, composed of the axial distance and the stream function, which construct an image-plane. Furthermore, Liu and Zhang (1989) improved their approach by introducing another unknown, the moment function, which represents a generalization of the Kutta-Joukowski lift theorem for 2D flow. The above approaches and applications are summarized by Liu (1991). Huang and Dulikravich (1986) and Dulikravich (1988, 1990) suggested that the streamwise coordinate system in which the stream function serves as a coordinate be referred to as the stream-function-coordinates (SFC). Applying this concept they gave an explicit formulation for 3D inviscid steady compressible flow and solved the incompressible flow around a cylinder and the subsonic flow past an airfoil.

Regarding von Mises coordinates, since Barron (1989) connected Martin's (1971) approach with the von Mises transformation and successfully solved the resulting elliptic equation to simulate incompressible potential flow past an airfoil, numerical simulations based on the von Mises transformation and stream function coordinates have been considerably extended, such as to incompressible lifting (Naeem and Barron 1989), axisymmetric (Barron et al. 1990) and design (Barron 1990) problems, as well as to transonic analysis and design problems (Barron and Naeem 1989, Naeem and Barron 1990, Barron and Naeem 1991, Barron and An 1991, An and Barron 1992).

1.3 Present Work

In this study, a new approach is developed to calculate two dimensional steady transonic flows past airfoils using the Euler equations in a stream function coordinate system. Through the introduction of stream function and von Mises transformation, a set of Euler-equivalent equations in stream function coordinates is formulated. It consists of three coupled equations with three unknowns. One is a geometrical variable, the streamline ordinate y, and the other two are physical quantities, density ρ and vorticity ω. All of them are unknown functions of the von Mises variables, abscissa x and stream function ψ. These three equations are numerically solved sequentially and iteratively. To solve the 'main equation' for y, which is a mathematically well classified and physically consistent second order partial differential equation, Murman and Cole's type-dependent difference scheme is applied. To treat the embedded shock wave correctly, the shock jump conditions are analyzed and a shock point operator is constructed in stream function coordinates.

In order to solve for density ρ, a traditional method is to use the Bernoulli equation. In the transonic range, however, the classical double density problem still exists in the new stream function coordinate formulation. From the author and his colleagues' experiences, even if the artificial density technique is applied in conjunction with the use of upwind differencing in supersonic regions, the supersonic pocket and the shock waves are still difficult to handle. This is perhaps because there is no obvious mechanism by which the artificial density provides dissipation to the y equation, as explained by Jameson (1976) or Hafez et al.(1979) for the potential equation and by Habashi and Hafez (1982b) or Hafez and Lovell (1983) for the stream function equation. To overcome this difficulty, instead of solving the algebraic Bernoulli equation, a first order partial or ordinary differential equation, called the 'secondary equation', is derived and solved to avoid the double density trouble. Once y and ρ are obtained, ω can be easily calculated from its definition.

Under the isentropic and irrotationality assumptions, the full potential-equivalent equations in stream function coordinates are formulated and several choices for the

'secondary variables' and the related equations are possible. If a further assumption of incompressibility is made, the Laplace-equivalent equation in the stream function coordinates can be derived.

In the first part of this dissertation, the Euler-equivalent equations and the full potential-equivalent equations are formulated in chapters 2 and 3, respectively. This constitutes the principal theoretical analysis and presents the basic mathematical models. The second part consists of numerical methodologies. In Chapter 4, numerical techniques related to our problems, such as type-dependent difference scheme, successive line overrelaxation (SLOR), first order equation marching strategy, etc., are discussed. In chapter 5, attention is paid to the shock wave treatment, including the analysis of the shock jump conditions and structure of the shock point operator. Chapter 6 extends the procedure given in the previous two chapters to a stretched coordinate system. Chapter 7 gives the results of analysis and design problems using the full potential formulation. Chapter 8 gives the Euler solution. In both these chapters, sample computations are conducted and the calculated results are compared with the available experimental data and other computations. In chapter 9, some extensions of the basic analysis have been made, including the extensions to axisymmetric flows, to unsteady flows, to viscous flows, to the arc length/stream function coordinates and to the (x, ζ) coordinates. They are direct and immediate extensions of the approach proposed in this dissertation and can be conducted in the future. In the last chapter, brief conclusions are given, the advantages and limitations of the present approach are discussed and possible ways to resolve the problems are suggested.

Chapter 2. Euler Formulation in SFC

2.1 Euler Equations in Stream Function Form

For a two dimensional, steady, inviscid fluid flow around an airfoil, the most accurate mathematical model is the Euler equations

$$\begin{pmatrix} \rho u \\ \rho u^2 + p \\ \rho uv \\ \rho uH \end{pmatrix}_x + \begin{pmatrix} \rho v \\ \rho uv \\ \rho v^2 + p \\ \rho vH \end{pmatrix}_y = 0 \tag{2-1}$$

where

$$H = \frac{\gamma}{\gamma - 1}\frac{p}{\rho} + \frac{u^2 + v^2}{2}$$

is total enthalpy per unit mass, ρ is density, u and v are velocity components in Cartesian coordinates (x, y), p is pressure and γ is the ratio of specific heats. The dependent variables ρ, u, v and p have been normalized by the quantities at free stream condition: density ρ_∞, speed V_∞ and dynamic pressure head $\rho_\infty V_\infty^2$. The independent variables x and y have been scaled by the airfoil chord length.

Introducing stream function ψ, such that

$$\psi_y = \rho u, \qquad \psi_x = -\rho v, \tag{2-2}$$

the first equation in (2-1), the continuity equation, is automatically satisfied and the Euler equations take the stream function form

$$\begin{pmatrix} \psi_y^2/\rho + p \\ -\psi_x\psi_y/\rho \\ \psi_y H \end{pmatrix}_x + \begin{pmatrix} -\psi_x\psi_y/\rho \\ \psi_x^2/\rho + p \\ -\psi_x H \end{pmatrix}_y = 0 \tag{2-3}$$

where

$$H = \frac{\gamma}{\gamma - 1}\frac{p}{\rho} + \frac{\psi_x^2 + \psi_y^2}{2\rho^2}$$

is the total enthalpy in stream function form. Here, only three equations are left with three unknowns ψ, ρ and p, as functions of x and y.

2.2 von Mises Transformation and Stream Function Coordinates

The explicit form of stream function $\psi = \psi(x, y)$ can be written in an implicit form as $F(x, y; \psi) = 0$, or in an alternative explicit form as $y = y(x, \psi)$. This process is equivalent to the introduction of the von Mises transformation (Pai 1956 or Ames 1965):

$$x \equiv \phi, \quad y = y(\phi, \psi) \quad \text{or} \quad \phi \equiv x, \quad \psi = \psi(x, y). \tag{2-4}$$

Now, notice that

$$x_\phi = 1, \quad x_\psi = 0 \quad \text{or} \quad \phi_x = 1, \quad \phi_y = 0 \tag{2-5}$$

so that the Jacobian of the transformation is

$$J = \frac{\partial(x, y)}{\partial(\phi, \psi)} = \det \begin{pmatrix} x_\phi & x_\psi \\ y_\phi & y_\psi \end{pmatrix} = y_\psi \tag{2-6}$$

and the differential operators are

$$\frac{\partial}{\partial x} = \frac{\partial}{\partial \phi} + \psi_x \frac{\partial}{\partial \psi}, \qquad \frac{\partial}{\partial y} = \psi_y \frac{\partial}{\partial \psi}. \tag{2-7}$$

Applying (2-7) to y gives

$$0 = y_\phi + \psi_x y_\psi, \qquad 1 = \psi_y y_\psi \tag{2-8}$$

which implies that

$$\psi_x = -\frac{y_\phi}{y_\psi}, \qquad \psi_y = \frac{1}{y_\psi}. \tag{2-9}$$

Therefore, the differential operators become

$$\frac{\partial}{\partial x} = \frac{\partial}{\partial \phi} - \frac{y_\phi}{y_\psi} \frac{\partial}{\partial \psi}, \qquad \frac{\partial}{\partial y} = \frac{1}{y_\psi} \frac{\partial}{\partial \psi}. \tag{2-10}$$

The Euler equations in stream function form (2-3) can be written in a compact form

$$\widetilde{F}_x + \widetilde{G}_y = 0 \tag{2-11}$$

where

$$\widetilde{F} = \begin{pmatrix} \psi_y^2/\rho + p \\ -\psi_x\psi_y/\rho \\ \psi_y H \end{pmatrix}, \qquad \widetilde{G} = \begin{pmatrix} -\psi_x\psi_y/\rho \\ \psi_x^2/\rho + p \\ -\psi_x H \end{pmatrix}.$$

If the Jacobian of the transformation $J = y_\psi \neq 0$ and finite, then the Euler equations in stream function form (2-11) can be transformed to

$$F_\phi - \frac{y_\phi}{y_\psi}F_\psi + \frac{1}{y_\psi}G_\psi = 0 \tag{2-12}$$

where

$$F = \begin{pmatrix} 1/(\rho y_\psi^2) + p \\ y_\phi/(\rho y_\psi^2) \\ H/y_\psi \end{pmatrix}, \qquad G = \begin{pmatrix} y_\phi/(\rho y_\psi^2) \\ y_\phi^2/(\rho y_\psi^2) + p \\ y_\phi H/y_\psi \end{pmatrix}.$$

Multiplying (2-12) by y_ψ, we have

$$y_\psi F_\phi - y_\phi F_\psi + G_\psi = 0$$

or

$$(y_\psi F)_\phi + (G - y_\phi F)_\psi = 0. \tag{2-13}$$

Substituting the expressions for F and G in (2-12) into (2-13) and simplifying the resulting equations, we get

$$\begin{pmatrix} 1/(\rho y_\psi) + p y_\psi \\ y_\phi/(\rho y_\psi) \\ H \end{pmatrix}_\phi + \begin{pmatrix} -p y_\phi \\ p \\ 0 \end{pmatrix}_\psi = 0 \tag{2-14}$$

where

$$H = \frac{\gamma}{\gamma - 1}\frac{p}{\rho} + \frac{1 + y_\phi^2}{2\rho^2 y_\psi^2}.$$

Noticing that $\phi \equiv x$, we can rewrite the Euler equations (2-14) in (x, ψ) coordinates

$$\begin{pmatrix} 1/(\rho y_\psi) + p y_\psi \\ y_x/(\rho y_\psi) \\ H \end{pmatrix}_x + \begin{pmatrix} -p y_x \\ p \\ 0 \end{pmatrix}_\psi = 0 \tag{2-15}$$

where

$$H = \frac{\gamma}{\gamma - 1}\frac{p}{\rho} + \frac{1 + y_x^2}{2\rho^2 y_\psi^2}.$$

Usually, the (x, ψ) coordinates are referred to as the stream function coordinates (SFC) as suggested by Huang and Dulikravich (1986). The Euler equations (2-15) in stream function coordinates (x, ψ) are completely equivalent to the Euler equations (2-1) in Cartesian coordinates (x, y) as long as the von Mises transformation is permissible for the problem under consideration. In this formulation, there are three dependent variables, streamline ordinate y, density ρ and pressure p, as unknown functions of two independent variables, abscissa x and stream function ψ.

The last equation in (2-15), $H_x = 0$, means that the total enthalpy H is invariant along a streamline. However, for a flow with uniform free stream, H is also invariant along any line. Therefore, H is a constant throughout the flow field. This is the homoenergetic assumption made by many Euler equation researchers, e.g. Ni (1982). The constant can be evaluated at free stream conditions

$$H = H_\infty = \frac{1}{2} + \frac{1}{(\gamma - 1)M_\infty^2}. \tag{2-16}$$

Thus, equations (2-15) become

$$(\frac{1}{\rho y_\psi} + p y_\psi)_x - (p y_x)_\psi = 0, \tag{2-17a}$$

$$(\frac{y_x}{\rho y_\psi})_x + p_\psi = 0, \tag{2-17b}$$

$$\frac{\gamma}{\gamma - 1}\frac{p}{\rho} + \frac{1 + y_x^2}{2\rho^2 y_\psi^2} = H_\infty. \tag{2-17c}$$

Here, the energy equation has been reduced to an algebraic equation for p, ρ and y derivatives due to the homoenergetic assumption.

Equations (2-2) and (2-9) imply that

$$u = \frac{1}{\rho y_\psi}, \quad v = \frac{y_x}{\rho y_\psi}, \tag{2-18}$$

and therefore, the velocity components can be easily calculated after equations (2-17) are solved.

2.3 Euler-Equivalent Equations in SFC

Equations (2-17) are not easy to solve simultaneously and directly. However, if we manage to solve one of the equations resulting from (2-17a) and (2-17b) for y and the other for ρ, and calculate p from the last algebraic equation (2-17c), then we might be successful. As a matter of fact, this approach is quite feasible because the prospective y equation will be a second order partial differential equation which is more convenient to classify and solve.

Expanding (2-17a) and (2-17b) gives

$$y_{x\psi} + y_\psi \frac{\rho_x}{\rho} - \rho y_\psi^3 p_x + \rho y_x y_\psi^2 p_\psi = 0, \tag{2-19a}$$

$$y_\psi y_{xx} - y_x y_{x\psi} - y_x y_\psi \frac{\rho_x}{\rho} + \rho y_\psi^2 p_\psi = 0. \tag{2-19b}$$

Differentiating (2-17c) with respect to x leads to

$$\begin{aligned} \frac{\gamma}{\gamma-1}\rho y_\psi^3 p_x = &-y_x y_\psi y_{xx} + (1+y_x^2) y_{x\psi} \\ &+ y_\psi (H_\infty \rho^2 y_\psi^2 + \frac{1+y_x^2}{2}) \frac{\rho_x}{\rho}, \end{aligned} \tag{2-20a}$$

and, with respect to ψ, leads to

$$\begin{aligned} \frac{\gamma}{\gamma-1}\rho y_\psi^2 p_\psi = &- y_x y_{x\psi} + \frac{1}{y_\psi}(1+y_x^2) y_{\psi\psi} \\ &+ (H_\infty \rho^2 y_\psi^2 + \frac{1+y_x^2}{2}) \frac{\rho_\psi}{\rho}. \end{aligned} \tag{2-20b}$$

Substituting p_x, p_ψ from (2-20a), (2-20b) into (2-19a) and (2-19b) yields

$$\begin{aligned} 2y_x y_\psi^2 y_{xx} + 2y_\psi (\frac{1}{\gamma-1} - 2y_x^2) y_{x\psi} + 2y_x(1+y_x^2) y_{\psi\psi} \\ = y_\psi^2 (2H_\infty \rho^2 y_\psi^2 - \frac{\gamma+1}{\gamma-1} + y_x^2) \frac{\rho_x}{\rho} \\ - y_x y_\psi (2H_\infty \rho^2 y_\psi^2 + 1 + y_x^2) \frac{\rho_\psi}{\rho}, \end{aligned} \tag{2-21a}$$

$$\frac{2\gamma}{\gamma-1} y_\psi^2 y_{xx} - \frac{2(2\gamma-1)}{\gamma-1} y_x y_\psi y_{x\psi} + 2(1+y_x^2) y_{\psi\psi}$$

$$= \frac{2\gamma}{\gamma-1} y_x y_\psi^2 \frac{\rho_x}{\rho} - y_\psi (2H_\infty \rho^2 y_\psi^2 + 1 + y_x^2) \frac{\rho_\psi}{\rho}. \tag{2-21b}$$

The vorticity is defined by

$$\omega = v_x - u_y$$

in Cartesian coordinates and expressed as

$$\omega = \frac{1}{y_\psi} \{ [\frac{y_x}{\rho}]_x - [\frac{1+y_x^2}{\rho y_\psi}]_\psi \} \tag{2-22}$$

in (x, ψ) coordinates, or

$$\begin{aligned} y_\psi^2 y_{xx} - 2y_x y_\psi y_{x\psi} + (1+y_x^2) y_{\psi\psi} \\ = y_x y_\psi^2 \frac{\rho_x}{\rho} - y_\psi (1+y_x^2) \frac{\rho_\psi}{\rho} + \rho\omega y_\psi^3 \end{aligned} \tag{2-23}$$

after expansion.

Solving equations (2-21a) and (2-21b) for ρ_x/ρ and ρ_ψ/ρ, substituting them into equation (2-23) and simplifying the resulting equation, we get

$$(y_\psi^2 - Z_1) y_{xx} - 2y_x y_\psi y_{x\psi} + (1+y_x^2) y_{\psi\psi} = Z_2 \tag{2-24}$$

where

$$Z_1 = \frac{\frac{2}{\gamma-1} y_\psi^2}{2H_\infty \rho^2 y_\psi^2 - (1+y_x^2)}$$

is the compressibility parameter and

$$Z_2 = \rho\omega y_\psi^3 \frac{2H_\infty \rho^2 y_\psi^2 + (1+y_x^2)}{2H_\infty \rho^2 y_\psi^2 - (1+y_x^2)}$$

incorporates the rotational effect.

Equation (2-24), which can be solved for y if ρ and ω are known, is a second order nonlinear nonhomogeneous partial differential equation. To classify this equation, consider its discriminant

$$\begin{aligned} \Delta &= (-2y_x y_\psi)^2 - 4(y_\psi^2 - Z_1)(1+y_x^2) \\ &= \frac{-4y_\psi^2}{H_\infty - (1+y_x^2)/(2\rho^2 y_\psi^2)} \{ H_\infty - \frac{1+y_x^2}{2\frac{\gamma-1}{\gamma+1}\rho^2 y_\psi^2} \}. \end{aligned} \tag{2-25}$$

The coefficient before the curly brackets is negative due to equation (2-17c). Thus, the type of equation (2-24) is hyperbolic (or elliptic) if

$$H_\infty - \frac{1+y_x^2}{2\frac{\gamma-1}{\gamma+1}\rho^2 y_\psi^2} < 0 \quad (\text{or} > 0).$$

On the other hand,

$$\begin{aligned} M^2 - 1 &= \frac{V^2}{a^2} - 1 \\ &= \frac{V^2}{\gamma p/\rho} - 1 \\ &= \frac{\frac{1}{\gamma-1}(1+y_x^2)/(\rho^2 y_\psi^2)}{H_\infty - (1+y_x^2)/(2\rho^2 y_\psi^2)} - 1 \\ &= \frac{-1}{H_\infty - (1+y_x^2)/(2\rho^2 y_\psi^2)}\{H_\infty - \frac{1+y_x^2}{2\frac{\gamma-1}{\gamma+1}\rho^2 y_\psi^2}\} \end{aligned} \tag{2-26}$$

where V is velocity, a is speed of sound and M is local Mach number. So, the local flow is supersonic (or subsonic) if

$$H_\infty - \frac{1+y_x^2}{2\frac{\gamma-1}{\gamma+1}\rho^2 y_\psi^2} < 0 \quad (\text{or} > 0).$$

Comparing equations (2-25) and (2-26), we conclude that if the local flow is supersonic (or subsonic), then the governing equation must be hyperbolic (or elliptic). Therefore, the classification of the governing equation remains invariant after the von Mises transformation, or in other words, the mathematical classification of the governing equation in stream function coordinates (x, ψ) is consistent with the physical nature of the local flow field. This feature provides the possibility of applying the type-dependent difference scheme proposed by Murman and Cole (1971) to numerically solve equation (2-24) for y.

It is obvious that equation (2-24) for y is coupled with ρ and ω through Z_1 and Z_2. Therefore, to solve equation (2-24) for y iteratively, ρ and ω must be updated from iteration to iteration. In order to update density ρ, we have several options:

i) V-PDE mode

Eliminating the term

$$y_\psi^2 y_{xx} - 2y_x y_\psi y_{x\psi} + (1+y_x^2) y_{\psi\psi}$$

from (2-23) and (2-24), we get

$$y_x y_\psi^2 \rho_x - y_\psi (1+y_x^2)\rho_\psi = (Z_1 y_{xx} + Z_3)\rho \tag{2-27}$$

where the compressibility parameter Z_1 is the same as in (2-24) and

$$Z_3 = Z_2 - \rho\omega y_\psi^3 = \frac{2\rho\omega y_\psi^3 (1+y_x^2)}{2H_\infty \rho^2 y_\psi^2 - (1+y_x^2)}$$

is the term representing the rotational effect. Equation (2-27) is a first order non-linear partial differential equation for ρ. From the theory of first order partial differential equations (Courant and Hilbert 1965), the slope of its characteristic curve is

$$\frac{d\psi}{dx} = -\frac{1+y_x^2}{y_x y_\psi}. \tag{2-28}$$

At infinity, $y_x \to 0, y_\psi \to 1$, and hence $d\psi/dx \to \infty$. Therefore, the characteristic curve of (2-27) at infinity is a vertical line in the (x,ψ) plane. For this reason, it is termed the V-PDE mode.

ii) H-PDE mode

Rewriting (2-21a) in the form

$$y_\psi^2 (2H_\infty \rho^2 y_\psi^2 - \frac{\gamma+1}{\gamma-1} + y_x^2)\frac{\rho_x}{\rho} - y_x y_\psi (2H_\infty \rho^2 y_\psi^2 + 1 + y_x^2)\frac{\rho_\psi}{\rho}$$

$$= 2y_x y_\psi^2 y_{xx} + 2y_\psi (\frac{1}{\gamma-1} - 2y_x^2) y_{x\psi} + 2y_x (1+y_x^2) y_{\psi\psi},$$

multiplying (2-23) by a factor of $2y_x$

$$2y_x^2 y_\psi^2 \frac{\rho_x}{\rho} - 2y_x y_\psi (1+y_x^2)\frac{\rho_\psi}{\rho} =$$

$$2y_x y_\psi^2 y_{xx} - 4y_x^2 y_\psi y_{x\psi} + 2y_x(1+y_x^2)y_{\psi\psi} - 2\rho\omega y_x y_\psi^3,$$

subtracting them and dividing the resulting equation by y_ψ, we get

$$y_\psi\{2H_\infty\rho^2 y_\psi^2 - (\frac{\gamma+1}{\gamma-1}+y_x^2)\}\frac{\rho_x}{\rho} - y_x\{2H_\infty\rho^2 y_\psi^2 - (1+y_x^2)\}\frac{\rho_\psi}{\rho}$$

$$= \frac{2}{\gamma-1}y_{x\psi} + 2\rho\omega y_x y_\psi^2$$

which can be written as

$$y_\psi(y_\psi^2 - Z_1)\rho_x - y_x y_\psi^2\rho_\psi = (Z_1 y_{x\psi} + Z_4)\rho \tag{2-29}$$

where Z_1 is the same as in (2-24) and the rotational effect is included in

$$Z_4 = \frac{2\rho\omega y_x y_\psi^4}{2H_\infty\rho^2 y_\psi^2 - (1+y_x^2)}.$$

Equation (2-29) is also a first order nonlinear partial differential equation for density ρ. However, in contrast to equation (2-27), the slope of its characteristic curve is

$$\frac{d\psi}{dx} = -\frac{y_x}{y_\psi}\frac{2H_\infty\rho^2 y_\psi^2 - (1+y_x^2)}{2H_\infty\rho^2 y_\psi^2 - (\frac{\gamma+1}{\gamma-1}+y_x^2)}. \tag{2-30}$$

At infinity, $y_x \to 0, y_\psi \to 1, \rho \to 1$, and therefore $d\psi/dx \to 0$. That is, the horizontal line at infinity is a characteristic curve of equation (2-29). Therefore, this method of updating ρ is called the H-PDE mode.

iii) ODE mode

Eliminating the ρ_ψ/ρ term from equations (2-21a) and (2-21b), we have

$$-\frac{2}{\gamma-1}\{y_x y_\psi^2 y_{xx} - y_\psi(1+y_x^2)y_{x\psi}\}$$

$$= y_\psi^2\{2H_\infty\rho^2 y_\psi^2 - \frac{\gamma+1}{\gamma-1}(1+y_x^2)\}\frac{\rho_x}{\rho}$$

or

$$-\frac{1}{\gamma-1}\{\frac{(1+y_x^2)_x}{y_\psi^2} - \frac{(1+y_x^2)(y_\psi^2)_x}{y_\psi^4}\} = 2\{H_\infty - \frac{1+y_x^2}{2\frac{\gamma-1}{\gamma+1}\rho^2 y_\psi^2}\}\rho\rho_x$$

which finally simplifies to

$$(\rho^2)_x = -\frac{1}{\gamma-1}[\frac{1+y_x^2}{y_\psi^2}]_x/\{H_\infty - \frac{1+y_x^2}{2\frac{\gamma-1}{\gamma+1}\rho^2 y_\psi^2}\}. \tag{2-31}$$

Equation (2-31) is a first order nonlinear ordinary differential equation for ρ^2 which can be solved by marching it from some initial values, step by step (cf. Johnson and Riess 1982). Numerical solutions can be obtained at all points except for sonic points and shock waves.

At a sonic point, equation (2-31) deteriorates to an indeterminate form because both numerator (mass flux rate) and denominator (critical velocity criterion) vanish and cannot be solved for ρ^2. Fortunately, ρ^2 can be obtained by requiring that the local velocity be equal to the local speed of sound, i.e.

$$\rho^2 = \frac{1+y_x^2}{2\frac{\gamma-1}{\gamma+1}H_\infty y_\psi^2}. \tag{2-32}$$

Across a shock wave, the differential equation (2-31) fails because ρ and derivatives of y are discontinuous. Thus, equation (2-31) should be replaced by the Rankine-Hugoniot shock relation (Landau and Lifshitz 1959)

$$\frac{\rho_+}{\rho_-} = \frac{\frac{\gamma+1}{2}(M^2)_-}{1+\frac{\gamma-1}{2}(M^2)_-}$$

where the squared Mach number upstream of the shock can be calculated from

$$(M^2)_- = [\frac{\frac{2}{\gamma-1}(1+y_x^2)}{2H_\infty\rho^2 y_\psi^2 - (1+y_x^2)}]_-.$$

Substituting the expression of $(M^2)_-$ into the Rankine-Hugoniot relation, the density downstream of the shock is given by

$$\rho_+ = [\frac{1+y_x^2}{2\frac{\gamma-1}{\gamma+1}H_\infty y_\psi^2\rho}]_-. \tag{2-33}$$

Here, the subscript "+" and "−" denote the quantities downstream and upstream of the shock, respectively. Equations (2-31)-(2-33) can be solved for density ρ.

After y is solved from (2-24) and ρ is updated from (2-27) or (2-29) or (2-31)-(2-33), the vorticity ω can be updated from its definition (2-22). These equations, (2-24), (2-27) or (2-29) or (2-31)-(2-33) and (2-22), constitute a complete set of the 'Euler-equivalent equations' in the stream function coordinates (x, ψ). For convenience, equation (2-24) is referred to as the 'main equation' for the corresponding 'main variable' y (geometric quantity) and equations (2-27) or (2-29) or (2-31)-(2-33) and (2-22) are referred to as the 'secondary equations' for the related 'secondary variables', ρ and ω (physical quantities). Having solved for y, ρ and ω, we can calculate the local Mach number and pressure coefficient from

$$M^2 = \frac{\frac{2}{\gamma-1}(1+y_x^2)}{2H_\infty \rho^2 y_\psi^2 - (1 + y_x^2)}, \tag{2-34}$$

$$C_p = 2(p - \frac{1}{\gamma M_\infty^2}) \tag{2-35}$$

where

$$p = \frac{\gamma-1}{\gamma}(H_\infty \rho - \frac{1+y_x^2}{2\rho y_\psi^2}).$$

Chapter 3. Full Potential Formulation in SFC

3.1 Non-Isentropic Irrotational Flows

For non-isentropic irrotational flows (Hafez et al. 1985), $\omega = 0$, the main equation (2-24) reduces to a homogeneous one

$$(y_\psi^2 - Z_1)y_{xx} - 2y_x y_\psi y_{x\psi} + (1 + y_x^2)y_{\psi\psi} = 0 \tag{3-1}$$

where the compressibility parameter is

$$Z_1 = \frac{\frac{2}{\gamma-1}y_\psi^2}{2H_\infty \rho^2 y_\psi^2 - (1 + y_x^2)}.$$

The secondary equations (2-27) and (2-29) are simplified because $Z_3 = 0$ and $Z_4 = 0$ while (2-31)—(2-33) remain the same:

i) V-PDE mode

$$y_x y_\psi^2 \rho_x - y_\psi(1 + y_x^2)\rho_\psi = Z_1 y_{xx}\rho; \tag{3-2}$$

ii) H-PDE mode

$$y_\psi(y_\psi^2 - Z_1)\rho_x - y_x y_\psi^2 \rho_\psi = Z_1 y_{x\psi}\rho; \tag{3-3}$$

iii) ODE mode

$$(\rho^2)_x = -\frac{1}{\gamma - 1}[\frac{1 + y_x^2}{y_\psi^2}]_x / \{H_\infty - \frac{1 + y_x^2}{2\frac{\gamma-1}{\gamma+1}\rho^2 y_\psi^2}\}, \tag{3-4a}$$

$$\rho^2 = \frac{1 + y_x^2}{2\frac{\gamma-1}{\gamma+1}H_\infty y_\psi^2} \qquad \text{at sonic points,} \tag{3-4b}$$

$$\rho_+ = [\frac{1 + y_x^2}{2\frac{\gamma-1}{\gamma+1}H_\infty y_\psi^2 \rho}]_- \qquad \text{at shock waves.} \tag{3-4c}$$

To obtain a more compact formulation, let

$$\tilde{R} = \rho^2. \tag{3-5}$$

Then, the main equation (3-1) reads

$$(y_\psi^2 - \tilde{Z}_1)y_{xx} - 2y_x y_\psi y_{x\psi} + (1 + y_x^2)y_{\psi\psi} = 0 \tag{3-6}$$

where

$$\tilde{Z}_1 = \frac{\frac{2}{\gamma-1}y_\psi^2}{2H_\infty \tilde{R} y_\psi^2 - (1 + y_x^2)}.$$

Accordingly, the secondary equations (3-2)—(3-4) are reduced to:

i) V-PDE mode

$$y_x y_\psi^2 \tilde{R}_x - y_\psi(1 + y_x^2)\tilde{R}_\psi = 2\tilde{Z}_1 y_{xx}\tilde{R}; \tag{3-7}$$

ii) H-PDE mode

$$y_\psi(y_\psi^2 - \tilde{Z}_1)\tilde{R}_x - y_x y_\psi^2 \tilde{R}_\psi = 2\tilde{Z}_1 y_{x\psi}\tilde{R}; \tag{3-8}$$

iii) ODE mode

$$\tilde{R}_x = -\frac{1}{\gamma - 1}[\frac{1 + y_x^2}{y_\psi^2}]_x / \{H_\infty - \frac{1 + y_x^2}{2\frac{\gamma-1}{\gamma+1}\tilde{R}y_\psi^2}\}, \tag{3-9a}$$

$$\tilde{R} = \frac{1 + y_x^2}{2\frac{\gamma-1}{\gamma+1}H_\infty y_\psi^2} \qquad \text{at sonic points,} \tag{3-9b}$$

$$\tilde{R}_+ = \{\frac{1 + y_x^2}{2\frac{\gamma-1}{\gamma+1}H_\infty y_\psi^2}\}_-^2 \frac{1}{\tilde{R}_-} \quad \text{at shock waves.} \tag{3-9c}$$

The main equation (3-6) and one of the secondary equations (3-7)—(3-9) construct a complete set of equations to solve for y and $\tilde{R}$.

3.2 Isentropic Rotational Flows

If the flows are isentropic and rotational, then

$$p = \frac{\rho^\gamma}{\gamma M_\infty^2} \tag{3-10}$$

holds and

$$\omega = \frac{1}{y_\psi}\{[\frac{y_x}{\rho}]_x - [\frac{1 + y_x^2}{\rho y_\psi}]_\psi\} \neq 0. \tag{3-11}$$

Expanding (3-11) leads to

$$y_\psi^2 y_{xx} - 2y_x y_\psi y_{x\psi} + (1+y_x^2) y_{\psi\psi} = y_x y_\psi^2 \frac{\rho_x}{\rho} - y_\psi (1+y_x^2)\frac{\rho_\psi}{\rho} + \rho\omega y_\psi^3 \tag{3-12}$$

Differentiating the isentropic relation (3-10) with respect to x and ψ yields

$$p_x = \frac{\rho^{\gamma-1}}{M_\infty^2}\rho_x, \qquad p_\psi = \frac{\rho^{\gamma-1}}{M_\infty^2}\rho_\psi. \tag{3-13}$$

Substituting these into the x- and y- momentum equations (2-19a) and (2-19b) gives

$$y_{x\psi} - y_\psi (y_\psi^2 \frac{\rho^{\gamma+1}}{M_\infty^2} - 1)\frac{\rho_x}{\rho} + y_x y_\psi^2 \frac{\rho^{\gamma+1}}{M_\infty^2}\frac{\rho_\psi}{\rho} = 0, \tag{3-14a}$$

$$y_\psi y_{xx} - y_x y_{x\psi} - y_x y_\psi \frac{\rho_x}{\rho} + y_\psi^2 \frac{\rho^{\gamma+1}}{M_\infty^2}\frac{\rho_\psi}{\rho} = 0. \tag{3-14b}$$

Solving (3-14a) and (3-14b) for ρ_x/ρ and ρ_ψ/ρ, substituting them into (3-12) and simplifying the resulting equation, we get

$$(y_\psi^2 - \frac{M_\infty^2}{\rho^{\gamma+1}})y_{xx} - 2y_x y_\psi y_{x\psi} + (1+y_x^2) y_{\psi\psi} = \rho\omega y_\psi^3. \tag{3-15}$$

Eliminating $y_{x\psi}$ from (3-14a) and (3-14b) gives

$$y_x y_\psi^2 \rho^\gamma \rho_x - y_\psi (1+y_x^2)\rho^\gamma \rho_\psi = M_\infty^2 y_{xx}. \tag{3-16}$$

Equation (3-14a) can be rewritten as

$$y_\psi (y_\psi^2 - \frac{M_\infty^2}{\rho^{\gamma+1}})\rho^\gamma \rho_x - y_x y_\psi^2 \rho^\gamma \rho_\psi = M_\infty^2 y_{x\psi}. \tag{3-17}$$

Substituting $y_{xx}, y_{x\psi}$ from (3-16) and (3-17) into equation (3-15) leads to

$$y_x (y_\psi^2 - \frac{M_\infty^2}{\rho^{\gamma+1}})\rho^\gamma \rho_x + y_\psi \{(1-y_x^2) - \frac{M_\infty^2}{\rho^{\gamma+1}}\frac{1+y_x^2}{y_\psi^2}\}\rho^\gamma \rho_\psi$$

$$= M_\infty^2 \{\frac{1+y_x^2}{y_\psi^2} y_{\psi\psi} - \rho\omega y_\psi\}. \tag{3-18}$$

The main equation (3-15), one of the secondary equations (3-16)—(3-18) and the vorticity definition (3-11) constitute a full set of equations to solve for y, ρ and ω.

3.3 Full Potential-Equivalent Equations in SFC

If the flows are isentropic and irrotational, then both $p = \rho^\gamma/(\gamma M_\infty^2)$ and $\omega = 0$ hold. Equations (3-15) and (3-18) can be reduced since the right hand sides contain the factor ω:

$$(y_\psi^2 - \frac{M_\infty^2}{\rho^{\gamma+1}})y_{xx} - 2y_x y_\psi y_{x\psi} + (1+y_x^2)y_{\psi\psi} = 0, \tag{3-19}$$

$$y_x y_\psi^2 \rho^\gamma \rho_x - y_\psi(1+y_x^2)\rho^\gamma \rho_\psi = M_\infty^2 y_{xx}, \tag{3-20}$$

$$y_\psi(y_\psi^2 - \frac{M_\infty^2}{\rho^{\gamma+1}})\rho^\gamma \rho_x - y_x y_\psi^2 \rho^\gamma \rho_\psi = M_\infty^2 y_{x\psi}, \tag{3-21}$$

$$y_x(y_\psi^2 - \frac{M_\infty^2}{\rho^{\gamma+1}})\rho^\gamma \rho_x + y_\psi\{(1-y_x^2) - \frac{M_\infty^2}{\rho^{\gamma+1}}\frac{1+y_x^2}{y_\psi^2}\}\rho^\gamma \rho_\psi$$
$$= M_\infty^2 \frac{1+y_x^2}{y_\psi^2} y_{\psi\psi}. \tag{3-22}$$

In order to simplify the formulation further, define the generalized density

$$R = \rho^{\gamma+1}. \tag{3-23}$$

Then, equations (3-19)—(3-22) become

$$(y_\psi^2 - \frac{M_\infty^2}{R})y_{xx} - 2y_x y_\psi y_{x\psi} + (1+y_x^2)y_{\psi\psi} = 0, \tag{3-24}$$

$$y_x y_\psi^2 R_x - y_\psi(1+y_x^2)R_\psi = (\gamma+1)M_\infty^2 y_{xx}, \tag{3-25}$$

$$y_\psi(y_\psi^2 - \frac{M_\infty^2}{R})R_x - y_x y_\psi^2 R_\psi = (\gamma+1)M_\infty^2 y_{x\psi}, \tag{3-26}$$

$$y_x(y_\psi^2 - \frac{M_\infty^2}{R})R_x + y_\psi\{(1-y_x^2) - \frac{M_\infty^2}{R}\frac{1+y_x^2}{y_\psi^2}\}R_\psi$$
$$= (\gamma+1)M_\infty^2 \frac{1+y_x^2}{y_\psi^2} y_{\psi\psi}. \tag{3-27}$$

The main equation (3-24) can be solved for the main variable y and one of the secondary equations (3-25)—(3-27) can be solved for the secondary variable R.

This set of equations is referred to as the full potential-equivalent equations in stream function coordinates (x, ψ). Checking the secondary equations (3-25)–(3-27) carefully, we find that equation (3-25) is the simplest to solve for R due to its linearity. Therefore, this equation should be given priority as much as possible unless other difficulties occur with it. After y and R are solved, the local Mach number and pressure coefficient can be calculated from

$$M^2 = \frac{M_\infty^2}{R}\frac{1+y_x^2}{y_\psi^2}, \tag{3-28}$$

$$C_p = \frac{2}{\gamma M_\infty^2}\{R^{\frac{\gamma}{\gamma+1}} - 1\}. \tag{3-29}$$

3.4 Other Forms of Secondary Equations

Apart from equations (3-25)—(3-27), several secondary equations for R can be derived. A few of them are listed below:

i) Conservative Form

Dividing equations (3-25) by y_ψ^2, we have

$$y_x R_x - \frac{1+y_x^2}{y_\psi}R_\psi = (\gamma+1)M_\infty^2\frac{y_{xx}}{y_\psi^2}$$

or

$$(y_x R)_x - (\frac{1+y_x^2}{y_\psi}R)_\psi = (\gamma+1)M_\infty^2\frac{y_{xx}}{y_\psi^2} + R\{y_{xx} - (\frac{1+y_x^2}{y_\psi})_\psi\}.$$

The term in the curly brackets is

$$y_{xx} - (\frac{1+y_x^2}{y_\psi})_\psi = \frac{y_\psi^2 y_{xx} - 2y_x y_\psi y_{x\psi} + (1+y_x^2)y_{\psi\psi}}{y_\psi^2}.$$

On the other hand, equation (3-24) can be rewritten in the form

$$y_\psi^2 y_{xx} - 2y_x y_\psi y_{x\psi} + (1+y_x^2)y_{\psi\psi} = \frac{M_\infty^2}{R}y_{xx}.$$

Therefore, we have

$$(y_x R)_x - (\frac{1+y_x^2}{y_\psi} R)_\psi = (\gamma+2) M_\infty^2 \frac{y_{xx}}{y_\psi^2}. \tag{3-30}$$

This is a conservative form of the secondary equation (3-25) and can also be used to solve for R.

ii) ODE Form

Eliminating the R_ψ term from (3-25) and (3-26) leads to

$$\{\frac{M_\infty^2}{R}\frac{1+y_x^2}{y_\psi^2} - 1\} R_x = (\gamma+1) M_\infty^2 [\frac{y_x}{y_\psi^2} y_{xx} - \frac{1+y_x^2}{y_\psi^3} y_{x\psi}].$$

The right hand side term is

$$\frac{\gamma+1}{2} M_\infty^2 [\frac{1+y_x^2}{y_\psi^2}]_x.$$

Hence, we have

$$R_x = \frac{\gamma+1}{2} M_\infty^2 [\frac{1+y_x^2}{y_\psi^2}]_x / \{\frac{M_\infty^2}{R}\frac{1+y_x^2}{y_\psi^2} - 1\}. \tag{3-31a}$$

Likewise,

$$R_\psi = \frac{\gamma+1}{2} M_\infty^2 [\frac{1+y_x^2}{y_\psi^2}]_\psi / \{\frac{M_\infty^2}{R}\frac{1+y_x^2}{y_\psi^2} - 1\}. \tag{3-31b}$$

It is interesting that equations (3-31a) and (3-31b) are similar and symmetric. Any one of these two ordinary differential equations can be chosen as a secondary equation. According to the theory of ordinary differential equations, R can be solved by marching (3-31a) or (3-31b) step by step along the x- or ψ- direction. However, when marching (3-31a) along x- direction across a sonic line or a shock wave, it is necessary to replace this equation by the sonic condition (cf. (3-28), for $M = 1$)

$$R = M_\infty^2 \frac{1+y_x^2}{y_\psi^2} \tag{3-32}$$

or by the Rankine-Hugoniot relation (cf. (3-4c))

$$R_+ = \{\frac{1+y_x^2}{2\frac{\gamma-1}{\gamma+1}H_\infty y_\psi^2}\}_-^{\gamma+1}\frac{1}{R_-} \tag{3-33}$$

where the subscripts '+' and '−' represent the downstream and upstream sides of the shock wave, respectively.

iii) Second Order PDE Form

Differentiating (3-25) and (3-26) with respect to ψ and x, respectively, we get the following equations

$$y_x y_\psi^2 R_{x\psi} - y_\psi(1+y_x^2)R_{\psi\psi} =$$

$$-(y_x y_\psi^2)_\psi R_x + [y_\psi(1+y_x^2)]_\psi R_\psi + (\gamma+1)M_\infty^2 y_{xx\psi}$$

and

$$y_\psi(y_\psi^2 - \frac{M_\infty^2}{R})R_{xx} - y_x y_\psi^2 R_{x\psi} =$$

$$-[y_\psi(y_\psi^2 - \frac{M_\infty^2}{R})]_x R_x + (y_x y_\psi^2)_x R_\psi + (\gamma+1)M_\infty^2 y_{x\psi x}.$$

Subtracting these equations to eliminate the third derivatives $y_{xx\psi}$ and $y_{x\psi x}$, we have

$$y_\psi(y_\psi^2 - \frac{M_\infty^2}{R})R_{xx} - 2y_x y_\psi^2 R_{x\psi} + y_\psi(1+y_x^2)R_{\psi\psi} =$$

$$\{(y_x y_\psi^2)_\psi - [y_\psi(y_\psi^2 - \frac{M_\infty^2}{R})]_x\}R_x + \{(y_x y_\psi^2)_x - [y_\psi(1+y_x^2)]_\psi\}R_\psi.$$

Substituting R_x, R_ψ from equations (3-31a) and (3-31b) into this equation, we obtain a second order partial differential equation for R with the same second order differential operator as in the y equation (3-24), but with a nonhomogeneous right hand side term

$$(y_\psi^2 - \frac{M_\infty^2}{R})R_{xx} - 2y_x y_\psi R_{x\psi} + (1+y_x^2)R_{\psi\psi} = G \tag{3-34}$$

where

$$G = \frac{\gamma+1}{2} M_\infty^2 \frac{H_1 + H_2}{y_\psi} / \{ \frac{M_\infty^2}{R} \frac{1+y_x^2}{y_\psi^2} - 1 \},$$

$$H_1 = \{ (y_x y_\psi^2)_\psi - [y_\psi (y_\psi^2 - \frac{M_\infty^2}{R})]_x \} [\frac{1+y_x^2}{y_\psi^2}]_x,$$

$$H_2 = \{ (y_x y_\psi^2)_x - [y_\psi (1+y_x^2)]_\psi \} [\frac{1+y_x^2}{y_\psi^2}]_\psi.$$

All of the above R equations, first order nonconservative partial differential equations (2-25)—(2-27), conservative partial differential equation (3-30), first order ordinary differential equations (3-31a)—(3-31b) and second order partial differential equation (3-34), can be used as secondary equations to solve for R in order to update the compressibility parameter M_∞^2/R in the main equation (3-24). Of course, the numerical solution procedure will be different from one to another.

3.5 Alternative Sets of Variables

Moreover, we can construct the full potential-equivalent equations in SFC using alternative sets of variables:

i) $(y - M^2)$ Set

Using the (M^2-R) relation (3-28) in the main equation (3-24) produces the main equation with the compressibility parameter expressed by M^2

$$(y_\psi^2 - M^2 \frac{y_\psi^2}{1+y_x^2}) y_{xx} - 2 y_x y_\psi y_{x\psi} + (1+y_x^2) y_{\psi\psi} = 0 \qquad (3\text{-}35)$$

where the squared Mach number has been used as the secondary variable. To derive the secondary equation for M^2, taking the logarithm of equation (3-28) and differentiating it with respect to x, we get

$$\frac{(M^2)_x}{M^2} = -\frac{R_x}{R} + [\frac{1+y_x^2}{y_\psi^2}]_x / [\frac{1+y_x^2}{y_\psi^2}].$$

From (3-31) and (3-28),

$$\frac{R_x}{R} = \frac{\gamma+1}{2}\frac{M^2}{M^2-1}[\frac{1+y_x^2}{y_\psi^2}]_x/[\frac{1+y_x^2}{y_\psi^2}].$$

Thus,

$$\frac{(M^2)_x}{M^2} = \frac{1+\frac{\gamma-1}{2}M^2}{1-M^2}[\frac{1+y_x^2}{y_\psi^2}]_x/[\frac{1+y_x^2}{y_\psi^2}]$$

or

$$(M^2)_x = \frac{M^2(1+\frac{\gamma-1}{2}M^2)}{1-M^2}\{ln[\frac{1+y_x^2}{y_\psi^2}]\}_x. \qquad (3\text{-}36a)$$

Similarly,

$$(M^2)_\psi = \frac{M^2(1+\frac{\gamma-1}{2}M^2)}{1-M^2}\{ln[\frac{1+y_x^2}{y_\psi^2}]\}_\psi. \qquad (3\text{-}36b)$$

To solve for the secondary variable M^2, the ordinary differential equations (3-36a) or (3-36b) can be marched along the x- or ψ- direction. This is similar to the R equations (3-31a) or (3-31b). Likewise, when marching (3-36a) across a sonic line or a shock wave, equation (3-36a) should be replaced by the sonic condition

$$M^2 = 1 \qquad (3\text{-}37)$$

or by the Rankine-Hugoniot relation (Landau and Lifshitz 1959)

$$(M^2)_+ = [\frac{1+\frac{\gamma-1}{2}(M^2)}{\gamma(M^2)-\frac{\gamma-1}{2}}]_-. \qquad (3\text{-}38)$$

ii) $(y-u)$ Set

From equation (2-18), $\rho = 1/(y_\psi u)$, we can rewrite the main equation (3-19) as

$$(y_\psi^2 - M_\infty^2 y_\psi^{\gamma+1}u^{\gamma+1})y_{xx} - 2y_x y_\psi y_{x\psi} + (1+y_x^2)y_{\psi\psi} = 0 \qquad (3\text{-}39)$$

where the x- velocity component u has been chosen as the secondary variable. The secondary equation to solve for u can be derived from $\omega = 0$:

$$(y_x y_\psi u)_x - [(1+y_x^2)u]_\psi = 0. \qquad (3\text{-}40)$$

iii) $(y-\sigma)$ Set

Letting density reciprocal

$$\sigma = \frac{1}{\rho} \tag{3-41}$$

be the secondary variable, then a new set of equations is obtained:

$$(y_\psi^2 - M_\infty^2 \sigma^{\gamma+1}) y_{xx} - 2 y_x y_\psi y_{x\psi} + (1 + y_x^2) y_{\psi\psi} = 0, \tag{3-42}$$

$$(y_x \sigma)_x - [\frac{1 + y_x^2}{y_\psi} \sigma]_\psi = 0. \tag{3-43}$$

iv) $(y-u-\rho)$ Set

Traditionally, the algebraic Bernoulli equation is used to update density ρ. In the transonic regime, however, the classical double valued density/mass-flux relation in stream function formulation still exists in this SFC formulation and is perhaps even more difficult to handle. As a compromise, the intermediate quantity u is solved first and the density ρ is evaluated by the Bernoulli equation afterwards. Thus, the following set of equations comes up:

$$(y_\psi^2 - \frac{M_\infty^2}{\rho^{\gamma+1}}) y_{xx} - 2 y_x y_\psi y_{x\psi} + (1 + y_x^2) y_{\psi\psi} = 0, \tag{3-44}$$

$$(y_x y_\psi u)_x - [(1 + y_x^2) u]_\psi = 0, \tag{3-45}$$

$$\rho = \{1 + \frac{\gamma - 1}{2} M_\infty^2 [1 - (1 + y_x^2) u^2]\}^{\frac{1}{\gamma-1}}. \tag{3-46}$$

More details regarding the full-potential-equivalent equations in stream function coordinates and its application to transonic airfoil calculations can be found in the paper of An and Barron (1992).

Chapter 4. Numerical Methodologies

4.1 Governing Equations and Boundary Conditions

Suppose an airfoil is placed in a two-dimensional air flow with free stream Mach number M_∞ at angle of attack α (Fig. 4-1a). The governing Euler-equivalent equations in stream function coordinates are (2-24), (2-27) and (2-22):

$$(y_\psi^2 - Z_1)y_{xx} - 2y_x y_\psi y_{x\psi} + (1+y_x^2)y_{\psi\psi} = Z_2, \tag{4-1a}$$

$$y_x y_\psi^2 \rho_x - y_\psi(1+y_x^2)\rho_\psi = (Z_1 y_{xx} + Z_3)\rho, \tag{4-1b}$$

$$\omega = \frac{1}{y_\psi}\{[\frac{y_x}{\rho}]_x - [\frac{1+y_x^2}{\rho y_\psi}]_\psi\} \tag{4-1c}$$

where

$$Z_1 = \frac{\frac{2}{\gamma-1}y_\psi^2}{2H_\infty\rho^2 y_\psi^2 - (1+y_x^2)},$$

$$Z_2 = \frac{2H_\infty\rho^2 y_\psi^2 + (1+y_x^2)}{2H_\infty\rho^2 y_\psi^2 - (1+y_x^2)}\rho\omega y_\psi^3,$$

$$Z_3 = \frac{2(1+y_x^2)}{2H_\infty\rho^2 y_\psi^2 - (1+y_x^2)}\rho\omega y_\psi^3.$$

On the airfoil, the boundary condition is simply Dirichlet

$$y = f_\pm(x) \tag{4-2a}$$

where $f_+(x)$ and $f_-(x)$ represent the shape functions of the upper and lower surfaces of the airfoil, respectively. In the far field, the stream function can be expressed as the sum of a uniform stream, a doublet and a vortex flow. In most cases, the doublet term is sufficiently small and can be ignored. Finally, the boundary condition at infinity is given in an explicit form for ψ (Atkins and Hassan 1985):

$$\psi(x,y) = y\cos\alpha - x\sin\alpha + \frac{\Gamma}{2\pi}ln\{x^2 + (1-M_\infty^2)y^2\}$$

in Cartesian coordinates, or in an implicit form for y:

$$y(x,\psi) = \frac{\psi}{\cos\alpha} + x\tan\alpha - \frac{\Gamma}{2\pi\cos\alpha}ln\{x^2 + (1-M_\infty^2)[y(x,\psi)]^2\} \tag{4-2b}$$

in stream function coordinates, where Γ is the circulation. This algebraic equation for $y = y(x, \psi)$ is nonlinear so that some kind of iteration algorithm (e.g. Newton's iteration) must be applied. In addition, at the trailing edge, the Kutta condition must be satisfied, i.e. the velocities

$$V_{TE} = \sqrt{[\frac{1 + y_x^2}{\rho^2 y_\psi^2}]_{TE}} \tag{4-2c}$$

calculated from upper and lower surfaces at the trailing edge must be equal to each other.

If the flow is assumed to be potential, the governing full potential-equivalent equations in stream function coordinates are (3-24) and (3-25):

$$(y_\psi^2 - \frac{M_\infty^2}{R})y_{xx} - 2y_x y_\psi y_{x\psi} + (1 + y_x^2)y_{\psi\psi} = 0, \tag{4-3a}$$

$$y_x y_\psi^2 F_x - y_\psi(1 + y_x^2)R_\psi = (\gamma + 1)M_\infty^2 y_{xx} \tag{4-3b}$$

where $R = \rho^{\gamma+1}$ is the generalized density. The boundary conditions on the airfoil, at infinity and at the trailing edge are the same as those in (4-2a), (4-2b) and (4-2c), respectively.

The sketches of the physical and computational domains and the boundary conditions are shown in Figs. 4-1a and 4-1b, respectively.

4.2 Type-Dependent Scheme for the Main Equation

Because the main equations (4-1a) for the Euler formulation and (4-3a) for the full potential formulation are well classified as hyperbolic/elliptic type depending on the local supersonic/subsonic flow property, it is possible to apply the type-dependent scheme to solve for y.

Equation (4-1a) can be rewritten as

$$A_1 y_{xx} + A_2 y_{x\psi} + A_3 y_{\psi\psi} = A_4 \tag{4-4}$$

where

$$A_1 = y_\psi^2 - Z_1, \quad A_2 = -2y_x y_\psi, \quad A_3 = 1 + y_x^2, \quad A_4 = Z_2$$

and

$$Z_1 = \frac{\frac{2}{\gamma-1} y_\psi^2}{2H_\infty \rho^2 y_\psi^2 - (1+y_x^2)},$$
$$Z_2 = \frac{2H_\infty \rho^2 y_\psi^2 + (1+y_x^2)}{2H_\infty \rho^2 y_\psi^2 - (1+y_x^2)} \rho\omega y_\psi^3.$$

The type-dependent scheme reads

$$\begin{aligned} &\{A_1[\nu\Delta_x + (1-\nu)\nabla_x]\nabla_x \\ &+A_2[\nu\delta_x + (1-\nu)\nabla_x]\delta_\psi \\ &+A_3\delta_{\psi\psi}\}y_{i,j} \quad = \quad A_4 \end{aligned} \tag{4-5}$$

where Δ, ∇ and δ are forward, backward and central difference quotient operators, respectively, and the switch parameter

$$\nu = \begin{cases} 1 & \text{for subsonic points,} \\ 0 & \text{for supersonic points.} \end{cases} \tag{4-6}$$

Expanding the type-dependent scheme (4-5) and rearranging the terms to express it in a tridiagonal coefficient matrix form, one gets

$$Ay_{i,j-1} + By_{i,j} + Cy_{i,j+1} = RHS \tag{4-7}$$

where

$$\begin{aligned} A &= \beta^2 A_3 - (1-\nu)\beta A_2/2, \\ B &= -2\beta^2 A_3 + (1-3\nu)A_1, \\ C &= \beta^2 A_3 + (1-\nu)\beta A_2/2, \end{aligned}$$

$$\begin{aligned} RHS = &-\nu A_1(y_{i+1,j} + y_{i-1,j}) + (1-\nu)A_1(2y_{i-1,j} - y_{i-2,j}) \\ &-\nu\beta A_2(y_{i+1,j+1} - y_{i+1,j-1} - y_{i-1,j+1} + y_{i-1,j-1})/4 \\ &+(1-\nu)\beta A_2(y_{i-1,j+1} - y_{i-1,j-1})/2 + \Delta x^2 A_4 \end{aligned}$$

for $i = 2, 3, ..., I_{max-1}, j = 2, 3, ..., J_{max-1}$ and $\beta = \Delta x/\Delta\psi$.

If the flow is potential, equation (4-3a) can be rewritten in the same form as (4-4), but the A's are slightly different:

$$A_1 y_{xx} + A_2 y_{x\psi} + A_3 y_{\psi\psi} = A_4 \tag{4-8}$$

where

$$A_1 = y_\psi^2 - \frac{M_\infty^2}{R}, \quad A_2 = -2y_x y_\psi, \quad A_3 = 1 + y_x^2, \quad A_4 = 0.$$

The system of difference equations with a tridiagonal coefficient matrix is the same as equation (4-7) except for the different A's as shown in equation (4-8).

Following Jones' (1980) 'patch relaxation method', the computational domain is divided into four subdomains as shown in Fig.4-2a. Each subdomain is swept sequentially by SLOR from left to right and, due to the nonlinearity of the equation, the whole process is iterated up to convergence.

4.3 Crank-Nicolson Scheme for the Secondary Equation

As mentioned in section 2.3, paragraph i), equation (4-1b) has vertical characteristics in the far field. From the theory of first order partial differential equations (Courant and Hilbert 1965), equation (4-1b) can be solved by marching it line by line from a non-characteristic curve. In our case, the horizontal far field boundary can be used at which density is specified $\rho = 1$, and equation (4-1b) can be marched to the airfoil from the lower and upper boundaries for lower and upper half planes, respectively (Fig.4-2b).

Equation (4-1b) can be rewritten as

$$B_1 \rho_x + B_2 \rho_\psi + B_3 \rho = 0 \tag{4-9}$$

where

$$B_1 = y_x y_\psi^2, \quad B_2 = -y_\psi(1 + y_x^2), \quad B_3 = -(Z_1 y_{xx} + Z_3)$$

and

$$Z_1 = \frac{\frac{2}{\gamma-1} y_\psi^2}{2H_\infty \rho^2 y_\psi^2 - (1 + y_x^2)},$$

$$Z_3 = \frac{2(1+y_x^2)}{2H_\infty \rho^2 y_\psi^2 - (1+y_x^2)} \rho \omega y_\psi^3.$$

Crank-Nicolson scheme is an implicit, second order accurate and unconditionally stable difference scheme. Applying it to (4-9) at point $(i, j-\frac{1}{2})$ for the lower half plane, we have

$$B_1 \frac{\rho_{i+1,j-\frac{1}{2}} - \rho_{i-1,j-\frac{1}{2}}}{2\Delta x} + B_2 \frac{\rho_{i,j} - \rho_{i,j-1}}{\Delta \psi} + B_3 \rho_{i,j-\frac{1}{2}} = 0.$$

Evaluating density ρ at $(j-\frac{1}{2})$ level by the average at j and $(j-1)$ levels and rearranging the equations in a tridiagonal form, one gets

$$\widetilde{A}\rho_{i-1,j} + \widetilde{B}\rho_{i,j} + \widetilde{C}\rho_{i+1,j} = \widetilde{RHS} \tag{4-10}$$

where

$$\widetilde{A} = -B_1, \quad \widetilde{B} = 4\beta B_2 + 2\Delta x B_3, \quad \widetilde{C} = B_1,$$

$$\widetilde{RHS} = B_1 \rho_{i-1,j-1} + (4\beta B_2 - 2\Delta x B_3)\rho_{i,j-1} - B_1 \rho_{i+1,j-1}$$

for $i = 2, 3, ..., I_{max-1}, \quad j = 2, 3, ..., J_{md1}$. Here $\beta = \Delta x / \Delta \psi$ and J_{md1} represents the "zero" streamline coinciding with the airfoil surface. It should be noted that B_1, B_2 and B_3 are the averages of the corresponding quantities at j and $(j-1)$. Similarly, for the upper half plane, Crank-Nicolson scheme yields

$$\widetilde{A}\rho_{i-1,j} + \widetilde{B}\rho_{i,j} + \widetilde{C}\rho_{i+1,j} = \widetilde{RHS} \tag{4-11}$$

where

$$\widetilde{A} = -B_1, \quad \widetilde{B} = -4\beta B_2 + 2\Delta x B_3, \quad \widetilde{C} = B_1,$$

$$\widetilde{RHS} = B_1 \rho_{i-1,j+1} - (4\beta B_2 + 2\Delta x B_3)\rho_{i,j+1} - B_1 \rho_{i+1,j+1}$$

for $i = 2, 3, ..., I_{max-1}, \quad j = J_{max-1}, J_{max-2}, ..., J_{md1}$. Likewise, B_1, B_2 and B_3 are the averages of the corresponding quantities at j and $(j+1)$.

If the flow is potential, equation (4-3b) can be rewritten as

$$B_1 R_x + B_2 R_\psi = B_3 \tag{4-12}$$

where

$$B_1 = y_x y_\psi^2, \quad B_2 = -y_\psi(1+y_x^2), \quad B_3 = (\gamma+1)M_\infty^2 y_{xx}.$$

Applying Crank-Nicolson scheme to (4-12) for lower and upper half planes, respectively, we get the following system of difference equations with a tridiagonal coefficient matrix:

$$\tilde{A}R_{i-1,j} + \tilde{B}R_{i,j} + \tilde{C}R_{i+1,j} = \widetilde{RHS} \tag{4-13}$$

where

$$\tilde{A} = -B_1, \quad \tilde{B} = 4\beta B_2, \quad \tilde{C} = B_1,$$

$$\widetilde{RHS} = \tilde{C}R_{i-1,j-1} + \tilde{B}R_{i,j-1} + \tilde{A}R_{i+1,j-1} + 4\Delta x B_3$$

for the lower half plane, and

$$\tilde{A} = -B_1, \quad \tilde{B} = -4\beta B_2, \quad \tilde{C} = B_1$$

$$\widetilde{RHS} = \tilde{C}R_{i-1,j+1} + \tilde{B}R_{i,j+1} + \tilde{A}R_{i+1,j+1} + 4\Delta x B_3$$

for the upper half plane, respectively. Likewise, B_1, B_2 and B_3 are the averages of the corresponding quantities at j and $(j-1)$ levels for the lower half plane and at j and $(j+1)$ levels for the upper half plane, respectively.

The systems of difference equations (4-10) and (4-11) for the Euler formulation, or equation (4-13) for the full potential formulation, have tridiagonal coefficient matrices and can be solved line by line horizontally using SLOR from far field boundaries to the airfoil. An iterative procedure is needed for the Euler formulation due to the nonlinearity of the B_3 term for ρ in equation (4-9), while no iteration procedure is needed for the full potential formulation because equation (4-12) is linear for R. It should be pointed out that the second derivative y_{xx} in the B_3 term of equation (4-9) or (4-12) should be type-dependent differenced to be consistent with the differencing in the y equation:

$$\begin{aligned} y_{xx} =& \frac{\nu}{\Delta x^2}(y_{i+1,j} - 2y_{i,j} + y_{i-1,j}) \\ &+ \frac{1-\nu}{\Delta x^2}(y_{i,j} - 2y_{i-1,j} + y_{i-2,j}) \end{aligned} \tag{4-14}$$

where the switch factor ν is defined in equation (4-6).

After ρ is solved, the vorticity can be updated from its definition (4-1c) and the local Mach number can be calculated from

$$M^2 = \frac{\frac{2}{\gamma-1}(1+y_x^2)}{2H_\infty \rho^2 y_\psi^2 - (1+y_x^2)} \tag{4-15a}$$

for the Euler formulation or from

$$M^2 = \frac{M_\infty^2}{R}\frac{1+y_x^2}{y_\psi^2} \tag{4-15b}$$

after R is solved for the full potential formulation.

The velocities at the trailing edge calculated from the upper surface, V_{TE}^+, and from the lower surface, V_{TE}^-, must be equal to each other. That is,

$$(\Delta V)_{TE} = V_{TE}^+ - V_{TE}^- = 0 \tag{4-16}$$

where the velocities $V_{TE}^\pm$ are given by (4-2c) and evaluated from the upper and lower surfaces of the airfoil, respectively. Equation (4-16) is the Kutta condition at the trailing edge. Furthermore, if (4-16) is not satisfied, more iterations are needed and the circulation Γ around the airfoil can be corrected from the following expression suggested by Hafez et al.(1985):

$$\Gamma^{(n+1)} = \Gamma^{(n)} + \beta_0 (\Delta V)_{TE} \tag{4-17}$$

where the superscripts (n) and $(n+1)$ indicate the iteration levels and the relaxation parameter β_0 can be determined from numerical tests. The numerical solution process can be described as follows:

First, the tridiagonal system of algebraic equations (4-7) is solved for y along a vertical line. Each vertical line is then successively relaxed from left to right in each subdomain and each subdomain is swept in the order of I, II, III and IV. The latest values of y are always used whenever they become available. After y is relaxed, the difference between the current and previous iterations is checked by

$$|y_{i,j}^{(n)} - y_{i,j}^{(n-1)}| < \varepsilon \tag{4-18}$$

for all grid points (i, j) where ε is the prescribed tolerance. If condition (4-18) is satisfied, the iterations are considered to have converged, otherwise, the iterations are repeated until convergence. After y is converged, ρ can be solved from equation (4-10) and (4-11) for the Euler formulation or from equation (4-13) for the full potential formulation. This time, the tridiagonal system of algebraic equations (4-10), (4-11) or (4-13) is solved along a horizontal line and each horizontal line is marched upward or downward to the airfoil. After ρ is converged, the Mach number M, vorticity ω (for the Euler formulation) are calculated and the Kutta condition is checked by (4-16). If it is not satisfied, the circulation Γ is updated by (4-17) and the procedure is repeated again until convergence. The Mach number is used to distinguish the grid point type: subsonic, supersonic or shock wave (see the next chapter). The computational flow chart is shown in Fig.4-3.

Chapter 5. Special Treatment of Shock Waves

5.1 Shock Jump Condition

After some numerical tests, it was found that the type-dependent scheme is effective only for subcritical flows and for supercritical flows with very weak shock waves. However, for a supercritical flow with moderate or strong shock waves, the computation either fails to converge or is forced to stop due to inaccurate intermediate values of the unknowns y and ρ during the iteration. Occasionally, the computation converges but gives inaccurate pressure distributions and incorrect shock wave positions. This means that the shock waves are not properly handled. Therefore, a special treatment of shock waves is necessary. In the early work of Murman and Cole (1971), the shock jump conditions are automatically involved in their scheme for the TSD equation. The sonic line and shock waves develop naturally during the course of iteration. No special shock wave treatment has been made in their computation. To improve the approach, Murman (1974) proposed the concept of shock point operator (SPO) for the TSD equation. Although his SPO cannot be applied here directly, his basic idea and analysis of the shock wave structure provides a useful hint for more accurate models, such as the full potential or Euler equations. The shock wave theory which has been developed rather completely, e.g. Courant and Friedrichs 1948, Shapiro 1953, Landau and Lifshitz 1959, etc., can be used to analyze the shock jump conditions and construct the shock point operator in stream function coordinates (x, ψ).

Suppose an oblique shock wave makes an angle β with the x axis, and V, α are the velocity and its angle with the x axis. u, v are x and y components. V_n, V_t are normal and tangential components to the shock. Superscripts '$\mp$' represent upstream and downstream of the shock (Fig.5-1). The tangential velocity conservation across a shock, $V_t^+ = V_t^-$, gives

$$V^+ cos(\beta - \alpha^+) = V^- cos(\beta - \alpha^-).$$

Expanding it yields

$$V^+cos\alpha^+cos\beta + V^+sin\alpha^+sin\beta$$
$$=V^-cos\alpha^-cos\beta + V^-sin\alpha^-sin\beta$$

or

$$(v^+ - v^-)sin\beta + (u^+ - u^-)cos\beta = 0.$$

Therefore,

$$\frac{v^+ - v^-}{u^+ - u^-} = -K \tag{5-1}$$

where $K = 1/tan\beta$ is the reciprocal of shock wave slope. The normal momentum conservation across a shock, $\rho^+V_n^+ = \rho^-V_n^-$, gives

$$\rho^+V^+sin(\beta - \alpha^+) = \rho^-V^-sin(\beta - \alpha^-).$$

Likewise, expanding yields

$$\rho^+V^+cos\alpha^+sin\beta - \rho^+V^+sin\alpha^+cos\beta$$
$$=\rho^-V^-cos\alpha^-sin\beta - \rho^-V^-sin\alpha^-cos\beta$$

or

$$(\rho^+u^+ - \rho^-u^-)sin\beta - (\rho^+v^+ - \rho^-v^-)cos\beta = 0.$$

Therefore,

$$\frac{\rho^+u^+ - \rho^-u^-}{\rho^+v^+ - \rho^-v^-} = K. \tag{5-2}$$

Equations (5-1) and (5-2) can be expressed in a compact form

$$[v] + K[u] = 0, \quad [\rho u] - K[\rho v] = 0$$

where [...] represents the jump of the corresponding quantities across the shock wave. Considering $\rho u y_\psi = 1$ and $v = y_x u$, we get the following oblique shock jump conditions in stream function coordinates (x, ψ):

$$[\frac{y_x}{\rho y_\psi}] + K[\frac{1}{\rho y_\psi}] = 0, \quad [\frac{1}{y_\psi}] - K[\frac{y_x}{y_\psi}] = 0. \tag{5-3}$$

For a shock wave perpendicular to the x axis, $\beta = \pi/2, K = 0$, and the shock jump conditions reduce to

$$[\frac{y_x}{\rho y_\psi}] = 0, \quad [\frac{1}{y_\psi}] = 0$$

or in a simpler form

$$[\frac{y_x}{\rho}] = 0, \quad [y_\psi] = 0. \tag{5-4}$$

These are the normal shock jump conditions in stream function coordinates (x, ψ).

5.2 Shock Point Operator

For a moderate transonic Mach number, the shock wave is approximately normal and, therefore, assumed to be an infinitesimally thin discontinuity surface located at point $(i-\frac{1}{2}, j)$ and perpendicular to the streamline. From shock jump conditions (5-4) in the previous section, only y_x/ρ and y_ψ are continuous across this discontinuity but other quantities are not (see Fig.5-2).

The normal shock jump conditions (5-4) gives

$$y_x^+ = \mu y_x^-, \qquad y_\psi^+ = y_\psi^- \tag{5-5}$$

where the density jump factor μ is given by the Rankine-Hugoniot relation for a normal shock (Shapiro 1953 or Landau and Lifshitz 1959)

$$\mu = \frac{\rho^+}{\rho^-} = \frac{\frac{\gamma+1}{2}(M^2)^-}{1+\frac{\gamma-1}{2}(M^2)^-}. \tag{5-6}$$

The squared Mach number at point $(i-\frac{1}{2}, j)^-$ can be evaluated by extrapolation from the two upstream grid points

$$(M^2)^-_{i-\frac{1}{2},j} = \frac{3}{2}M^2_{i-1,j} - \frac{1}{2}M^2_{i-2,j}. \tag{5-7}$$

Thus, the shock jump conditions (5-5) can be rewritten as

$$(y_x)^+_{i-\frac{1}{2},j} = \mu_j (y_x)^-_{i-\frac{1}{2},j}, \quad (y_\psi)^+_{i-\frac{1}{2},j} = (y_\psi)^-_{i-\frac{1}{2},j} \tag{5-8}$$

where

$$\mu_j = \frac{\frac{\gamma+1}{4}(3M^2_{i-1,j} - M^2_{i-2,j})}{1 + \frac{\gamma-1}{4}(3M^2_{i-1,j} - M^2_{i-2,j})}$$

is the density jump factor on the j^{th} streamline.

Finally, we construct the difference approximation to y_{xx} at a shock point $i = i_s$, i.e. the grid point just behind the shock:

$$\begin{aligned}
(y_{xx})_{i,j} &= \frac{1}{\Delta x}[(y_x)_{i+\frac{1}{2},j} - (y_x)^+_{i-\frac{1}{2},j}] \\
&= \frac{1}{\Delta x}[(y_x)_{i+\frac{1}{2},j} - \mu_j(y_x)^-_{i-\frac{1}{2},j}] \\
&= \frac{1}{\Delta x}[\frac{1}{\Delta x}(y_{i+1,j} - y_{i,j}) - \frac{\mu_j}{\Delta x}(y_{i-1,j} - y_{i-2,j})] \\
&= \frac{1}{\Delta x^2}(y_{i+1,j} - y_{i,j} - \mu_j y_{i-1,j} + \mu_j y_{i-2,j}) \qquad (5\text{-}9)
\end{aligned}$$

where the first part of the shock jump condition (5-8) and the following difference formulae have been used:

$$\begin{aligned}
(y_x)_{i+\frac{1}{2},j} &= \frac{1}{\Delta x}(y_{i+1,j} - y_{i,j}), \\
(y_x)^-_{i-\frac{1}{2},j} &= \frac{1}{\Delta x}(y_{i-1,j} - y_{i-2,j}).
\end{aligned}$$

Similarly, the cross derivative can be given by

$$\begin{aligned}
(y_{x\psi})_{i,j} =& \frac{1}{\Delta x}[(y_\psi)_{i+\frac{1}{2},j} - (y_\psi)^+_{i-\frac{1}{2},j}] \\
=& \frac{1}{\Delta x}[(y_\psi)_{i+\frac{1}{2},j} - (y_\psi)^-_{i-\frac{1}{2},j}] \\
=& \frac{1}{2\Delta x}[(y_\psi)_{i+1,j} + (y_\psi)_{i,j} - 3(y_\psi)_{i-1,j} + (y_\psi)_{i-2,j}] \\
=& \frac{1}{4\Delta x \Delta \psi}(y_{i+1,j+1} - y_{i+1,j-1} + y_{i,j+1} - y_{i,j-1} \\
& - 3y_{i-1,j+1} + 3y_{i-1,j-1} + y_{i-2,j+1} - y_{i-2,j-1}) \qquad (5\text{-}10)
\end{aligned}$$

where the second part of the shock jump condition (5-8), the arithmetical average

$$(y_\psi)_{i+\frac{1}{2},j} = \frac{1}{2}[(y_\psi)_{i+1,j} + (y_\psi)_{i,j}],$$

the extrapolation formula

$$(y_\psi)_{i-\frac{1}{2},j} = \frac{3}{2}(y_\psi)_{i-1,j} - \frac{1}{2}(y_\psi)_{i-2,j}$$

and the central difference for y_ψ

$$(y_\psi)_{k,j} = \frac{1}{2\Delta\psi}(y_{k,j+1} - y_{k,j-1}), \quad k = i-2, i-1, i, i+1$$

have been used. Equations (5-9) and (5-10) define the so-called shock point operator (SPO) in stream function coordinates (x, ψ). Numerical tests show that the first derivatives, y_x, ρ_x, etc., do not need to be specially treated across shock waves.

5.3 Type-Dependent Scheme with Shock Point Operator

Due to the special treatment of the grid point at a shock wave, we have to revise the type-dependent difference scheme (4-7) and Crank-Nicolson schemes in (4-10) and (4-11) for the Euler formulation and (4-13) for the full potential formulation.

The system of difference equations for y is still of the same form as in (4-7):

$$Ay_{i,j-1} + By_{i,j} + Cy_{i,j+1} = RHS \tag{5-11}$$

but the coefficients A, B, C and the RHS term have to be modified:

$$A = \beta^2 A_3 - \begin{cases} (1-\nu)\beta A_2/2 & \text{if } i \neq i_s \\ \beta A_2/4 & \text{if } i = i_s, \end{cases}$$

$$B = -2\beta^2 A_3 + \begin{cases} (1-3\nu)A_1 & \text{if } i \neq i_s \\ -A_1 & \text{if } i = i_s, \end{cases}$$

$$C = \beta^2 A_3 + \begin{cases} (1-\nu)\beta A_2/2 & \text{if } i \neq i_s \\ \beta A_2/4 & \text{if } i = i_s, \end{cases}$$

$$RHS = \begin{cases} -\nu A_1(y_{i+1,j} + y_{i-1,j}) + (1-\nu)A_1(2y_{i-1,j} - y_{i-2,j}) \\ -\nu\beta A_2(y_{i+1,j+1} - y_{i+1,j-1} - y_{i-1,j+1} + y_{i-1,j-1})/4 \\ +(1-\nu)\beta A_2(y_{i-1,j+1} - y_{i-1,j-1})/2 + \Delta x^2 A_4 & \text{if } i \neq i_s \\ \\ -A_1(y_{i+1,j} - \mu_j y_{i-1,j} + \mu_j y_{i-2,j}) \\ -\beta A_2(y_{i+1,j+1} - y_{i+1,j-1} - 3y_{i-1,j+1} \\ +3y_{i-1,j-1} + y_{i-2,j+1} - y_{i-2,j-1})/4 + \Delta x^2 A_4 & \text{if } i = i_s \end{cases}$$

where $\beta = \Delta x/\Delta\psi$ and $i = 2,3,...,I_{max-1}, j = 2,3,...,J_{max-1}$. The A's are given by (4-4) for the Euler formulation and by (4-8) for the full potential formulation.

For the ρ equation (4-9), the corresponding Crank-Nicolson scheme with shock point operator gives the same forms of difference equation, its coefficients and its RHS term as those in equations (4-10)-(4-11) for the Euler formulation and equation (4-13) for the full potential formulation, but the second derivative y_{xx} in the B_3 expression should be approximated by the type-dependent difference with shock point operator, cf. equation (5-9):

$$y_{xx} = \begin{cases} \frac{\nu}{\Delta x^2}(y_{i+1,j} - 2y_{i,j} + y_{i-1,j}) + \frac{1-\nu}{\Delta x^2}(y_{i,j} - 2y_{i-1,j} + y_{i-2,j}), & i \neq i_s \\ \frac{1}{\Delta x^2}(y_{i+1,j} - y_{i,j} - \mu_j y_{i-1,j} + \mu_j y_{i-2,j}), & i = i_s \end{cases} \tag{5-12}$$

where the switch parameter ν and the density jump factor μ_j are defined in (4-6) and (5-6).

In order to determine the type of local flow at grid point (i,j), we have to check the flow property at two adjacent grid points, the current point (i,j) and the immediate upstream point $(i-1,j)$. The criterion is shown in the following table:

$M^2_{i-1,j}$	$M^2_{i,j}$	Local flow type at (i,j)
< 1	< 1	Subsonic point
< 1	> 1	Sonic point
> 1	> 1	Supersonic point
> 1	< 1	Shock point

In computational practice, the sonic point need not be distinguished because there is no jump across it but the shock point must be identified carefully and it is a key step in getting a convergent solution in supercritical transonic flow computation.

Chapter 6. Coordinate Stretching Transformation

6.1 Jones' Stretching Transformation

In order to improve accuracy by increasing the number of grid points on the airfoil, without consuming too much computational time, some kind of coordinate stretching transformation may be applied to pack mesh points for larger gradient regions and spread out mesh points for smaller gradient regions. Jones' (1980) algebraic stretching transformation for independent variables is a simple and effective one:

$$x = Ae^{-B\xi^2}tan\xi, \quad \psi = Dtan\eta \tag{6-1}$$

where $-\pi/2 < \xi < \pi/2, -\pi/2 < \eta < \pi/2$, A, B and D are constants determined from numerical tests. The derivatives of x and ψ with respect to ξ and η are

$$x_\xi = Ae^{-B\xi^2}(sec^2\xi - 2B\xi tan\xi),$$

$$\frac{x_{\xi\xi}}{x_\xi} = 2\frac{tan\xi - Bsin\xi cos\xi - B\xi}{1 - 2B\xi sin\xi cos\xi} - 2B\xi,$$

$$\psi_\eta = Dsec^2\eta,$$

$$\frac{\psi_{\eta\eta}}{\psi_\eta} = 2tan\eta.$$

The differential operators are transformed as

$$\frac{\partial}{\partial x} = \frac{1}{x_\xi}\frac{\partial}{\partial \xi}, \quad \frac{\partial}{\partial \psi} = \frac{1}{\psi_\eta}\frac{\partial}{\partial \eta}$$

$$\frac{\partial^2}{\partial x^2} = \frac{1}{x_\xi^2}\frac{\partial^2}{\partial \xi^2} - \frac{x_{\xi\xi}}{x_\xi^3}\frac{\partial}{\partial \xi},$$

$$\frac{\partial^2}{\partial x \partial \psi} = \frac{1}{x_\xi \psi_\eta}\frac{\partial^2}{\partial \xi \partial \eta},$$

$$\frac{\partial^2}{\partial \psi^2} = \frac{1}{\psi^2}\frac{\partial^2}{\partial \eta^2} - \frac{\psi_{\eta\eta}}{\psi_\eta^3}\frac{\partial}{\partial \eta}.$$

The Jacobian of the transformation is

$$J = \frac{\partial(x,\psi)}{\partial(\xi,\eta)} = ADe^{-B\xi^2}(sec^2\xi - 2B\xi tan\xi)sec^2\eta.$$

It can be seen that $J \neq 0, \infty$ for $-\pi/2 < \xi < \pi/2, -\pi/2 < \eta < \pi/2$, hence the Jones' transformation does not have any singularities.

For further simplification of boundary conditions, a new dependent variable Y may be introduced by

$$y = Y + \psi. \tag{6-2}$$

After this dependent variable transformation, the derivatives of y with respect to x and ψ are transformed to

$$y_x = \frac{Y_\xi}{x_\xi}, \quad y_\psi = \frac{Y_\eta}{\psi_\eta} + 1,$$

$$y_{xx} = \frac{Y_{\xi\xi}}{x_\xi^2} - \frac{x_{\xi\xi}}{x_\xi^3}Y_\xi, \quad y_{x\psi} = \frac{Y_{\xi\eta}}{x_\xi\psi_\eta}, \quad y_{\psi\psi} = \frac{Y_{\eta\eta}}{\psi_\eta^2} - \frac{\psi_{\eta\eta}}{\psi_\eta^3}Y_\eta.$$

8.2 Main Equation for Y in Stretched Coordinates

After the transformations (6-1) and (6-2), the main equation (4-1a) for the Euler formulation becomes

$$A_1Y_{\xi\xi} + A_2Y_{\xi\eta} + A_3Y_{\eta\eta} + A_4Y_\xi + A_5Y_\eta = A_6 \tag{6-3}$$

where

$$\begin{cases} A_1 = (Y_\eta + \psi_\eta)^2 - \psi_\eta^2 Z_1 \\ A_2 = -2Y_\xi(Y_\eta + \psi_\eta) \\ A_3 = \quad Y_\xi^2 + x_\xi^2 \\ A_4 = -A_1 x_{\xi\xi}/x_\xi \\ A_5 = -A_3\psi_{\eta\eta}/\psi_\eta \\ A_6 = \quad x_\xi^2\psi_\eta^2 Z_2, \end{cases}$$

$$Z_1 = \frac{\frac{2}{\gamma-1}x_\xi^2(Y_\eta+\psi_\eta)^2}{2H_\infty\rho^2x_\xi^2(Y_\eta+\psi_\eta)^2-\psi_\eta^2(Y_\xi^2+x_\xi^2)},$$

$$Z_2 = \frac{2H_\infty\rho^2x_\xi^2(Y_\eta+\psi_\eta)^2+\psi_\eta^2(Y_\xi^2+x_\xi^2)}{2H_\infty\rho^2x_\xi^2(Y_\eta+\psi_\eta)^2-\psi_\eta^2(Y_\xi^2+x_\xi^2)}\rho\omega(\frac{Y_\eta}{\psi_\eta}+1)^3.$$

For the full potential formulation, the main equation (4-3a) leads to

$$A_1Y_{\xi\xi}+A_2Y_{\xi\eta}+A_3Y_{\eta\eta}+A_4Y_\xi+A_5Y_\eta=A_6 \tag{6-4}$$

where

$$\begin{cases} A_1=(Y_\eta+\psi_\eta)^2-\psi_\eta^2M_\infty^2/R \\ A_2=-2Y_\xi(Y_\eta+\psi_\eta) \\ A_3=\quad Y_\xi^2+x_\xi^2 \\ A_4=-A_1x_{\xi\xi}/x_\xi \\ A_5=-A_3\psi_{\eta\eta}/\psi_\eta \\ A_6=0. \end{cases}$$

On the airfoil, the boundary condition is

$$Y=f_\pm[x(\xi)]. \tag{6-5a}$$

In the far field, the boundary condition can be derived from (4-2b):

$$\begin{aligned} Y(\xi,\eta) =& Dtan\eta(\frac{1}{cos\alpha}-1)+Ae^{-B\xi^2}tan\xi tan\alpha \\ &-\frac{\Gamma}{2\pi cos\alpha}ln\{A^2e^{-2B\xi^2}tan^2\xi \\ &+(1-M_\infty^2)[Y(\xi,\eta)+Dtan\eta]^2\}. \end{aligned} \tag{6-5b}$$

At the trailing edge, the Kutta condition must be satisfied so that the velocities

$$V_{TE}=\sqrt{[\frac{\psi_\eta^2(Y_\xi^2+x_\xi^2)}{\rho^2x_\xi^2(Y_\eta+\psi_\eta)^2}]_{TE}} \tag{6-5c}$$

calculated from lower and upper surfaces at the trailing edge are equal to each other.

After transformations (6-1) and (6-2), the normal shock jump conditions (5-4): become

$$[\frac{Y_\xi}{\rho x_\xi}]=0, \quad [\frac{Y_\eta}{\psi_\eta}+1]=0.$$

Because x_ξ, ψ_η are continuous everywhere, the shock jump conditions reduce to the same form as in (5-4):

$$[\frac{Y_\xi}{\rho}] = 0, \quad [Y_\eta] = 0 \tag{6-6}$$

or

$$Y_\xi^+ = \mu Y_\xi^-, \quad Y_\eta^+ = Y_\eta^-$$

where $\mu = \rho^+/\rho^-$ is the density jump factor across the shock. In more detail, the shock jump conditions in the stretched coordinates are (cf. Fig.5-2)

$$(Y_\xi)^+_{i-\frac{1}{2},j} = \mu_j (Y_\xi)^-_{i-\frac{1}{2},j}, \quad (Y_\eta)^+_{i-\frac{1}{2},j} = (Y_\eta)^-_{i-\frac{1}{2},j} \tag{6-7}$$

where the density jump factor on the j^{th} streamline is

$$\mu_j = \frac{\frac{\gamma+1}{4}(3M^2_{i-1,j} - M^2_{i-2,j})}{1 + \frac{\gamma-1}{4}(3M^2_{i-1,j} - M^2_{i-2,j})}.$$

Finally, we can construct the shock point operator in Jones' stretched coordinates:

$$(Y_{\xi\xi})_{i,j} = \frac{1}{\Delta\xi^2}(Y_{i+1,j} - Y_{i,j} - \mu_j Y_{i-1,j} + \mu_j Y_{i-2,j}) \tag{6-8}$$

and

$$\begin{aligned}(Y_{\xi\eta})_{i,j} = \frac{1}{4\Delta\xi\Delta\eta}(&Y_{i+1,j+1} - Y_{i+1,j-1} + Y_{i,j+1} - Y_{i,j-1} \\ &- 3Y_{i-1,j+1} + 3Y_{i-1,j-1} + Y_{i-2,j+1} - Y_{i-2,j-1}).\end{aligned} \tag{6-9}$$

Using the type-dependent scheme with shock point operator in equation (6-3) for the Euler formulation, we get the following system of difference equations:

$$AY_{i,j-1} + BY_{i,j} + CY_{i,j+1} = RHS \tag{6-10}$$

where

$$A = \beta^2 A_3 - 1/2\beta\Delta\xi A_5 - \begin{cases} (1-\nu)\beta A_2/2 & \text{if } i \neq i_s \\ \beta A_2/4 & \text{if } i = i_s, \end{cases}$$

$$B = -2\beta^2 A_3 + \begin{cases} (1-3\nu)A_1 + (1-\nu)\Delta\xi A_4 & \text{if } i \neq i_s \\ -A_1 & \text{if } i = i_s, \end{cases}$$

$$C = \beta^2 A_3 + 1/2\beta\Delta\xi A_5 + \begin{cases} (1-\nu)\beta A_2/2 & \text{if } i \neq i_s \\ \beta A_2/4 & \text{if } i = i_s, \end{cases}$$

$$RHS = \begin{cases} -\nu A_1(Y_{i+1,j} + Y_{i-1,j}) + (1-\nu)A_1(2Y_{i-1,j} - Y_{i-2,j}) \\ -\nu\beta A_2(Y_{i+1,j+1} - Y_{i+1,j-1} - Y_{i-1,j+1} + Y_{i-1,j-1})/4 \\ +(1-\nu)\beta A_2(Y_{i-1,j+1} - Y_{i-1,j-1})/2 \\ -\nu\Delta\xi A_4(Y_{i+1,j} - Y_{i-1,j})/2 + (1-\nu)\Delta\xi A_4 Y_{i-1,j} \\ +\Delta\xi^2 A_6 \qquad\qquad \text{if } i \neq i_s \\ \\ -A_1(Y_{i+1,j} - \mu_j Y_{i-1,j} + \mu_j Y_{i-2,j}) \\ -\beta A_2(Y_{i+1,j+1} - Y_{i+1,j-1} - 3Y_{i-1,j+1} \\ \quad +3Y_{i-1,j-1} + Y_{i-2,j+1} - Y_{i-2,j-1})/4 \\ -\Delta\xi A_4(Y_{i+1,j} - Y_{i-1,j})/2 \\ +\Delta\xi^2 A_6 \qquad\qquad \text{if } i = i_s \end{cases}$$

for $i = 2, 3, ..., I_{max-1}$, $j = 2, 3, ..., J_{max-1}$ and $\beta = \Delta\xi/\Delta\eta$.

For the full potential formulation, the system of difference equations is the same as equation (6-10) but the A's are differently defined as in equation (6-4).

6.3 Secondary Equation for ρ in Stretched Coordinates

Applying transformations (6-1) and (6-2) to the secondary equation (4-1b) for the Euler formulation, we have

$$B_1\rho_\xi + B_2\rho_\eta + B_3\rho = 0 \tag{6-11}$$

where

$$\begin{cases} B_1 = Y_\xi(Y_\eta + \psi_\eta)^2 \\ B_2 = -(Y_\eta + \psi_\eta)(Y_\xi^2 + x_\xi^2) \\ B_3 = -\psi_\eta^2(Y_{\xi\xi} - \frac{x_{\xi\xi}}{x_\xi}Y_\xi)Z_1 - x_\xi^2\psi_\eta^2 Z_3, \end{cases}$$

$$Z_1 = \frac{\frac{2}{\gamma-1}x_\xi^2(Y_\eta + \psi_\eta)^2}{2H_\infty\rho^2 x_\xi^2(Y_\eta + \psi_\eta)^2 - \psi_\eta^2(Y_\xi^2 + x_\xi^2)},$$

$$Z_3 = \frac{2\psi_\eta^2(Y_\xi^2 + x_\xi^2)}{2H_\infty\rho^2 x_\xi^2(Y_\eta + \psi_\eta)^2 - \psi_\eta^2(Y_\xi^2 + x_\xi^2)}\rho\omega(\frac{Y_\eta}{\psi_\eta} + 1)^3.$$

For the full potential formulation, the secondary equation in (ξ, η) coordinates is

$$B_1 R_\xi + B_2 R_\eta = B_3 \tag{6-12}$$

where

$$\begin{cases} B_1 = Y_\xi (Y_\eta + \psi_\eta)^2 \\ B_2 = -(Y_\eta + \psi_\eta)(Y_\xi^2 + x_\xi^2) \\ B_3 = (\gamma+1) M_\infty^2 \psi_\eta^2 (Y_{\xi\xi} - \frac{x_{\xi\xi}}{x_\xi} Y_\xi). \end{cases}$$

The Crank-Nicolson scheme for equation (6-11) of the Euler formulation or (6-12) of the full potential formulation produces the same forms of difference equation, its coefficients and its RHS term as in equation (4-10) and (4-11) or (4-13), but the B's take different forms from (4-9) as shown in (6-11) for the Euler formulation or (6-12) for the full potential formulation. In addition, the second derivatives $Y_{\xi\xi}$ in the expression of B_3 should be approximated by type-dependent difference with shock point operator:

$$Y_{\xi\xi} = \begin{cases} \frac{\nu}{\Delta\xi^2}(Y_{i+1,j} - 2Y_{i,j} + Y_{i-1,j}) + \frac{1-\nu}{\Delta\xi^2}(Y_{i,j} - 2Y_{i-1,j} + Y_{i-2,j}), & i \neq i_s \\ \frac{1}{\Delta\xi^2}(Y_{i+1,j} - Y_{i,j} - \mu_j Y_{i-1,j} + \mu_j Y_{i-2,j}), & i = i_s. \end{cases} \tag{6-13}$$

For the Euler formulation, the vorticity and the local Mach number can be calculated from

$$\omega = \frac{1}{Y_\eta + \psi_\eta} \{ \frac{\psi_\eta}{x_\xi} [\frac{Y_\xi}{\rho x_\xi}]_\xi - [\frac{\psi_\eta (Y_\xi^2 + x_\xi^2)}{\rho x_\xi^2 (Y_\eta + \psi_\eta)}]_\eta \} \tag{6-14}$$

and

$$M^2 = \frac{\frac{2}{\gamma-1}\psi_\eta^2 (Y_\xi^2 + x_\xi^2)}{2H_\infty \rho^2 x_\xi^2 (Y_\eta + \psi_\eta)^2 - \psi_\eta^2 (Y_\xi^2 + x_\xi^2)}. \tag{6-15}$$

The local Mach number for the full potential formulation is expressed by

$$M^2 = \frac{M_\infty^2}{R} \frac{\psi_\eta^2 (Y_\xi^2 + x_\xi^2)}{x_\xi^2 (Y_\eta + \psi_\eta)^2}. \tag{6-16}$$

The equations for the Kutta condition and for updating the circulation around the airfoil are the same as those in (4-16) and (4-17) where V_{TE} should be calculated from (6-5c). The pressure coefficient C_p is also expressed by (2-35) for the Euler formulation and by (3-29) for the full potential formulation.

Chapter 7. Full Potential Analysis and Design

The governing equations for irrotational and isentropic fluid flow are the full potential-equivalent equations derived in Chapter 3. There are several options for secondary equations and the corresponding secondary variables. For analysis problems, we can chose the (y, R) set of equations (3-24) and (3-25) to solve:

$$(y_\psi^2 - \frac{M_\infty^2}{R})y_{xx} - 2y_x y_\psi y_{x\psi} + (1 + y_x^2)y_{\psi\psi} = 0, \tag{7-1a}$$

$$y_x y_\psi^2 R_x - y_\psi(1 + y_x^2)R_\psi = (\gamma + 1)M_\infty^2 y_{xx} \tag{7-1b}$$

where $R = \rho^{\gamma+1}$ is the generalized density. The boundary conditions on the airfoil, at infinity and at the trailing edge are the same as in the Euler formulation: (4-2a), (4-2b) and (4-2c). The difference equations which should be solved are equation (5-11) for y and equations (4-13) for R, but the A's and B's should be adjusted accordingly.

For design problems, however, due to the different boundary condition on the airfoil, an alternative set of governing equations is selected. The main equation is still (3-24), but the secondary equation is changed to (3-26):

$$y_\psi(y_\psi^2 - \frac{M_\infty^2}{R})R_x - y_x y_\psi^2 R_\psi = (\gamma + 1)M_\infty^2 y_{x\psi} \tag{7-2}$$

The boundary conditions for the design problem are the same as in the analysis problems, except on the airfoil whose shape is unknown. There, the pressure (or velocity) distribution is specified, hence, the generalized density is also specified:

$$R_s(x) = [1 + \frac{\gamma}{2}M_\infty^2 C_{ps}(x)]^{\frac{\gamma+1}{\gamma}} \tag{7-3}$$

where $C_{ps}(x)$ is the prescribed surface pressure coefficient. On the airfoil, the Bernoulli equation in stream function coordinates leads to

$$F(x)y_\psi^2 - y_x^2 = 1 \tag{7-4}$$

where

$$F(x) = \frac{2}{(\gamma-1)M_\infty^2}\{(1+\frac{\gamma-1}{2}M_\infty^2)[R_s(x)]^{\frac{2}{\gamma+1}} - R_s(x)\}$$

is a known function of x. Equation (7-4) is a Neumann boundary condition on the airfoil when solving (7-1a) for y. Equation (7-3) is a Dirichlet boundary condition on the airfoil when solving (7-2) for R. At infinity, $R = 1$. If the problem is symmetric, the condition $R_\psi = 0$ on a symmetry line off the airfoil should be applied. If streamlines do not intersect each other on the airfoil, then $y_\psi > 0$, and if, furthermore, $F(x) \neq 0$ on the airfoil, then equation (7-4) gives

$$y_\psi = \sqrt{\frac{1+y_x^2}{F(x)}}.$$

For most practical transonic flows the required conditions are easily satisfied as long as $C_{ps}(x)$ is reasonably specified. Differencing y_ψ with second order accuracy, we get

$$y_{i,1} = \frac{1}{3}[4y_{i,2} - y_{i,3} - 2G(x_i)] \tag{7-5}$$

where

$$G(x_i) = \Delta\psi\sqrt{\frac{1+(y_x^2)_{i,1}}{F(x_i)}}.$$

Considering this boundary condition, we modify system (5-11) as below: for j=2, equation (5-11) becomes

$$[B+\frac{4}{3}A]y_{i,2} + [C-\frac{1}{3}A]y_{i,3} = RHS + \frac{2}{3}AG(x_i) \tag{7-6}$$

Replacing the first equation in system (5-11) by (7-6), solving the resulting system of equations and applying (7-5), we can obtain the desired airfoil contour $f(x_i) = y_{i,1}$ without any further iteration of the airfoil shape.

Equation (7-2) for R has different characteristic curves than equation (7-1b). In fact, the slope of the characteristic curves of equation (7-2) is

$$\frac{d\psi}{dx} = -\frac{y_x y_\psi}{y_\psi^2 - M_\infty^2/R}. \tag{7-7}$$

At infinity, $d\psi/dx = 0$. So, the horizontal far field boundary is a characteristic curve, but the vertical boundaries are not. Therefore, the marching process can be carried out from left to right. The whole domain can be divided into the same four subdomains to march R as for the y equation in Fig.4-2a.

For full potential analysis and design problems, only symmetric flows have been calculated. Figs.7-1 — 7-3 are comparisons of the calculated Cp distributions for a NACA 0012 airfoil with experimental data from the laboratories at ONERA and NAE for M_∞=0.703, 0.803 and 0.835. The computational domain (x, ψ) has been covered by a 65x33 uniform grid for moderate M_∞ (Fig.7-1). For higher Mach numbers (Fig.7-2 and 7-3), a denser 81x31 mesh in the stretched coordinates (ξ, η) has been used. The agreement between computed pressure coefficient and the available experimental data is quite satisfactory. For supercritical transonic flows, the shock waves can be captured by the type-dependent scheme plus the shock point operator (SPO).

Figs.7-4 — 7-8 show the Cp distributions for a NACA 0012 calculated by different sets of equations and the associated secondary variables. Fig.7-4 shows the calculated result for the (y, R) set of equations (3-24) and (3-25). Fig.7-5 is the result of calculations in which R is solved from the first order ODE (3-31a). Fig.7-6 shows the calculated Cp distribution by solving the set of equations in which R is solved from the second order PDE (3-34). Fig.7-7 depicts the calculated result using the (y, M^2) set of equations (3-35) and (3-36a). Fig.7-8 show the result of the computation from the (y, u, ρ) set of equations (3-44)—(3-46). Other sets of equations also have been tried and all of these computations have given acceptable results. However, the set of (y, R) with the first order PDE for R, i.e. equation (3-25), is the simplest due to its linearity for R and gives a more accurate result especially for the supercritical flows. Therefore, this set of equations appears to be the optimal choice.

Fig.7-9 indicates the typical convergence history of the full potential calculation. The horizontal axis gives the total iteration number and the vertical axis is the

logarithm of the error of R between two successive iterations. For subcritical Mach number, the convergence is fast and the maximum error decreases steeply. For supercritical flow, however, the convergence rate is much slower and the maximum error decreases slowly with oscillations.

Fig.7-10 shows the designed contours of a 6 percent biconvex airfoil compared with the exact shape (Abbott and von Doenhoff 1959). The specified $C_{ps}(x)$ on the airfoil comes from the experiments at NASA (Knetchtel 1959) for M_∞= 0.909. Figs.7-11 and 7-12 give the designed NACA 0012 airfoil contours compared with the exact shape (Abbott and von Doenhoff 1959). The specified $C_{ps}(x)$ is from NAE (Ohman 1979) for M_∞=0.490 (subcritical case) and from ONERA (Thibert and Grandjacques 1979) for M_∞=0.803 (supercritical case). In the example in Fig.7-11, a coarser uniform grid of 65x33 has been used and, in the computation of Fig.7-12, a finer clustered grid of 81x31 has been used. Here, we can see that the present full potential approach is capable of designing airfoil contours with satisfactory accuracy.

Chapter 8. Euler Solutions

The developed approach using the Euler-equivalent equations in stream function coordinates has also been used to calculate transonic flows past airfoils at zero and non-zero angle of attack. Both subcritical and supercritical Mach numbers have been considered. For unstretched stream function coordinates (x, ψ), a 65x65 uniform mesh covers the computational domain of $-2 \leq x \leq 3, -2.5 \leq \psi \leq 2.5$ and the airfoil is located between 0 and 1 with 13 grid points on it. For stretched coordinates (ξ, η), a 65x65 uniform grid system covers the computational domain of $-1.54 \leq \xi \leq 1.54, -1.54 \leq \eta \leq 1.54$ corresponding to a domain of $-7.04 \leq x \leq 7.04, -19.47 \leq \psi \leq 19.47$ in clustered (x, ψ) coordinates. The airfoil is placed between -0.5 and 0.5 and contains 25 grid points on its surface.

The computations are executed for the set of equations (2-24), (2-27) and (2-22) for y, ρ and ω. The corresponding difference equations are (5-11) for y and (4-10), (4-11) for ρ. The vorticity ω is calculated using central differences for all x and ψ differentiations. The iteration includes three levels of loops. The most internal loop is the y iteration, the intermediate level is for ρ and the most external iteration loop is for ω, or for Γ. The convergence criterion, the Kutta condition (4-16), must be satisfied. The computational flow chart is given in Fig.4-3.

Most calculations have been carried out on a PC machine. The typical computational time on a 25 MHz 386 IBM compatible computer with 387 Math Coprocessor is about 20 minutes for supercritical flows and 5 minutes for subcritical flows.

Figs.8-1 — 8-12 show the comparisons of surface Cp distributions between the calculated results and experimental data or other computations. Figs.8-1 — 8-2 are Cp distributions for a NACA 0012 in subcritical flows: M_∞=0.490 and 0.696 at zero angle of attack. Figs.8-3 — 8-5 show comparisons of computed and experimental Cp distributions on a NACA 0012 in supercritical flows: M_∞=0.756, 0.803 and 0.814. For moderate M_∞ (Fig.8-3), the coarse uniform grid in (x, ψ) has been used. For higher Mach numbers (Figs.8-4, 8-5), the finer clustered grid in (ξ, η)

has been used. The experimental data in Figs.8-1 — 8-5 are obtained from a laboratory of ONERA, France, (Thibert and Grandjacques 1979) and a laboratory of NAE, Canada, (Ohman 1979). Fig.8-6 shows the comparison of Cp distributions for a NACA 0012, M_∞=0.8, α=1.25 between the present clustered grid calculation and another Euler computation by Viviand (1985) using the O type 320x64 grid. Figs.8-7 — 8-8 show Cp distributions on the 6 percent biconvex airfoil at subcritical M_∞=0.840 and supercritical M_∞=0.909, respectively, compared with the experimental data from a laboratory of NASA (Knetchtel 1959). Figs.8-9 — 8-12 give the Cp distributions for the NACA 0012 at M_∞= 0.502 and various angles of attack: α=0, 2, 4 and 6 degrees. From these plots we can see that the present approach can accurately predict Cp distributions for both subcritical and supercritical flows. The small discrepancies between the calculated and experimental results at leading and trailing edges and at shock waves are expected because the experimental results necessarily involve the effect of viscosity.

Figs.8-13(a)—(d) show the effect of type-dependent (TD) differencing and shock point operator (SPO) in a typical supercritical calculation: NACA 0012, M_∞=0.803, α=0. Fig.8-13(a) gives the result of central differencing with neither TD nor SPO. The computed Cp distribution is totally incorrect and the shock wave cannot be captured. Fig.8-13(b) shows the result of only TD differencing without SPO. The calculated Cp distribution is inaccurate and the shock wave location is too far backward. Fig.8-13(c) shows the result of TD differencing plus relevant SPO, i.e. SPO is used in $y_{xx}, y_{x\psi}$ terms only. The calculation gives a satisfactory Cp distribution and the shock wave can be captured accurately. Fig.8-13(d) shows the result of TD differencing plus too much SPO, i.e. SPO is used not only in $y_{xx}, y_{x\psi}$ terms but also in y_x term. The computed Cp distribution is inaccurate and oscillations occur at the shock wave region. Comparing these pictures we conclude that the TD differencing plus relevant SPO is an effective scheme to calculate transonic flows and the SPO is a crucial tool to capture the embedded shock waves.

Figs. 8-14(a)—(h) demonstrate the evolution of iteration and convergence process

for a typical supercritical calculation: NACA 0012, M_∞=0.803, α=0. The Cp distributions on the airfoil after the following numbers of iterations are plotted: 31, 67, 103, 165, 251, 380, 449 and 528. From these plots we can see that before 165 iterations the calculated flow field has no shock wave. After 165 iterations, a shock wave is formed and pushed backward. The accuracy becomes better and better with the process of iterations. The computation converges after 528 iterations and gives a satisfactory solution.

Fig. 8-15 shows the convergence history for several typical calculations. The horizontal ordinate is the total number of iterations for y and the vertical ordinate is the logarithm of the error of ρ. For subcritical flow (M_∞=0.703), the iteration converges very fast, the error decays to order 10^{-4} within 100 iterations. For supercritical flow with no obvious shock wave (M_∞=0.756), the iteration converges slower and oscillation occurs, but it does not take long to decay the error to order 10^{-3}. However, for supercritical flow with a shock wave (M_∞=0.803), the convergence becomes very low and the calculation oscillates. It takes a long time (more than 500 iterations) to decay the error to order 10^{-2}.

Figs.8-16 — 8-17 show the effect of the stretching coordinate transformation. For the subcritical case, without and with the stretching coordinate transformation, the Cp distributions for the NACA 0012 at M_∞=0.703 and α=0 are shown in Figs.8-16(a) and (b), respectively. The accuracy improvement is not obvious as the unstretched discretization has already given a good result. However, for the supercritical case, the accuracy is improved considerably as shown in Figs.8-17(a) and (b). The stretched coordinate discretization gives a more accurate Cp distribution and shock wave location.

Chapter 9. Further Extensions

9.1 Extension to Axisymmetric Flows

Similar to the two dimensional case, for an inviscid compressible axisymmetric flow, the governing Euler equations take the following form

$$(\rho ur)_x + (\rho vr)_r = 0, \tag{9-1a}$$

$$\rho u u_x + \rho v u_r + p_x = 0, \tag{9-1b}$$

$$\rho u v_x + \rho v v_r + p_r = 0, \tag{9-1c}$$

$$p = \frac{\rho^\gamma}{\gamma M_\infty^2}. \tag{9-1d}$$

where u and v represent velocity components along the axial (x) and radial (r) directions, respectively. The coordinates (x, r) define a point in a meridian plane. Here, the isentropic assumption is made so that the energy equation is replaced by the isentropic relation (9-1d). After using the continuity equation, the axial and radial momentum equations (9-1b) and (9-1c) can be rewritten as

$$(\rho u^2 + p)_x + (\rho uv)_r + \frac{\rho uv}{r} = 0,$$

$$(\rho uv)_x + (\rho v^2 + p)_r + \frac{\rho v^2}{r} = 0.$$

Introducing Stokes stream function ψ such that

$$\psi_r = \rho ur, \qquad \psi_x = -\rho vr, \tag{9-2}$$

the continuity equation (9-1a) is automatically satisfied and the above momentum equations become

$$(\frac{\psi_r^2}{\rho r^2} + p)_x - (\frac{\psi_x \psi_r}{\rho r^2})_r - \frac{\psi_x \psi_r}{\rho r^3} = 0, \tag{9-3a}$$

$$-(\frac{\psi_x \psi_r}{\rho r^2})_x + (\frac{\psi_x^2}{\rho r^2} + p)_r + \frac{\psi_x^2}{\rho r^3} = 0. \tag{9-3b}$$

Making the von Mises transformation

$$x \equiv x, \qquad r = r(x, \psi) \tag{9-4}$$

and assuming that the Jacobian $J = \partial(x,r)/\partial(x,\psi) = r_\psi$ is non-zero and finite, we can get a single-valued transformation and the transformed operators:

$$\frac{\partial}{\partial x} = \frac{\partial}{\partial x} - \frac{r_x}{r_\psi}\frac{\partial}{\partial \psi}, \qquad \frac{\partial}{\partial r} = \frac{1}{r_\psi}\frac{\partial}{\partial \psi}.$$

Using these in (9-3a) and (9-3b) leads to

$$(\frac{1}{\rho r^2 r_\psi^2} + p)_x - \frac{r_x}{r_\psi}(\frac{1}{\rho r^2 r_\psi^2} + p)_\psi + \frac{1}{r_\psi}(\frac{r_x}{\rho r^2 r_\psi^2})_\psi + \frac{r_x}{\rho r^3 r_\psi^2} = 0,$$

$$(\frac{r_x}{\rho r^2 r_\psi^2})_x - \frac{r_x}{r_\psi}(\frac{r_x}{\rho r^2 r_\psi^2})_\psi + \frac{1}{r_\psi}(\frac{r_x^2}{\rho r^2 r_\psi^2} + p)_\psi + \frac{r_x^2}{\rho r^3 r_\psi^2} = 0$$

or

$$r_\psi(\frac{1}{\rho r^2 r_\psi^2})_x + \frac{r_{x\psi}}{\rho r^2 r_\psi^2} + \frac{r_x}{\rho r^3 r_\psi} + r_\psi p_x - r_x p_\psi = 0,$$

$$r_\psi(\frac{r_x}{\rho r^2 r_\psi^2})_x + \frac{r_x r_{x\psi}}{\rho r^2 r_\psi^2} + \frac{r_x^2}{\rho r^3 r_\psi} + p_\psi = 0.$$

Differentiating (9-1d) with respect to x and ψ,

$$p_x = \rho^{\gamma-1}\rho_x/M_\infty^2, \qquad p_\psi = \rho^{\gamma-1}\rho_\psi/M_\infty^2,$$

substituting p_x, p_ψ into the above momentum equations and simplifying, we get

$$-r_{x\psi} - \frac{r_x r_\psi}{r} + r_\psi(r^2 r_\psi^2 \frac{\rho^{\gamma+1}}{M_\infty^2} - 1)\frac{\rho_x}{\rho} - r_x r^2 r_\psi^2 \frac{\rho^{\gamma+1}}{M_\infty^2}\frac{\rho_\psi}{\rho} = 0, \tag{9-5a}$$

$$r_\psi r_{xx} - r_x r_{x\psi} - \frac{r_x^2 r_\psi}{r} - r_x r_\psi \frac{\rho_x}{\rho} + r^2 r_\psi^2 \frac{\rho^{\gamma+1}}{M_\infty^2}\frac{\rho_\psi}{\rho} = 0. \tag{9-5b}$$

The vorticity expression can be transformed to (x,ψ) coordinates as below:

$$\begin{aligned}\omega &= v_x - u_r \\ &= -[\frac{\psi_x}{\rho r}]_x - [\frac{\psi_r}{\rho r}]_r \\ &= \frac{1}{r_\psi}\{[\frac{r_x}{\rho r}]_x - [\frac{1+r_x^2}{\rho r r_\psi}]_\psi\}\end{aligned} \tag{9-6}$$

or in expanded form

$$r_\psi^2 r_{xx} - 2r_x r_\psi r_{x\psi} + (1+r_x^2) r_{\psi\psi} + \frac{r_\psi^2}{r}$$
$$= r_x r_\psi^2 \frac{\rho_x}{\rho} - r_\psi (1+r_x^2) \frac{\rho_\psi}{\rho} + \rho\omega r r_\psi^3. \tag{9-7}$$

Solving (9-5a) and (9-5b) for ρ_x/ρ and ρ_ψ/ρ, substituting them into (9-7) and simplifying the resulting equation, we get

$$(r_\psi^2 - \frac{M_\infty^2}{\rho^{\gamma+1} r^2}) r_{xx} - 2r_x r_\psi r_{x\psi} + (1+r_x^2) r_{\psi\psi} + \frac{r_\psi^2}{r} = \rho\omega r r_\psi^3. \tag{9-8}$$

Equation (9-8) which can be solved for r, is almost the same as equation (3-15) for the two dimensional case, except for an extra term r_ψ^2/r on the left hand side and slight changes in the compressibility parameter and in the rotational term. Eliminating $r_{x\psi}$ from (9-5a) and (9-5b) gives

$$r_x r_\psi^2 \rho^\gamma \rho_x - r_\psi (1+r_x^2) \rho^\gamma \rho_\psi = M_\infty^2 \frac{r_{xx}}{r^2}. \tag{9-9}$$

Equation (9-5a) can be rewritten as

$$r_\psi (r_\psi^2 - \frac{M_\infty^2}{\rho^{\gamma+1} r^2}) \rho^\gamma \rho_x - r_x r_\psi^2 \rho^\gamma \rho_\psi = M_\infty^2 (\frac{r_{x\psi}}{r^2} + \frac{r_x r_\psi}{r^3}). \tag{9-10}$$

Eliminating r_{xx} and $r_{x\psi}$ from (9-9), (9-10) and (9-8), we get

$$r_x (r_\psi^2 - \frac{M_\infty^2}{\rho^{\gamma+1} r^2}) \rho^\gamma \rho_x + r_\psi \{(1-r_x^2) - \frac{M_\infty^2}{\rho^{\gamma+1} r^2} \frac{1+r_x^2}{r_\psi^2}\} \rho^\gamma \rho_\psi$$
$$= M_\infty^2 \{\frac{1+r_x^2}{r_\psi^2} \frac{r_{\psi\psi}}{r^2} + \frac{1+2r_x^2}{r^3} - \rho\omega \frac{r_\psi}{r}\}. \tag{9-11}$$

Any one of equations (9-9)–(9-11) can be chosen to solve for ρ. At last, ω can be calculated from its definition (9-6) after r and ρ are solved. Equations (9-8), one of (9-9)–(9-11) and (9-6) constitute a set of equations governing inviscid axisymmetric flows. Similar to the two dimensional case, equation (9-8) is termed the 'main equation' for the corresponding 'main variable' r, and equations (9-9)–(9-11) are

called the 'secondary equations' for the 'secondary variable' ρ. After solving for r and ρ, the local Mach number can be evaluated by

$$M^2 = \frac{\frac{2}{\gamma-1}(1+r_x^2)}{2H_\infty \rho^2 r^2 r_\psi^2 - (1+r_x^2)}. \tag{9-12}$$

The pressure coefficient C_p is also expressed by (2-35).

For irrotational flows, $\omega = 0$, equations (9-8)-(9-11) can be simplified. Defining the generalized density $R = \rho^{\gamma+1}$ (cf. (3-23)), equations (9-8)-(9-11) become

$$(r_\psi^2 - \frac{M_\infty^2}{Rr^2})r_{xx} - 2r_x r_\psi r_{x\psi} + (1+r_x^2)r_{\psi\psi} + \frac{r_\psi^2}{r} = 0, \tag{9-13}$$

$$r_x r_\psi^2 R_x - r_\psi(1+r_x^2)R_\psi = (\gamma+1)M_\infty^2 \frac{r_{xx}}{r^2}, \tag{9-14}$$

$$r_\psi(r_\psi^2 - \frac{M_\infty^2}{Rr^2})R_x - r_x r_\psi^2 R_\psi = (\gamma+1)M_\infty^2(\frac{r_{x\psi}}{r^2} + \frac{r_x r_\psi}{r^3}), \tag{9-15}$$

$$r_x(r_\psi^2 - \frac{M_\infty^2}{Rr^2})R_x + r_\psi\{(1-r_x^2) - \frac{M_\infty^2}{Rr^2}\frac{1+r_x^2}{r_\psi^2}\}R_\psi$$

$$= (\gamma+1)M_\infty^2\{\frac{1+r_x^2}{r_\psi^2}\frac{r_{\psi\psi}}{r^2} + \frac{1+2r_x^2}{r^3}\}. \tag{9-16}$$

Among the secondary equations (9-14)-(9-16), the linear equation (9-14) for R is the simplest. Therefore, priority should be given to it unless other difficulties occur. The local Mach number is given by

$$M^2 = \frac{M_\infty^2}{R}\frac{1+y_x^2}{r^2 r_\psi^2} \tag{9-17}$$

and the pressure coefficient expression is the same as in (3-29).

In addition, if the flow is incompressible, then the flow field is governed by a single equation for $r = r(x,\psi)$:

$$r_\psi^2 r_{xx} - 2r_x r_\psi r_{x\psi} + (1+r_x^2)r_{\psi\psi} + \frac{r_\psi^2}{r} = 0. \tag{5-18}$$

This equation has been obtained by Barron et al.(1990). To remove the singularity at $r = 0$ and get a homogeneous boundary condition at infinity, they have introduced a new dependent variable $\tilde{r}$ defined by

$$\tilde{r}(x,\psi) = \frac{1}{2}r^2(x,\psi) - \psi \tag{9-19}$$

so that equation (9-18) becomes

$$(\tilde{r}_\psi + 1)^2 \tilde{r}_{xx} - 2\tilde{r}_x(\tilde{r}_\psi + 1)\tilde{r}_{x\psi} + (\tilde{r}_x^2 + 2\tilde{r} + 2\psi)\tilde{r}_{\psi\psi} = 0. \qquad (9\text{-}20)$$

9.2 Extension to Unsteady Flows

Srinivasan and Spalding (1986) solved shock tube flows using one dimensional unsteady gas dynamics equations for primitive variables in stream function coordinates by a floating grid finite difference method and claimed that the method can locate the contact discontinuity in temperature and density profiles precisely. Kalman (1960) also applied a similar idea to the oscillation of a zero-temperature plasma. In this section, we will derive a wave-like equation governing one dimensional unsteady compressible fluid flows as an extension of the approach in previous chapters.

For one dimensional unsteady flow of the inviscid isentropic gas, the governing equations are

$$\rho_t + (\rho u)_x = 0, \qquad (9\text{-}21a)$$

$$\rho u_t + \rho u u_x + p_x = 0, \qquad (9\text{-}21b)$$

$$p = \frac{\rho^\gamma}{\gamma M_\infty^2} \qquad (9\text{-}21c)$$

where the density ρ, velocity u and pressure p are unknown functions of time t and coordinate x. The continuity equation (9-21a) is automatically satisfied through the introduction of the stream function ψ such that

$$\psi_x = \rho, \quad \psi_t = -\rho u \qquad (9\text{-}22)$$

or

$$\rho = \psi_x, \quad u = -\frac{\psi_t}{\psi_x}. \qquad (9\text{-}23)$$

Differentiating the isentropic equation (9-21c) with respect to x gives

$$p_x = \frac{\rho^{\gamma-1}}{M_\infty^2}\rho_x = \frac{\psi_x^{\gamma-1}}{M_\infty^2}\psi_{xx}. \tag{9-24}$$

Substituting (9-23) and (9-24) into the momentum equation (9-21b) and simplifying, we get the governing equation for stream function ψ:

$$\psi_x^2\psi_{tt} - 2\psi_t\psi_x\psi_{tx} + (\psi_t^2 - \frac{\psi_x^{\gamma+1}}{M_\infty^2})\psi_{xx} = 0. \tag{9-25}$$

The discriminant of this equation

$$\Delta = 4\frac{\psi_x^{\gamma+3}}{M_\infty^2} \tag{9-26}$$

is always positive because $\psi_x = \rho > 0$. Therefore, equation (9-25) is always hyperbolic, which is consistent with the physical nature of the flow.

Making a von Mises-like transformation

$$t \equiv \tau, \quad x = x(\tau, \psi) \tag{9-27}$$

changes the roles of x from independent variable to dependent and ψ from dependent variable to independent. If the Jacobian $J = \partial(t,x)/\partial(\tau,\psi) = x_\psi$ is non-zero and finite, then the transformation is one-to-one and no singularities exist throughout the flow field. After the transformation, the differential operators are

$$\frac{\partial}{\partial t} = \frac{\partial}{\partial \tau} - \frac{x_\tau}{x_\psi}\frac{\partial}{\partial \psi}, \quad \frac{\partial}{\partial x} = \frac{1}{x_\psi}\frac{\partial}{\partial \psi}.$$

Therefore,

$$\psi_t = -\frac{x_\tau}{x_\psi}, \quad \psi_x = \frac{1}{x_\psi},$$

$$\psi_{tt} = -\frac{x_\psi^2 x_{\tau\tau} - 2x_\tau x_\psi x_{\tau\psi} + x_\tau^2 x_{\psi\psi}}{x_\psi^3},$$

$$\psi_{tx} = -\frac{x_\psi x_{\tau\psi} - x_\tau x_{\psi\psi}}{x_\psi^3}, \quad \psi_{xx} = -\frac{x_{\psi\psi}}{x_\psi^3}.$$

Substituting these into (9-25), we finally obtain the governing equation for one dimensional unsteady isentropic flows in stream function coordinates (τ, ψ):

$$M_\infty^2 x_\psi^{\gamma+1} x_{\tau\tau} = x_{\psi\psi}. \tag{9-28}$$

This nonlinear second order partial differential equation is always hyperbolic, or more precisely, it is a wave equation with a variable propagation speed, because its discriminant

$$\Delta = 4M_\infty^2 x_\psi^{\gamma+1} \tag{9-29}$$

is always positive ($x_\psi = 1/\rho > 0$). The dependent variable $x = x(\tau, \psi)$, as the unknown function of time τ and stream function ψ, is to be solved from (9-28). After x is obtained, the density, velocity and pressure can be easily calculated by

$$\rho = \frac{1}{x_\psi}, \quad u = x_\tau, \quad p = \frac{1}{\gamma M_\infty^2 x_\psi^\gamma}. \tag{9-30}$$

9.3 Extension to Viscous Flows

The formulation for inviscid incompressible rotational flows can be extended to the viscous case. For a two dimensional steady incompressible viscous flow, the governing Navier-Stokes equations are

$$u_x + v_y = 0, \tag{9-31a}$$

$$uu_x + vu_y + p_x = (u_{xx} + u_{yy})/Re, \tag{9-31b}$$

$$uv_x + vv_y + p_y = (v_{xx} + v_{yy})/Re, \tag{9-31c}$$

$$\omega = v_x - u_y \tag{9-31d}$$

where Re is Reynolds number and u, v, p and ω have the same meaning as before. Introducing stream function ψ and eliminating p from (9-31b) and (9-31c), we can obtain the following stream-function/vorticity formulation in the viscous case:

$$\psi_{xx} + \psi_{yy} = -\omega, \tag{9-32a}$$

$$\psi_y \omega_x - \psi_x \omega_y = (\omega_{xx} + \omega_{yy})/Re. \tag{9-32b}$$

After the von Mises transformation, the Poisson equation (9-32a) becomes

$$y_\psi^2 y_{xx} - 2y_x y_\psi y_{x\psi} + (1+y_x^2) y_{\psi\psi} = \omega y_\psi^3. \tag{9-33}$$

This equation is the same as for inviscid fluid flow. It can be solved for y when ω is prescribed or somehow determined. Likewise, after the von Mises transformation,

$$\omega_x = \omega_x - \frac{y_x}{y_\psi}\omega_\psi, \quad \omega_y = \frac{1}{y_\psi}\omega_\psi,$$

$$\begin{aligned}\omega_{xx} = &\frac{1}{y_\psi^2}\{y_\psi^2\omega_{xx} - 2y_x y_\psi \omega_{x\psi} + y_x^2\omega_{\psi\psi}\} \\ &- \frac{1}{y_\psi^3}\{y_\psi^2 y_{xx} - 2y_x y_\psi y_{x\psi} + y_x^2 y_{\psi\psi}\}\omega_\psi,\end{aligned}$$

$$\omega_{yy} = \frac{1}{y_\psi^2}\omega_{\psi\psi} - \frac{1}{y_\psi^3} y_{\psi\psi}\omega_\psi.$$

Therefore, the vorticity equation (9-32b) can be transformed to

$$\begin{aligned}y_\psi^2\omega_{xx} - 2y_x y_\psi \omega_{x\psi} + &(1+y_x^2)\omega_{\psi\psi} \\ &= Re\, y_\psi \omega_x + y_\psi^2 \omega\omega_\psi.\end{aligned} \tag{9-34}$$

This is also a second order non-homogeneous partial differential equation of elliptic type and can be solved for ω if y is obtained. Equation (9-34) is considered as a linear equation in the sense that the coefficients of the second derivatives of ω do not depend on ω itself. The second order differential operator for ω in this equation is the same as that for y in equation (9-33). On the other hand, it is also considered as a nonlinear equation due to the last term on the right hand side, but the degree of nonlinearity in (9-34) is much less than that in equation (9-33).

Equations (9-33) and (9-34) constitute a set of coupled equations for y and ω governing two dimensional incompressible viscous flows in stream function coordinates (x, ψ). Similar to the inviscid case, equation (9-33) and (9-34) are called the 'main

equation' and the 'secondary equation', respectively. After y and ω are determined, the velocity components can be evaluated by

$$u = \frac{1}{y_\psi}, \quad v = \frac{y_x}{y_\psi}. \tag{9-35}$$

For rotational flows, the Bernoulli equation in integral form does not exist. So, in order to get pressure after y and ω are solved, it is necessary to deduce the pressure equation in (x, ψ) coordinates. Differentiating equations (9-31b) and (9-31c) with respect to x and y, respectively, and adding them together, we have

$$p_{xx} + p_{yy} + u_x^2 + 2u_y v_x + v_y^2 = 0. \tag{9-36}$$

From (9-31d) and (9-31a),

$$v_x = u_y + \omega, \quad v_y = -u_x.$$

Then, equation (9-36) becomes

$$p_{xx} + p_{yy} + 2(u_x^2 + u_y^2 + u_y\omega) = 0. \tag{9-37}$$

In stream function coordinates (x, ψ),

$$u_x = -\frac{1}{y_\psi^3}(y_\psi y_{x\psi} - y_x y_{\psi\psi}), \quad u_y = -\frac{1}{y_\psi^3} y_{\psi\psi}, \tag{9-38}$$

$$p_{xx} + p_{yy} = \frac{1}{y_\psi^2}\{y_\psi^2 p_{xx} - 2y_x y_\psi p_{x\psi} + (1 + y_x^2)p_{\psi\psi}\} - \omega p_\psi. \tag{9-39}$$

Here, equation (9-33) has been used to simplify the expression in (9-39). Substituting (9-38) and (9-39) into (9-37), we finally obtain the p equation:

$$\begin{aligned} y_\psi^2 p_{xx} - 2y_x y_\psi p_{x\psi} + (1 + y_x^2)p_{\psi\psi} \\ = y_\psi^2 \omega p_\psi + \frac{2}{y_\psi^2}(y_{xx} y_{\psi\psi} - y_{x\psi}^2). \end{aligned} \tag{9-40}$$

This second order linear partial differential equation for p is also elliptic with the same operator as in equation (9-33). It can also be obtained from the Poisson equation for pressure in the section III-E-2 of Roache's book (1976):

$$\Delta^2 p = 2(\psi_{xx}\psi_{yy} - \psi_{xy}^2) \tag{9-41}$$

through the von Mises transformation. Equation (9-40) can be used to solve for p after y and ω are known.

To summarize, for a two dimensional steady incompressible viscous flow, instead of solving Navier-Stokes equations in primitive variable form or in stream-function/vorticity form, we can solve the two coupled equations (9-33) for $y(x,\psi)$ and (9-34) for $\omega(x,\psi)$. Once y and ω are solved, pressure p can be solved from equation (9-40) and velocity components u and v can be calculated by (9-35). All of the equations (9-33), (9-34) and (9-40) for the corresponding variable y, ω and p have the same second order differential operator and, therefore, are of the same elliptic type. However, (9-33) is highly nonlinear, while (9-34) and (9-40) are slightly nonlinear and linear, respectively.

9.4 Arc Length/Stream Function Formulation

In previous chapters, we always assumed that the von Mises transformation is permissible throughout the flow field. For most flow problems of practical interest this assumption is valid, especially for thin airfoils with sharp or slightly blunt leading edges at small angle of attack. In this case, the distance between the leading edge and the forward stagnation point is very small, hence, there is no reverse flow region or the reverse flow region is negligibly small. As a first approximation, the assumption that the stagnation point exactly coincides with the leading edge can be made so that no reverse flow appears at all.

However, when the leading edge is blunt and the angle of attack is not small, a reverse flow region cannot be neglected and the assumption of coincidence between

leading edge and stagnation point does not hold. In this case, the x-velocity component u becomes zero and the Jacobian goes to infinity at certain points (see Fig.9.1, points B and D), hence, the von Mises transformation is singular and the multi-value problem occurs (see Fig.9.1, points A, C and E). A possible way to overcome this difficulty is the use of arc length s to replace x in von Mises coordinates. Next, we will derive a so-called arc length/stream function formulation from the basic principles of differential geometry and the governing equations of incompressible potential flows.

Suppose two families of curves, $s = const.$ and $\psi = const.$, overlay the (x, y) plane and form a regular coordinate net in which each s-curve intersects with a ψ-curve at only one point and neither an s-curve nor a ψ-curve intersects with itself (see Fig.9.2). Consider a coordinate transformation

$$x = x(s, \psi), \quad y = y(s, \psi). \tag{9-42}$$

For the time being, s and ψ are arbitrary curvilinear coordinates and do not yet have any specific physical meaning. The differentials of (9-42) are

$$dx = x_s ds + x_\psi d\psi, \quad dy = y_s ds + y_\psi d\psi.$$

The squared length of an arbitrary element arc in (x, y) plane can be expressed by the first fundamental form

$$\begin{aligned} dS^2 &= dx^2 + dy^2 \\ &= E ds^2 + 2F ds d\psi + G d\psi^2 \end{aligned} \tag{9-43}$$

where

$$E = x_s^2 + y_s^2, \quad F = x_s x_\psi + y_s y_\psi, \quad G = x_\psi^2 + y_\psi^2$$

are the metrics of the transformation. By the chain rule,

$$\frac{\partial}{\partial x} = s_x \frac{\partial}{\partial s} + \psi_x \frac{\partial}{\partial \psi}, \quad \frac{\partial}{\partial y} = s_y \frac{\partial}{\partial s} + \psi_y \frac{\partial}{\partial \psi}.$$

Applying these operators to x and y, respectively, we have

$$x_s s_x + x_\psi \psi_x = 1, \quad x_s s_y + x_\psi \psi_y = 0,$$

$$y_s s_x + y_\psi \psi_x = 0, \quad y_s s_y + y_\psi \psi_y = 1.$$

Solving for s_x, s_y, ψ_x, ψ_y gives

$$s_x = \frac{y_\psi}{J}, \quad s_y = -\frac{x_\psi}{J}, \quad \psi_x = -\frac{y_s}{J}, \quad \psi_y = \frac{x_s}{J} \tag{9-44}$$

where the Jacobian of the transformation is

$$J = \frac{\partial(x,y)}{\partial(s,\psi)} = \det \begin{pmatrix} x_s & x_\psi \\ y_s & y_\psi \end{pmatrix} = x_s y_\psi - x_\psi y_s.$$

It is easy to verify that

$$J^2 = EG - F^2. \tag{9-45}$$

If the Jacobian is non-zero and finite, then the transformation (9-42) is one-to-one and there are no singularities throughout the domain. In this case, the differential operators are transformed as

$$\frac{\partial}{\partial x} = \frac{y_\psi}{J}\frac{\partial}{\partial s} - \frac{y_s}{J}\frac{\partial}{\partial \psi}, \quad \frac{\partial}{\partial y} = -\frac{x_\psi}{J}\frac{\partial}{\partial s} + \frac{x_s}{J}\frac{\partial}{\partial \psi} \tag{9-46}$$

and

$$\begin{aligned} \frac{\partial^2}{\partial x^2} &= \frac{1}{J^2}\{y_\psi^2 \frac{\partial^2}{\partial s^2} - 2y_s y_\psi \frac{\partial^2}{\partial s \partial \psi} + y_s^2 \frac{\partial^2}{\partial \psi^2}\} \\ &\quad + \{\frac{y_\psi}{J}(\frac{y_\psi}{J})_s - \frac{y_s}{J}(\frac{y_\psi}{J})_\psi\}\frac{\partial}{\partial s} \\ &\quad + \{-\frac{y_\psi}{J}(\frac{y_s}{J})_s + \frac{y_s}{J}(\frac{y_s}{J})_\psi\}\frac{\partial}{\partial \psi}, \end{aligned} \tag{9-47a}$$

$$\begin{aligned} \frac{\partial^2}{\partial y^2} &= \frac{1}{J^2}\{x_\psi^2 \frac{\partial^2}{\partial s^2} - 2x_s x_\psi \frac{\partial^2}{\partial s \partial \psi} + x_s^2 \frac{\partial^2}{\partial \psi^2}\} \\ &\quad + \{\frac{x_\psi}{J}(\frac{x_\psi}{J})_s - \frac{x_s}{J}(\frac{x_\psi}{J})_\psi\}\frac{\partial}{\partial s} \\ &\quad + \{-\frac{x_\psi}{J}(\frac{x_s}{J})_s + \frac{x_s}{J}(\frac{x_s}{J})_\psi\}\frac{\partial}{\partial \psi}. \end{aligned} \tag{9-47b}$$

Assuming that s is the arc length along a streamline and ψ is the stream function, then the second order differential operators in (9-47) can be significantly reduced. Applying (9-47) to stream function ψ yields

$$\psi_{xx} = -\frac{y_\psi}{J}(\frac{y_s}{J})_s + \frac{y_s}{J}(\frac{y_s}{J})_\psi, \tag{9-48a}$$

$$\psi_{yy} = -\frac{x_\psi}{J}(\frac{x_s}{J})_s + \frac{x_s}{J}(\frac{x_s}{J})_\psi. \tag{9-48b}$$

It is noted that the first two terms on the right hand sides of equations (9-47a) and (9-47b) vanish because ψ is independent of s and the second derivative of ψ with respect to ψ is also zero. Only the last terms involving the first derivative of ψ with respect to ψ remain.

The inviscid incompressible irrotational flow is governed by the Laplace equation for stream function ψ

$$\nabla^2\psi = \psi_{xx} + \psi_{yy} = 0. \tag{9-49}$$

Substituting (9-48) into (9-49) gives

$$y_\psi(\frac{y_s}{J})_s - y_s(\frac{y_s}{J})_\psi + x_\psi(\frac{x_s}{J})_s - x_s(\frac{x_s}{J})_\psi = 0$$

or

$$x_s(Gy_{ss} - 2Fy_{s\psi} + Ey_{\psi\psi}) = y_s(Gx_{ss} - 2Fx_{s\psi} + Ex_{\psi\psi}) \tag{9-50}$$

where the metrics E, F and G are defined in (9-43). Equation (9-50) is a second order nonlinear partial differential equation for y and x as functions of s and ψ. In this equation, the unknown variables $y(s,\psi)$ and $x(s,\psi)$ are coupled with each other and have a symmetric or interchangeable format. So, this equation can be used to solve for y if x has been obtained, and vice versa. The type of this equation is elliptic for y as well as for x because the discriminants for both y and x are less than zero:

$$\Delta^{(y)} = 4x_s^2(F^2 - EG) = -4x_s^2J^2 < 0, \tag{9-51a}$$

$$\Delta^{(x)} = 4y_s^2(F^2 - EG) = -4y_s^2J^2 < 0. \tag{9-51b}$$

Nevertheless, one equation (9-50) is not enough to solve for two unknowns y and x. Another independent equation is needed to complete the formulation. It is known that along a streamline, $\psi = const.$ or $d\psi = 0$, hence equation (9-43) reduces to

$$dS^2 = Eds^2.$$

On the other hand, along a streamline, $S = s$, or

$$dS = ds.$$

Comparing these two equations, we get $E = 1$, or

$$x_s^2 + y_s^2 = 1. \tag{9-52}$$

This first order partial differential equation is also symmetric or interchangeable for x and y.

Equations (9-50) and (9-52) constitute a set of equations called the arc length /stream function formulation for incompressible potential flows and can be solved simultaneously for y and x under certain boundary conditions. In principle, the choice of equation to be solved for y and the other for x is completely arbitrary. However, for conventional flow problems, in which x- axis roughly represents the main flow direction, it is recommended to use (9-50) as the y equation and (9-52) as the x equation. The second order equation (9-50) can be solved by SLOR in the whole region and the first order equation (9-52) can be marched along a streamline and proceeded streamline by streamline.

9.5 Laplace-Equivalent Equation in (x, ζ) Coordinates

For the purpose of cascade design, Ye (1991) developed a 'decomposition method' to solve steady incompressible potential flows in a more general curvilinear non-orthogonal coordinate system (x, ζ). The key point of the method is that the governing Laplace equation is decomposed into two equations in (x, ζ) coordinates. One is the y equation which functions as a grid generation equation and the other

is the equation for the stream function ψ. The two equations have a common differential operator. The most attractive advantage of this method is that the choice of the ζ coordinate is more flexible. This method can also be used to solve airfoil flows as long as boundary conditions are properly specified. Next, we will briefly outline this method. Let

$$x \equiv x, \quad y = y(x, \zeta) \tag{9-53}$$

define a coordinate transformation which transforms the Cartesian coordinates (x, y) into new coordinates (x, ζ). If the Jacobian $J = \partial(x, y)/\partial(x, \zeta) \neq 0, \infty$ then the transformation is one-to-one and invertible. After this transformation, the differential operators are

$$\frac{\partial}{\partial x} = \frac{\partial}{\partial x} - \frac{y_x}{y_\zeta}\frac{\partial}{\partial \zeta}, \quad \frac{\partial}{\partial y} = \frac{1}{y_\zeta}\frac{\partial}{\partial \zeta},$$

$$\begin{aligned}\frac{\partial^2}{\partial x^2} =& \frac{1}{y_\zeta^2}\{y_\zeta^2\frac{\partial^2}{\partial x^2} - 2y_x y_\zeta \frac{\partial^2}{\partial x \partial \zeta} + y_x^2\frac{\partial^2}{\partial \zeta^2}\} \\ & -\frac{1}{y_\zeta^3}\{y_\zeta^2 y_{xx} - 2y_x y_\zeta y_{x\zeta} + y_x^2 y_{\zeta\zeta}\}\frac{\partial}{\partial \zeta},\end{aligned}$$

$$\frac{\partial^2}{\partial y^2} = \frac{1}{y_\zeta^2}\frac{\partial}{\partial \zeta^2} - \frac{1}{y_\zeta^3}y_{\zeta\zeta}\frac{\partial}{\partial \zeta}.$$

Therefore, the Laplace operator becomes

$$\begin{aligned}\nabla^2 =& \frac{\partial^2}{\partial x^2} + \frac{\partial^2}{\partial y^2} \\ =& \frac{1}{y_\zeta^2}\{y_\zeta^2\frac{\partial^2}{\partial x^2} - 2y_x y_\zeta \frac{\partial^2}{\partial x \partial \zeta} + (1 + y_x^2)\frac{\partial^2}{\partial \zeta^2}\} \\ & -\frac{1}{y_\zeta^3}\{y_\zeta^2 y_{xx} - 2y_x y_\zeta y_{x\zeta} + (1 + y_x^2) y_{\zeta\zeta}\}\frac{\partial}{\partial \zeta}.\end{aligned}$$

Defining the differential operator

$$L = y_\zeta^2\frac{\partial^2}{\partial x^2} - 2y_x y_\zeta \frac{\partial^2}{\partial x \partial \zeta} + (1 + y_x^2)\frac{\partial^2}{\partial \zeta^2}, \tag{9-54}$$

one can express the Laplace operator symbolically as

$$\nabla^2(...) = \frac{1}{y_\zeta^3}\{y_\zeta L(...) - (...)_\zeta L(y)\} \tag{9-55}$$

where (...) represents any continuously twice differentiable function. The governing equation for an incompressible potential flow is the Laplace equation for stream function ψ in Cartesian coordinates

$$\nabla^2\psi = \psi_{xx} + \psi_{yy} = 0. \tag{9-56}$$

Using Laplace operator (9-55) in equation (9-56) produces a Laplace-equivalent equation in (x, ζ) coordinates

$$y_\zeta L(\psi) - \psi_\zeta L(y) = 0. \tag{9-57}$$

Suppose a curve $\zeta(x, y) = const.$ defines a coordinate line of a curvilinear coordinate system (x, ζ) and satisfies Laplace equation $\nabla^2\zeta = 0$, then one gets

$$y_\zeta L(\zeta) - L(y) = 0. \tag{9-58}$$

Moreover, equation (9-58) can be further reduced to

$$L(y) = y_\zeta^2 y_{xx} - 2y_x y_\zeta y_{x\zeta} + (1 + y_x^2)y_{\zeta\zeta} = 0 \tag{9-59}$$

because $L(\zeta) \equiv 0$. Recalling (9-57), we must have

$$L(\psi) = y_\zeta^2\psi_{xx} - 2y_x y_\zeta \psi_{x\zeta} + (1 + y_x^2)\psi_{\zeta\zeta} = 0. \tag{9-60}$$

In this way, Laplace equation (9-56) has been decomposed into two equations (9-59) and (9-60) which constitute a set of Laplace-equivalent equations in (x, ζ) coordinates governing incompressible potential flows. The first nonlinear equation for y serves as a grid generation equation which defines the y distribution from (x, ζ) discretization. The second linear equation can be solved for ψ if y has been solved from the first equation. It should be pointed out that although there are two equations, one of which plays the role of grid generation, used in this formulation the resulting CPU time does not increase too much due to the same differential operator in the two equations.

Chapter 10. Conclusions

1. The newly developed approach based on the Euler-equivalent equations, and the full potential-equivalent equations as well, in a stream function coordinate system, is able to simulate transonic flows past two dimensional airfoils. The embedded shock waves in supercritical flows can be captured automatically in the process of iterations. The calculated results compare well with existing experimental data and other computations.

2. The Euler-equivalent equations in stream function coordinates consist of a main equation for the corresponding main variable, streamline ordinate y, and a secondary equation for the secondary variable, density ρ, and an equation for the vorticity ω. These three equations are coupled together and must be solved simultaneously or iteratively. In the full potential-equivalent equations, only two equations are used: one is for y and the other for R, the generalized density.

3. The main equation for y is a second order nonlinear partial differential equation which is solved by SLOR using type-dependent (TD) differencing plus shock point operator (SPO). The shock point operator is a crucial tool to capture the embedded shock waves.

4. The secondary equation for ρ in the Euler formulation, or for R in the full potential formulation, is a first order partial differential equation. For analysis problems, it is solved horizontally and marched vertically from far field boundaries to the airfoil. For the full potential design problem, the secondary equation for R is solved vertically and marched horizontally. In any case, the Crank-Nicolson scheme is effective in solving these equations.

5. Most existing transonic codes require grid generation which takes a significant proportion of the CPU time and the storage requirements. This time-consuming step is completely avoided in the present approach because a single set of equations plays the double role of grid generation and governing the flow.

6. For analysis problems, all boundary conditions are Dirichlet which are easy to

implement.

7. For design problems, the airfoil contour can be obtained in a non-iterative manner because the airfoil shape is a part of the solution of the main equation.

8. The method used for calculation of the density is advantageous. Traditionally, the algebraic Bernoulli equation is solved for ρ, but the classic double-density problem is very difficult to handle. This difficulty is successfully overcome by marching the first order density equation.

9. The approach can be extended to handle a variety of flows, such as axisymmetric flow, unsteady flow, viscous flow, internal flow and so on. Some other streamwise coordinate systems each of which has its own advantages, can also be applied to solve the proposed problems.

10. The approach has some limitations. First of all, a very important property of the Euler equations in Cartesian coordinates, i.e. the homogeneous property, is destroyed after the von Mises transformation so that the opportunity to apply some current Euler solver techniques seems to be lost. In addition, if the flow is supercritical, the convergence is slow. Some possible ways to overcome this difficulty may be to employ the multi-grid method, the preconditioned conjugate gradient method, the implementation of a direct solver for the system of algebraic equations, and so on.

REFERENCES

Abbott, I and von Doenhoff, A. E. Theory of Airfoil Section, Dover Publ. Inc., N. Y. pp. 113-115

Ames, W. F. 1965. Nonlinear Partial Differential Equations in Engineering, Academic Press, New York, pp. 6-7, 31-33

An, C.-F. and Barron, R. M. 1992. Numerical solution of transonic full- potential-equivalent equations in von Mises coordinates, Intl. J. Num. Methods in Fluids (in press)

Andre, P., Clermont, J. R. and Lande, M. E. 1989. Analysis of incompressible flows by the stream tube method: computation of axisymmetric converging flows and free surface flows, Numerical Method for Laminar and Turbulent Flows, Vol.6, Part II, Proc. 6th Intl. Conf. held in Swansea, UK, ed. by C. Taylor et al., Pineridge Press, pp. 1439-1448

Atkins, H. L. and Hassan, H. A. 1985. A new stream function formulation for the steady Euler equations, AIAA J., Vol. 23, No. 5, pp. 701-706

Ballhaus, W. F., Jameson, A. and Albert, J. 1978. Implicit approximate- factorization schemes for steady transonic flow problems, AIAA J., Vol. 16, No. 6, pp. 573-579

Barron, R. M. 1989. Computation of incompressible potential flow using von Mises coordinates, Mathematics and Computers in Simulation, Vol. 31, pp. 177-188

Barron, R. M. and Naeem, R. K. 1989. Numerical solution of transonic flows on a streamfunction co-ordinate system, Intl. J. Num. Methods in Fluids, Vol. 9, pp. 1183-1193

Barron, R. M, 1990. A non-iterative technique for design of aerofoils in incompressible potential flow, Comm. Appl. Num. Methods, Vol. 6, pp. 557-564

Barron, R. M., Zhang, S., Chandna, A. and Rudraiah, N. 1990. Axisymmetric potential flow calculations. part 1: analysis mode, Comm. Appl. Num. Methods,

Vol. 6, pp. 437-445

Barron, R. M. and Naeem, R. K. 1991. 2-D transonic calculations on a flow-based grid system, Mathematics and Computers in Simulation, Vol. 33, pp. 65-67

Barron, R. M. and An, C.-F. 1991. Analysis and design of transonic airfoils using streamwise coordinates, Proc. 3rd Intl. Conf. on Inve.. Design Concepts and Optimization in Eng. Sci., held in Washington, D. C., USA, ed. by G. S. Dulikravich, pp. 359-370

Beam, R. M. and Warming, R. F. 1976. An implicit finite-difference algorithm for hyperbolic systems in conservation-law form, J. Comp. Phys., Vol. 22, pp. 87-110

Breeze-Stringfellow, A. and Burggraf, O.R. 1983. Computation of propeller nacelle interference flows using streamtube co-ordinates, Proc. Appl. Mech., Bioeng. and Fluids Eng. Conf., held in Houston, USA, ed. by K. N. Ghia and U. Ghia, pp. 107-116

Chan, S. T. K., Brashears, M. R. and Young, V. Y. C. 1975. Finite element analysis of transonic flow by the method of weighted residuals, AIAA paper 75-79

Chen, K.-M., Zhang, D.-F. and Zhu, Z.-G. 1989. A universal image-plane method for direct-, inverse- and hybrid problems of compressible cascade flow on arbitrary stream sheet of revolution: part II — numerical solution, Numerical Methods in Laminar and Turbulent Flows, Vol. 6, Part II, Proc. 6th Intl. Conf. held in Swansea, UK, ed. by C. Taylor et al., Pineridge Press, pp. 1355-1365

Clermont, L. R. and Lande, M. E. 1986. A method for the simulation of plane or axisymmetric flows of incompressible fluids based on the concept of the stream function, Eng. Computations, Vol. 3, No. 4, pp. 339-347

Courant, R. and Friedrichs, K. O. 1948. Supersonic Flow and Shock Waves, Interscience Publishers, Inc., New York, pp. 116-172

Courant, R. and Hilbert, D. 1965. Methods of Mathematical Physics, Vol. II, Interscience Publishers, Inc., New York

Duda, J. L. and Vrentas, J. S. 1967. Fluid mechanics of laminar liquid jets, Chem. Eng. Sci., Vol. 22, pp. 855-869

Dulikravich, G. S. 1988. Analysis of artificial dissipation models for the transonic full-potential equation, AIAA J., Vol. 26, No. 10, pp. 1238-1245

Dulikravich, G. S. 1990. A stream-function-coordinate (SFC) concept in aerodynamic shape design, AGARD VKI Lecture Series, Brussels, Belgium

Ecer, A and Akay, H. U. 1983. A finite element formulation for steady transonic Euler equations, AIAA J., Vol. 21, No. 3, pp. 343-350

Engquist, B. and Osher, S. 1980. Stable and entropy satisfying approximations for transonic flow calculations, Math. of Comp., Vol. 34, No. 149, pp. 45-75

Greywall, M. S. 1985. Streamwise computation of 2-D incompressible potential flows, J. Comp. Phys., Vol. 59, pp. 224-231

Habashi, W. G. and Hafez, M. 1982a. Finite element solutions of transonic flow problems, AIAA J., Vol. 20, No. 10, pp. 1368-1376

Habashi, W. G. and Hafez, M. 1982b. Finite element stream function solutions for transonic turbomachinery flows, AIAA paper 82-1268

Habashi, W. G., Kotiuga, P. L. and McLean, L. A. 1985. Finite element simulation of transonic flows by modified potential and stream function methods, Engineering Analysis, Vol. 2, No. 3, pp. 150-154

Hafez, M. and Ahrad, J. 1988. Numerical simulation of rotational flows, Symposium Transsonicum III, ed. by J. Zierep and H. Oertel, Springer- Verlag, pp. 339-354

Hafez, M. and Cheng, H. K. 1977. Shock-fitting applied to relaxation solutions of transonic small-disturbance equations, AIAA J., Vol. 15, No. 6, pp. 786-793

Hafez, M., Habashi, W. G. and Kotiuga, P. L. 1985. Short communications: conservative calculations of non-isentropic transonic flows, Intl. J. Num. Methods in Fluids, Vol. 5, pp. 1047-1057

Hafez, M. and Lovell, D. 1983. Numerical solution of transonic stream function equation, AIAA J., Vol. 21, No. 3, pp. 327-335

Hafez, M. and Lovell, D. 1988. Improved relaxation schemes for transonic potential calculations, Intl. J. Num. Methods in Fluids, Vol. 8, pp. 1-6

Hafez, M., South, J. and Murman, E. M. 1979. Artificial compressibility methods for numerical solutions of transonic full potential equation, AIAA J., Vol. 17, No. 8, pp. 838-844

Hafez, M., Whitlow Jr., W. and Osher, S. 1987. Improved finite-difference schemes for transonic potential flow calculations, AIAA J., Vol. 25, No. 11, pp. 1456-1462

Hafez, M., Yam, C., Tang, K. and Dwyer, H. 1989. Calculations of rotational flows using stream function, AIAA paper 89-0474

Harten, A. 1983. A high resolution scheme for the computation of weak solutions of hyperbolic conservation laws, J. Comp. Phys., Vol. 49, pp. 357-393

Holst, T.L. and Ballhaus, W. F. 1979. Fast conservative schemes for the full potential equation applied to transonic flows, AIAA J., Vol. 17, No. 2, pp. 145-152

Huang, C.-Y. and Dulikravich, G. S. 1986. Stream function and stream function coordinate (SFC) formulation for inviscid flow field calculations, Computer Methods in Appl. Mech. and Eng., Vol. 59, pp. 155-177

Huang, C.-Y. 1987. Optimization of explicit time-stepping algorithms and stream-function-coordinate (SFC) concept for fluid dynamics problems, Ph.D. dissertation, University of Texas at Austin

Jameson, A. 1974. Iterative solution of transonic flows over airfoils and wings, including flows at Mach 1, Comm. Pure Appl. Math., Vol. 27, pp. 283-309

Jameson, A. 1976. Numerical computation of transonic flows with shock waves, Symposium Transsonicum II, ed. by K. Oswatitsch and D. Rues, Springer-Verlag, pp. 384-414

Jameson, A., Schmidt, W. and Turkel, E. 1981. Numerical solution of the Euler equations by finite volume methods using Runge-Kutta time stepping schemes, AIAA paper 81-1259

Jameson, A. and Yoon, S. 1987. Lower-upper implicit schemes with multiple grids for the Euler equations, AIAA J., Vol. 25, No. 7, pp. 929-935

Jeppson, R.W. 1970. Inverse formulation and finite difference solution for flow

from a circular orifice, J. Fluid Mech., Vol. 40, Part 1, pp. 215-223

Johnson L. W. and Riess, D. 1982. Numerical Analysis, Addison-Wesley Publishing Company, Reading, MA, USA, pp. 350-445

Jones, D. J. and Dickenson, R. G. 1980. A description of the NAE two-dimensional transonic small disturbance computer method, NAE Tech. Rept., LTR-HA-39, Ottawa, Canada

Kalman, G. 1960. Nonlinear oscillations and nonstationary flow in a zero temperature plasma, Annals of Physics, Vol. 10, No. 1, pp. 1-61

Knetchtel, E. D. 1959. Experimental investigation at transonic speeds of pressure distributions over wedge and circular-arc-airfoil sections and evaluation of perforated wall interference, NASA TN D-15

Landau, L. D. and Lifshitz, E. M. 1959. Fluid Mechanics, translated from Russian by J. B. Sykes and W. H. Reid, Pergamon Press, London, pp. 310-346

Liu, G.-L. and Tao, C. 1989. A universal image-plane method for inverse and hybrid problems of compressible cascade flow on arbitrary stream sheet of revolution: part I — theory, Numerical Methods in Laminar and Turbulent Flows, Vol.6, Part II, Proc. 6th Intl. Conf. held in Swansea, UK, ed. by C. Taylor et al., Pineridge Press, pp. 1343-1354

Liu, G.-L. and Zhang, D.-F. 1989. The moment function formulation of inverse and hybrid problems for blade-to-blade compressible viscous flow along axisymmetric stream sheet, Numerical Methods in Laminar and Turbulent Flows, Vol.6, Part II, Proc. 6th Intl. Conf. held in Swansea, UK, ed. by C. Taylor et al., Pineridge Press, pp. 1289-1300

Liu, G.-L. 1991. Research on inverse, hybrid and optimization problems in engineering sciences with emphasis on turbomachine aerodynamics: review of Chinese advances, Proc. 3rd Intl. Conf. on Inverse Design Concepts and Optimization in Eng. Sci., held in Washington, D. C., USA, ed. by G. S. Dulikravich, pp. 145-163

Martin, M. H. 1971. The flow of a viscous fluid. I, Archives for Rational Mechanics and Analysis, Vol. 41, pp. 266-286

Moretti, G. 1985. Fast Euler solver for steady one-dimensional flows, Computers and Fluids, Vol. 13, No. 1, pp. 61-81

Murman, E. M. and Cole, J. D. 1971. Calculation of plane steady transonic flows, AIAA J., Vol. 9, No. 1, pp. 114-121

Murman, E. M. 1974. Analysis of embedded shock waves calculated by relaxation methods, AIAA J., Vol. 12, No. 5, pp. 626-633

Murman, E. M. and Krupp, J. A. 1974. Solution of the transonic potential equation using a mixed finite difference system, Lecture Notes in Physics, Vol. 8, ed. by M. Holt, Springer-Verlag, pp. 199-206

Naeem, R. K. and Barron, R. M. 1989. Lifting airfoil calculations using von Mises variables, Comm. Appl. Num. Methods, Vol. 5, pp. 203-210

Naeem, R. K. and Barron, R. M. 1990. Transonic computations on a natural grid, AIAA J., Vol. 28, No. 10, pp. 1836-1838

Ni, R.-H. 1982. A multiple-grid scheme for solving the Euler equations, AIAA J., Vol. 20, No. 11, pp. 1565-1571

Ohman, L. H. 1979. Experimental data base for computer program assessment, AGARD AR-138, pp. A1-20 — A1-33

Osher, S. and Chakravarthy, S. 1983. Upwind schemes and boundary conditions with applications to Euler equations in general geometries, J. Comp. Phys., Vol. 50, pp. 447-481

Osher, S., Hafez, M. and Whitlow Jr., W. 1985. Entropy condition satisfying approximations for the full potential equation of transonic flow, Math. of Comp., Vol. 44, No. 169, pp. 1-29

Owen, D. R. and Pearson, C. E. 1988. Numerical solution of a class of steady-state Euler equations by a modified streamline method, AIAA paper 88-0625

Pai, S.-I. 1956. Viscous Flow Theory I: Laminar Flow, D. Van Nostrand Company, Inc., Princeton, NJ, USA, pp. 152-154

Pearson, C. E. 1981. Use of streamline coordinates in the numerical solution of compressible flow problems, J. Comp, Phys., Vol. 42, pp. 257-265

Pulliam, T. H. and Chaussee, D. S. 1981. A digital form of an implicit approximate-factorization algorithm, J. Comp. Phys., Vol. 39, pp. 347-363

Pulliam, T. H. 1987. The Euler equations in computational fluid dynamics, AIAA Professional Study Seminar, Euler Solvers Workshop, Monterey, CA, USA

Roache, P. J. 1976. Computational Fluid Dynamics, Hermosa Publishers, Chinese translation by X.-C. Zhong and X.-Z. Liu, Science Press, Beijing, China, 1983, pp. 240-243

Shapiro, A. H. 1953. The Dynamics and Thermodynamics of Compressible Fluid Flow, Vol. I, The Ronald Press Company, New York, pp. 112-158, 529-592

Sherif, A. and Hafez, M. 1988. Computation of three-dimensional transonic flows using two stream functions, Intl. J. Num. Methods in Fluids, Vol. 8, pp. 17-29

Srinivasan, K. and Spalding, D. B. 1986. The stream function coordinate system for solution of one-dimensional unsteady compressible flow problems, Appl. Math. Modelling, Vol. 10, pp. 278-283

Steger, J. L. and Lomax, H. 1972. Transonic flow past two-dimensional airfoils by relaxation procedures, AIAA J., Vol. 10, No. 1, pp. 49-54

Steger, J. L. 1978. Implicit finite-difference simulation of flow about arbitrary two-dimensional geometries, AIAA J., Vol. 16, No. 7, pp. 679-686

Steger, J. L. and Warming, R. F. 1981. Flux vector splitting of the inviscid gasdynamic equations with application of finite-difference methods, J. Comp. Phys., Vol. 40, pp. 263-293

Takahashi, K. 1982. A numerical analysis of flow using streamline coordinates (The case of two-dimensional steady incompressible flow), Bulletin of the JSME, Vol. 25, No. 209, pp. 1696-1702

Takahashi, K. and Tsukiji, T. 1985. Numerical analysis of a laminar jet using a streamline coordinate system, Transactions of the CSME, Vol. 9, No. 3, pp. 165-170

Thibert, J. J., Grandjacques, M. 1979. Experimental data base for computer program assessment, AGARD AR-138, pp. A1-1 — A1-19

Tsukiji, T. and Takahashi, K. 1989. Numerical analysis of an axisymmetric jet using a streamline coordinate system, JSME Intl. J., Vol. 30, No. 267, pp. 1406-1413

Viviand, H. 1985. Test Cases for Inviscid Flow Field Methods, AGARD-AR-211, pp. 6-1 — 6-68

von Mises, R. 1927. Bemerkungen zur Hydrodynamik, ZAMM, Vol. 7, p. 425

Wang, B.-G. 1985. New iterative algorithm between stream function and density for transonic cascade flow, AIAA paper 85-1594

Wu, C.-H. 1952. A general theory of 3-D flow in subsonic and supersonic turbomachines of axial-, radial- and mixed-flow types, NACA TN 2604

Yang, T. and Nelson, C. D. 1979. Griffith diffusers, J. Fluids Eng., Vol. 101, pp. 473-477

Ye, H. 1991. The computation of fluid flow in a curvilinear non-orthogonal coordinate system, M.Sc. thesis at the University of Windsor, Windsor, Ontario, Canada

Fig. 4-1a Physical Plane

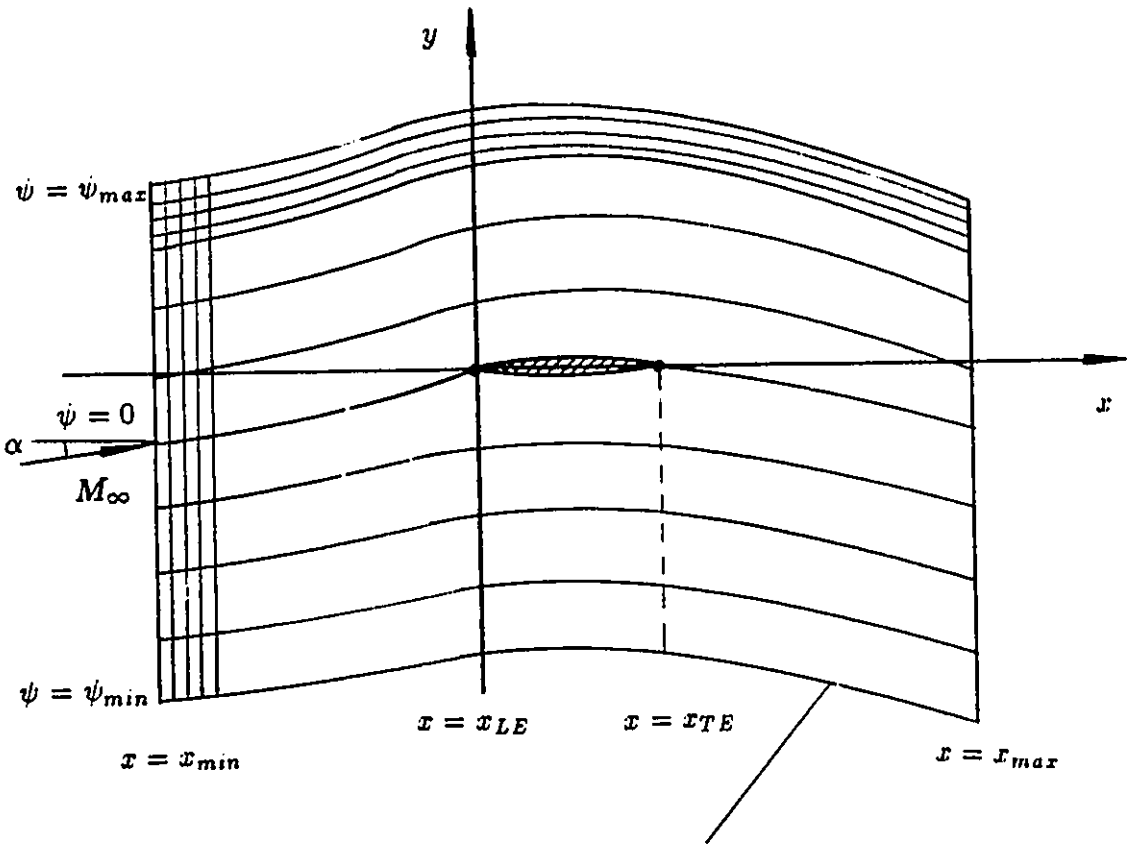

$$\psi(x,y) = y\cos\alpha - x\sin\alpha + \frac{\Gamma}{2\pi} ln\{x^2 + (1 - M_\infty^2)y^2\}$$

Fig. 4-1b Computational Plane

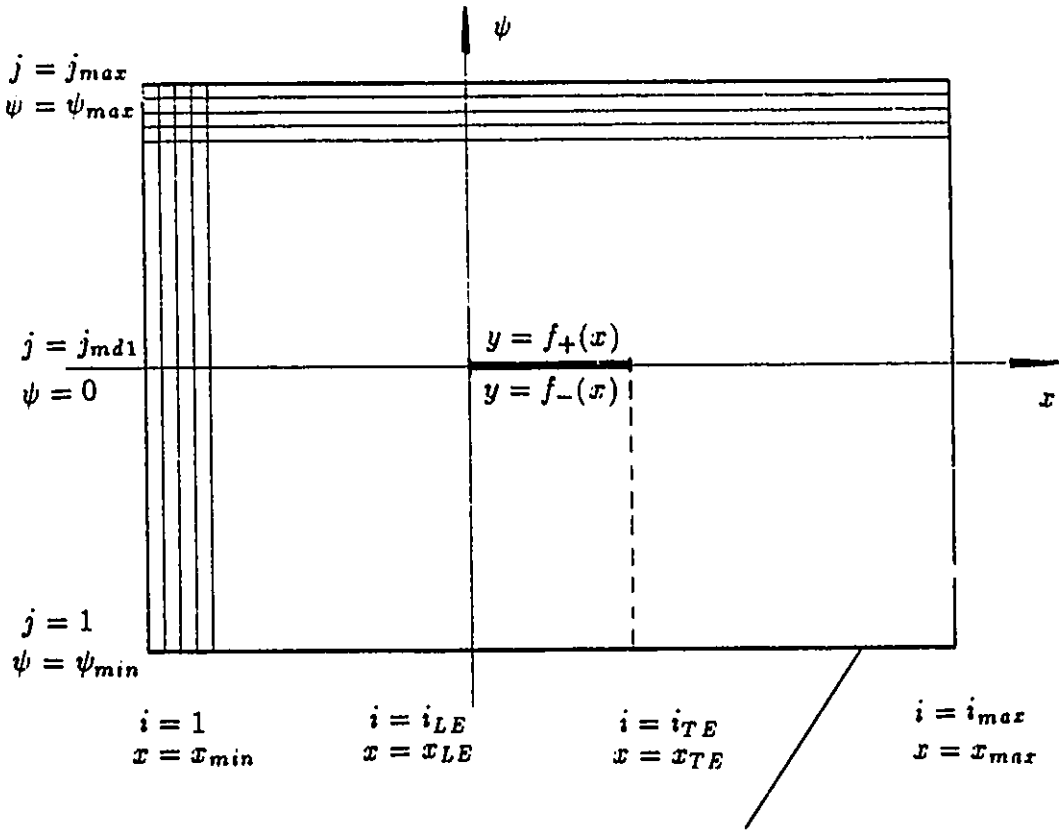

$$y(x,\psi) = \frac{\psi}{cos\alpha} + xtan\alpha - \frac{\Gamma}{2\pi cos\alpha} ln\{x^2 + (1 - M_\infty^2)[y(x,\psi)]^2\}$$

Fig. 4-2a y Equation Sweeping

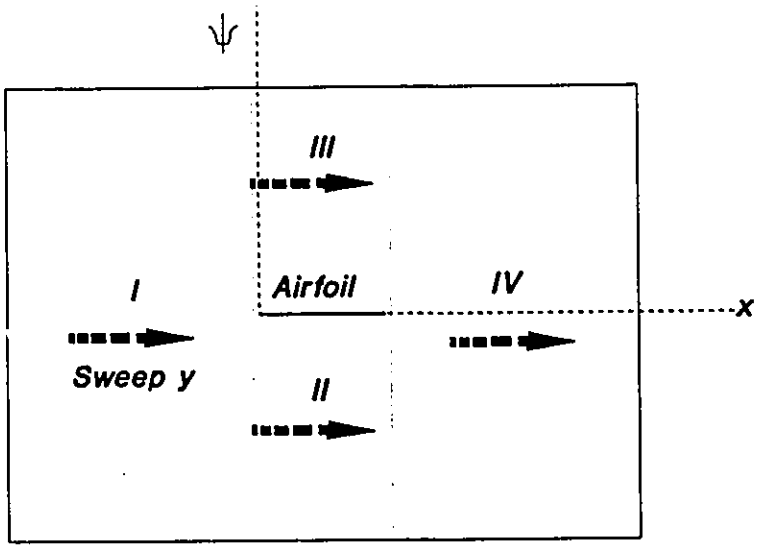

$$(y_\psi^2 - Z_1)y_{xx} - 2y_x y_\psi y_{x\psi} + (1 + y_x^2)y_{\psi\psi} = Z_2$$

Fig. 4-2b Density Equation Marching

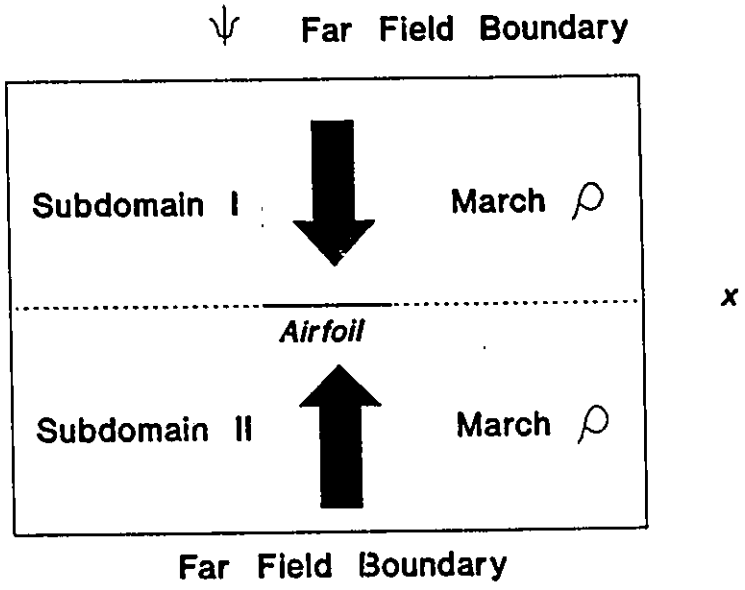

$$y_x y_\psi^2 \rho_x - y_\psi (1 + y_x^2)\rho_\psi = (Z_1 y_{xx} + Z_3)\rho$$

Fig. 4-3 Computational Flow Chart

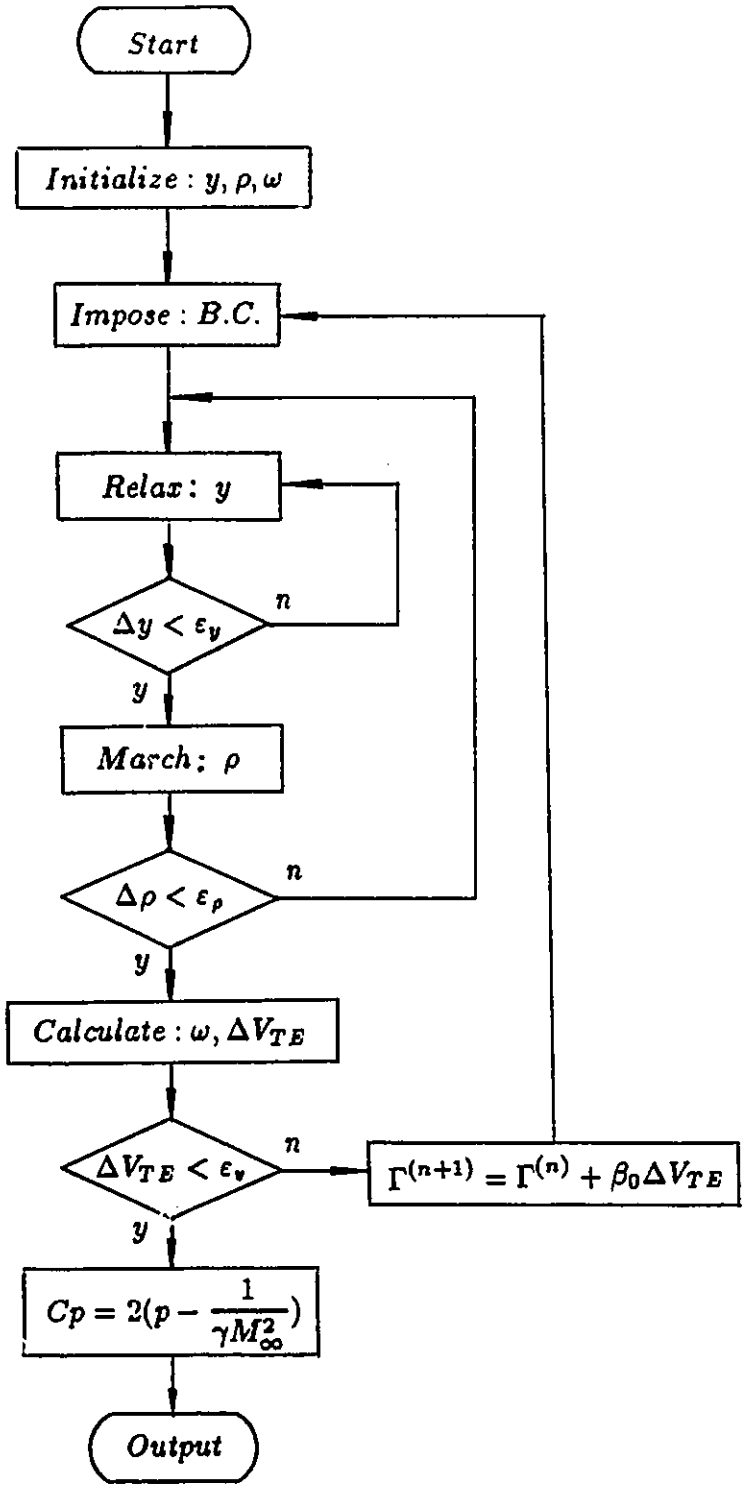

Fig. 5-1 Shock Jump Condition

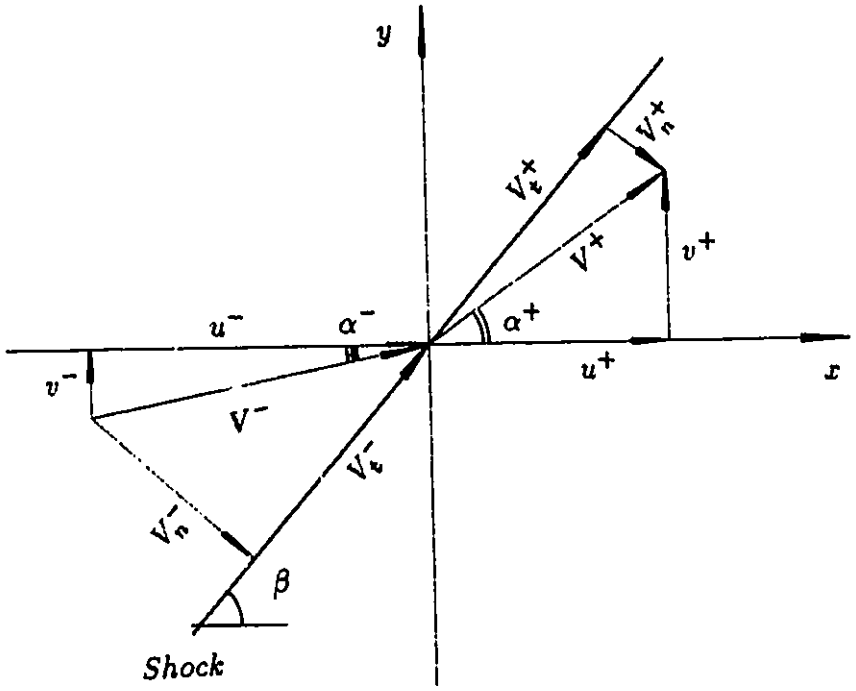

$$u^- = V^- cos\alpha^- \qquad u^+ = V^+ cos\alpha^+$$

$$v^- = V^- sin\alpha^- \qquad v^+ = V^+ sin\alpha^+$$

$$V_n^- = V^- sin(\beta - \alpha^-) \qquad V_n^+ = V^+ sin(\beta - \alpha^+)$$

$$V_t^- = V^- cos(\beta - \alpha^-) \qquad V_t^+ = V^+ cos(\beta - \alpha^+)$$

Fig. 5-2 Shock Point Operator

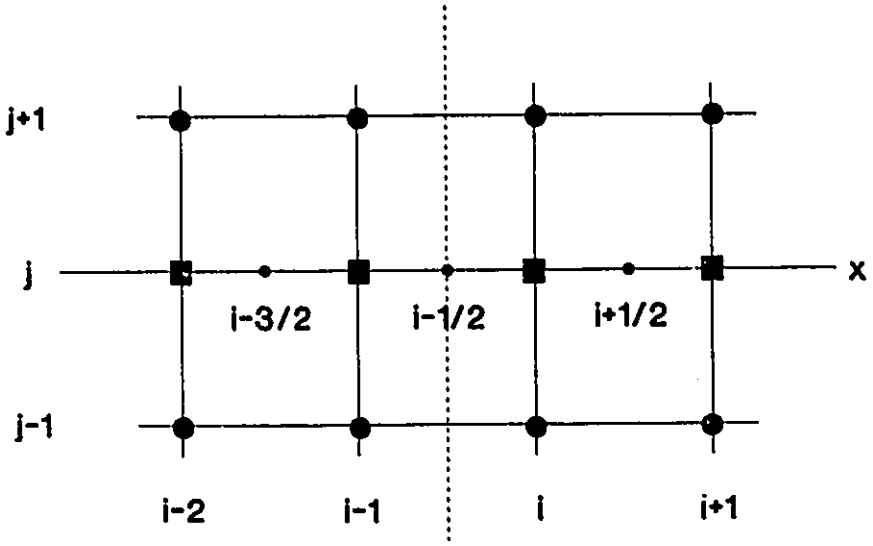

$$(y_{xx})_{i,j} = \frac{1}{\Delta x^2}(y_{i+1,j} - y_{i,j} - \mu_j y_{i-1,j} + \mu_j y_{i-2,j})$$

$$(y_{x\psi})_{i,j} = \frac{1}{4\Delta x \Delta \psi}(y_{i+1,j+1} - y_{i+1,j-1} + y_{i,j+1} - y_{i,j-1} - 3y_{i-1,j+1} + 3y_{i-1,j-1} + y_{i-2,j+1} - y_{i-2,j-1})$$

Fig. 7-1 Cp Comparison (1)

NACA 0012, α =0

M=0.703

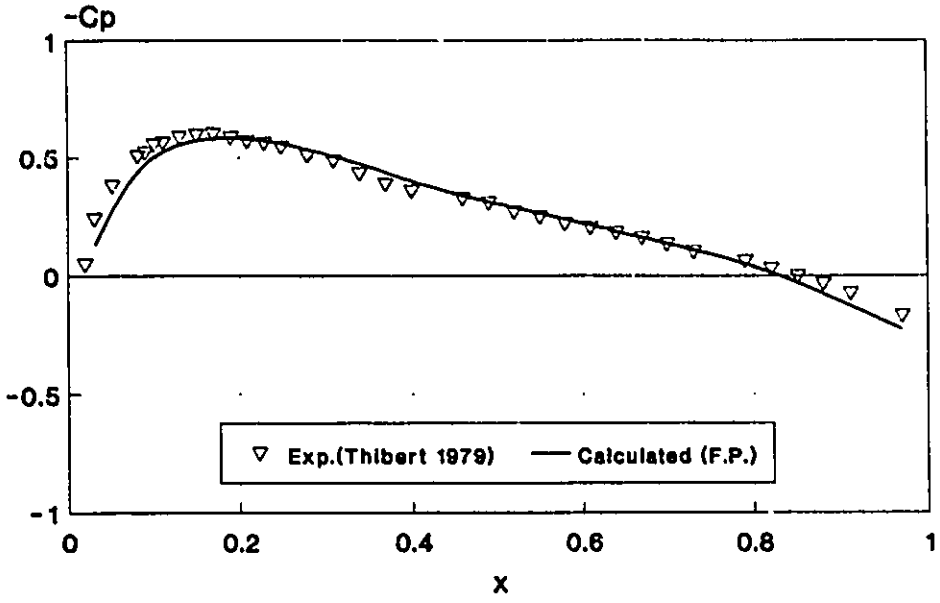

Fig. 7-2 Cp Comparison (2)

NACA 0012, α =0
M=0.803

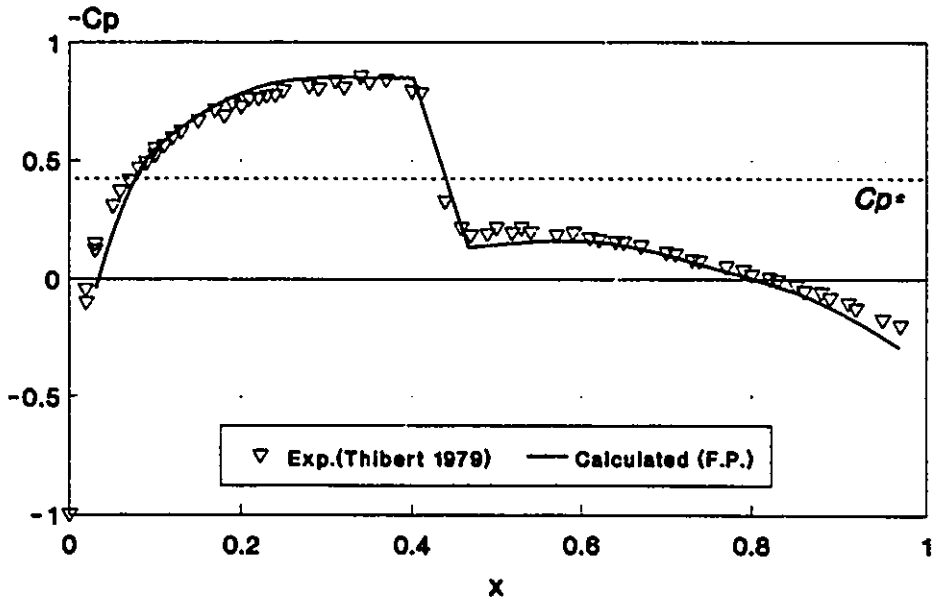

FIG. 7-3 Cp Comparison (3)
NACA 0012, α=0
M=0.835

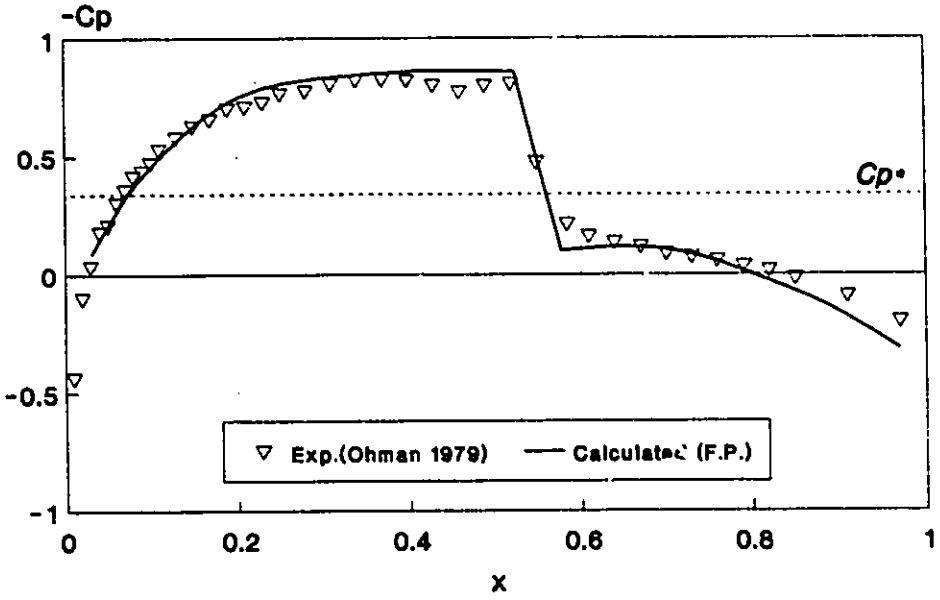

FIG. 7-4 Different Set of Variables (1)
NACA 0012, M=0.490, α=0

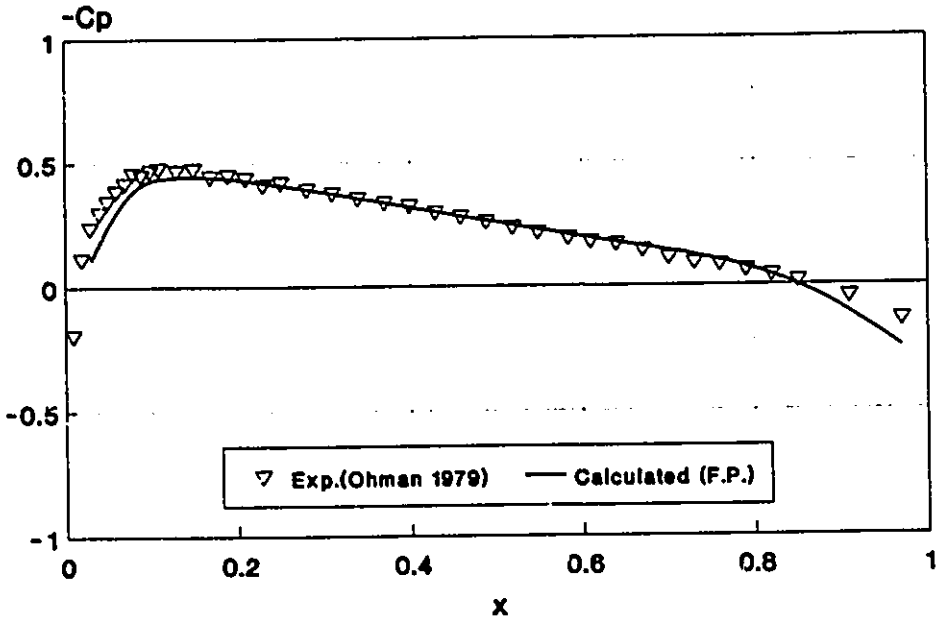

(y-R) Set :

$$(y_\psi^2 - \frac{M_\infty^2}{R})y_{xx} - 2y_x y_\psi y_{x\psi} + (1+y_x^2)y_{\psi\psi} = 0 \qquad (3\text{-}24)$$

$$y_x y_\psi^2 R_x - y_\psi(1+y_x^2)R_\psi = (\gamma+1)M_\infty^2 y_{xx} \qquad (3\text{-}25)$$

Fig. 7-5 Different Set of Variables (2)
NACA 0012, M=0.502, α=0

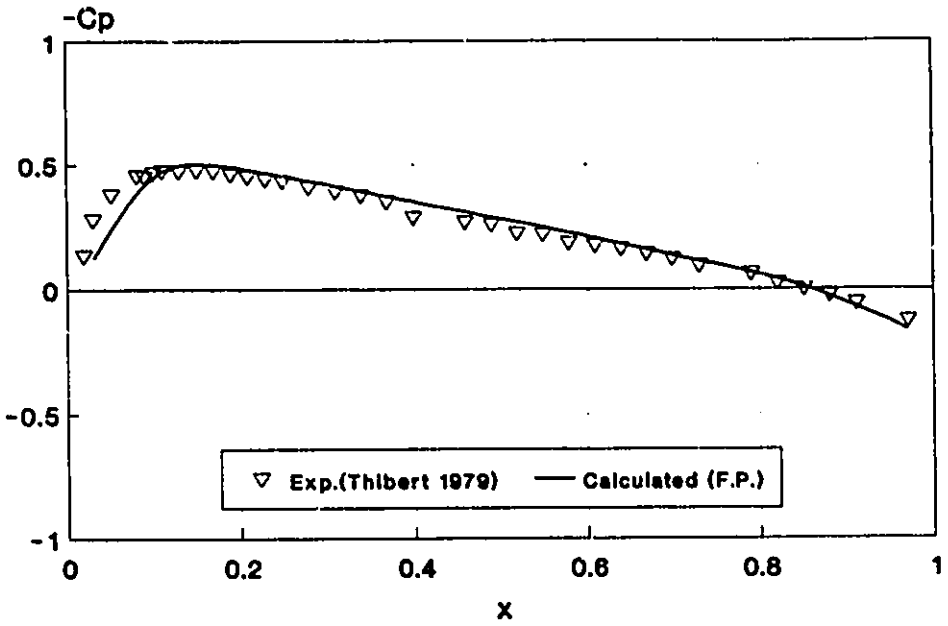

1st order ODE for R :

$$R_x = \frac{\gamma+1}{2} M_\infty^2 [\frac{1+y_x^2}{y_\psi^2}]_x / \{\frac{M_\infty^2}{R}\frac{1+y_x^2}{y_\psi^2} - 1\} \qquad (3\text{-}31a)$$

FIG. 7-6 Different Set of Variables (3)
NACA 0012, M=0.490, α=0

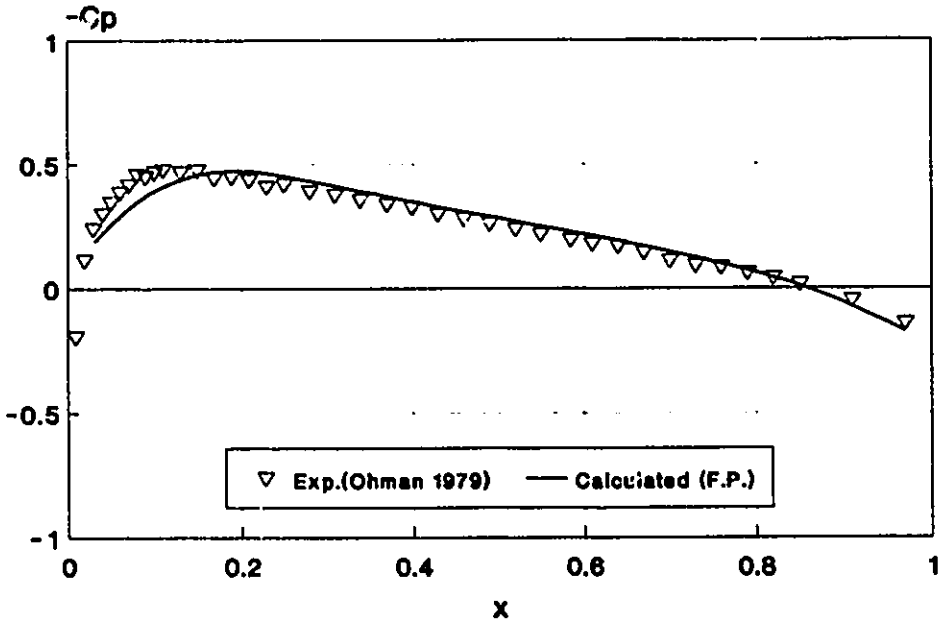

2nd order PDE for R :

$$(y_\psi^2 - \frac{M_\infty^2}{R})R_{xx} - 2y_x y_\psi R_{x\psi} + (1 + y_x^2)R_{\psi\psi} = G \qquad (3\text{-}34)$$

FIG. 7-7 Different Set of Variables (4)
NACA 0012, M=0.693, α=0

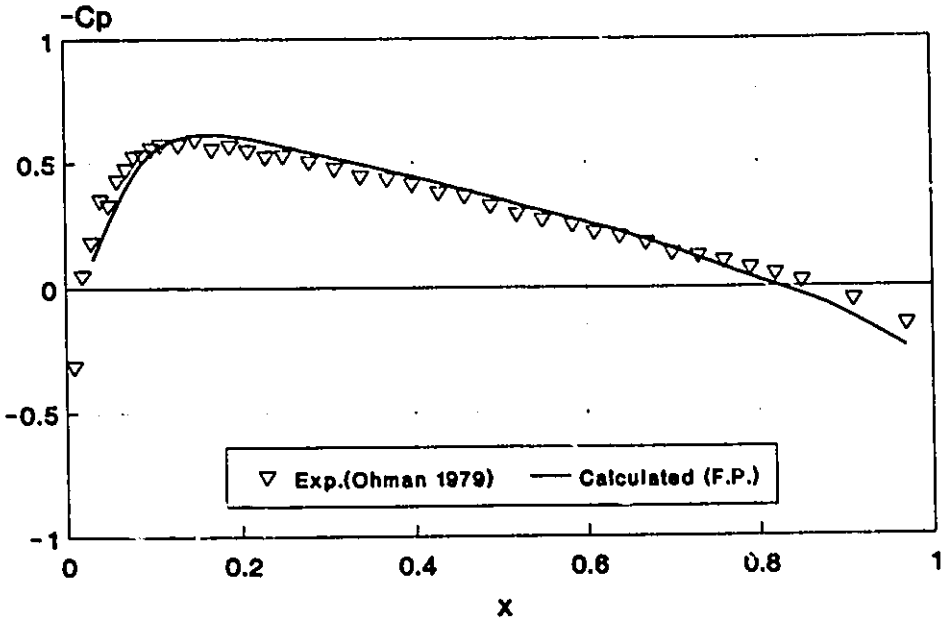

($y\text{-}M^2$) Set :

$$(y_\psi^2 - M^2\frac{y_\psi^2}{1+y_x^2})y_{xx} - 2y_x y_\psi y_{x\psi} + (1+y_x^2)y_{\psi\psi} = 0 \qquad (3\text{-}35)$$

$$(M^2)_x = \frac{M^2(1+\frac{\gamma-1}{2}M^2)}{1-M^2}\{ln[\frac{1+y_x^2}{y_\psi^2}]\}_x \qquad (3\text{-}36a)$$

FIG. 7-8 Different Set of Variables (5)
NACA 0012, M=0.696, α =0

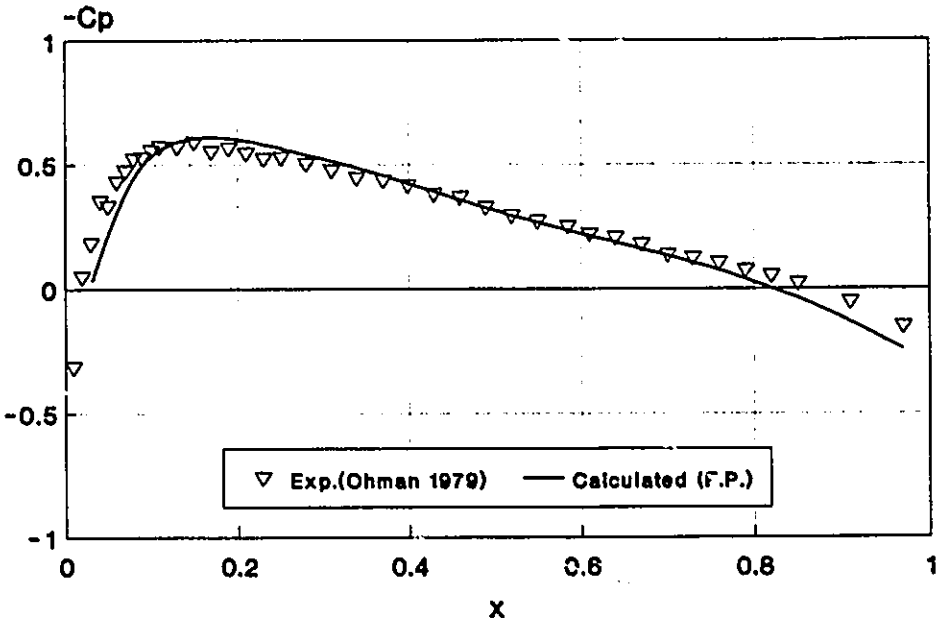

(y-u-ρ) Set :

$$(y_\psi^2 - \frac{M_\infty^2}{\rho^{\gamma+1}})y_{xx} - 2y_x y_\psi y_{x\psi} + (1+y_x^2)y_{\psi\psi} = 0 \qquad (3\text{-}44)$$

$$(y_x y_\psi u)_x - [(1+y_x^2)u]_\psi = 0 \qquad (3\text{-}45)$$

$$\rho = \{1 + \frac{\gamma-1}{2}M_\infty^2[1-(1+y_x^2)u^2]\}^{\frac{1}{\gamma-1}} \qquad (3\text{-}46)$$

Fig. 7-9 Convergence History (1)
NACA 0012, Full Potential

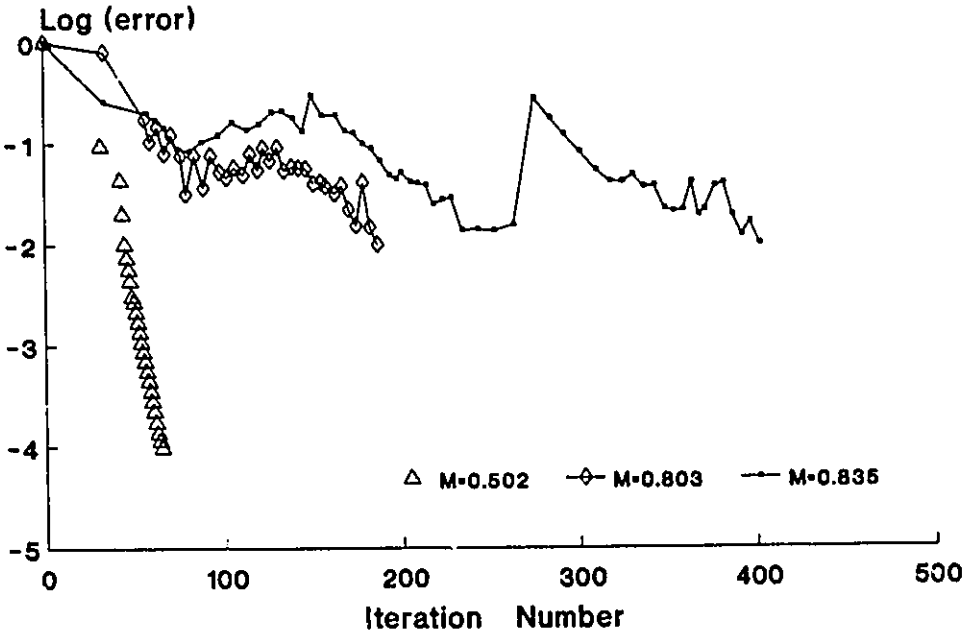

FIG. 7-10 Designed Biconvex(6%) Airfoil
M = 0.909, α =0
65x33 grid

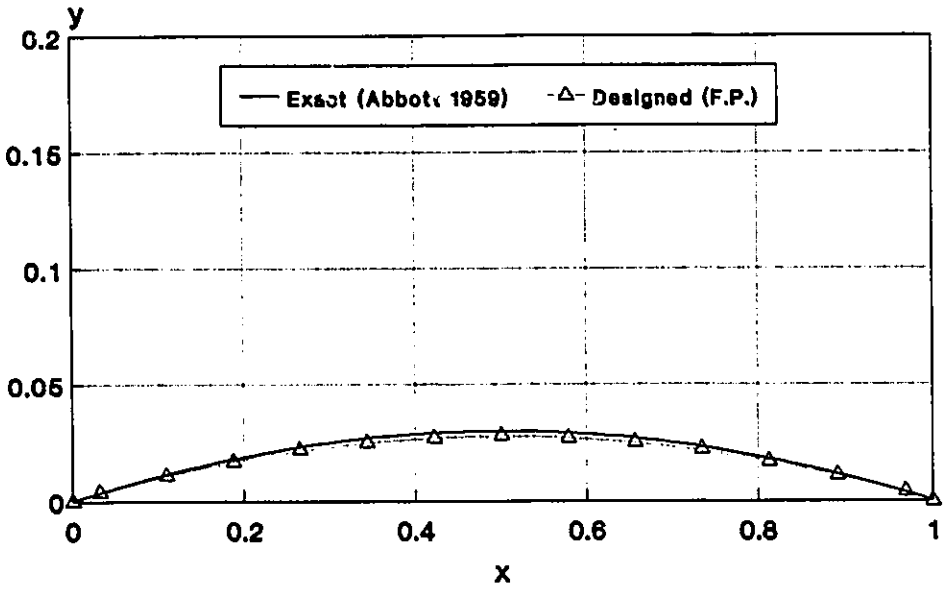

FIG.7-11 Designed NACA 0012 Airfoil (1)
M = 0.490, α =0
65x33 grid

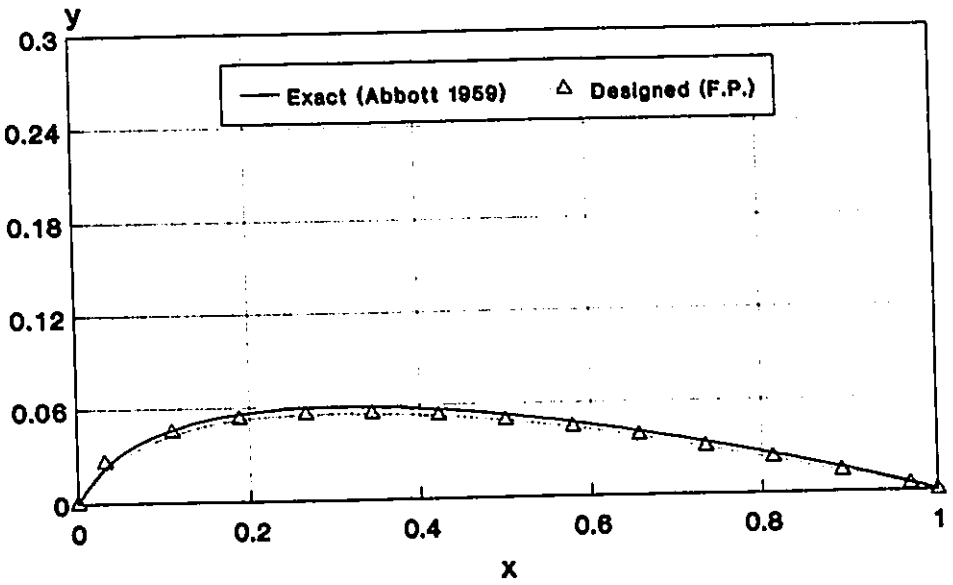

FIG.7-12 Designed NACA 0012 Airfoil (2)
M = 0.803, α =0
81x31 grid

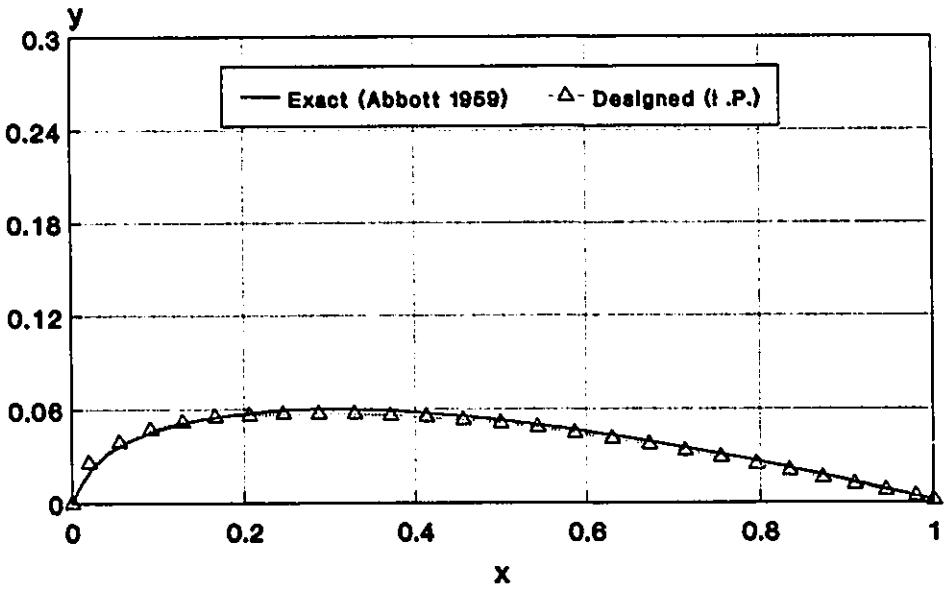

FIG. 8-1 Cp Comparison (1)
NACA 0012, α =0
M=0.490

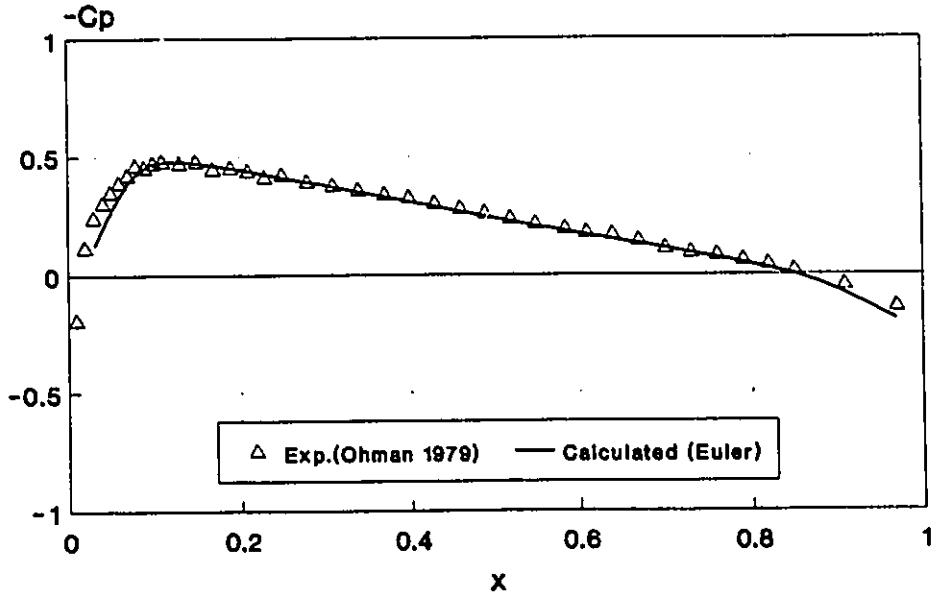

FIG. 8-2 Cp Comparison (2)
NACA 0012, α=0
M=0.696

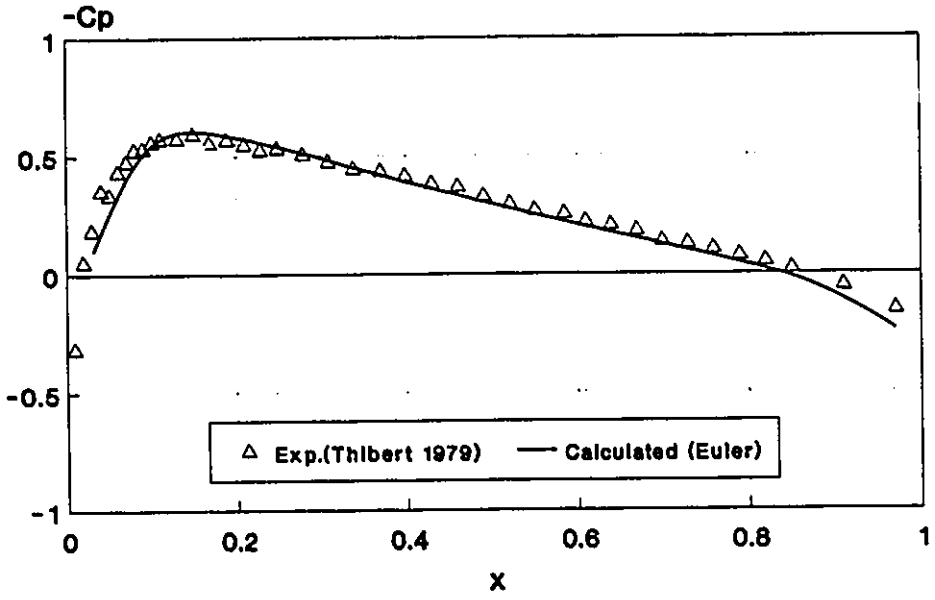

Fig. 8-3 Cp Comparison (3)
NACA 0012, α =0
M=0.756

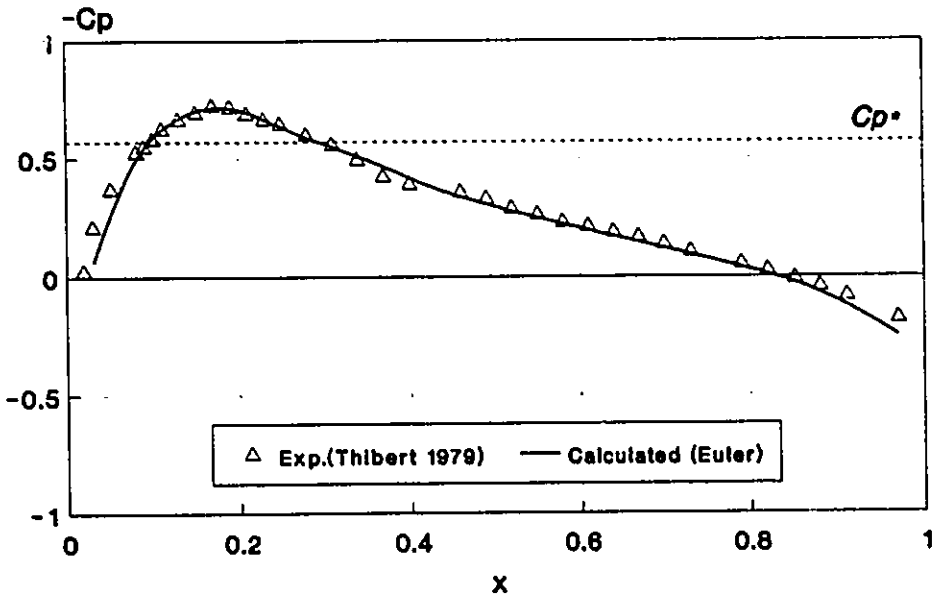

Fig. 8-4 Cp Comparison (4)
NACA 0012, α =0
M = 0.803

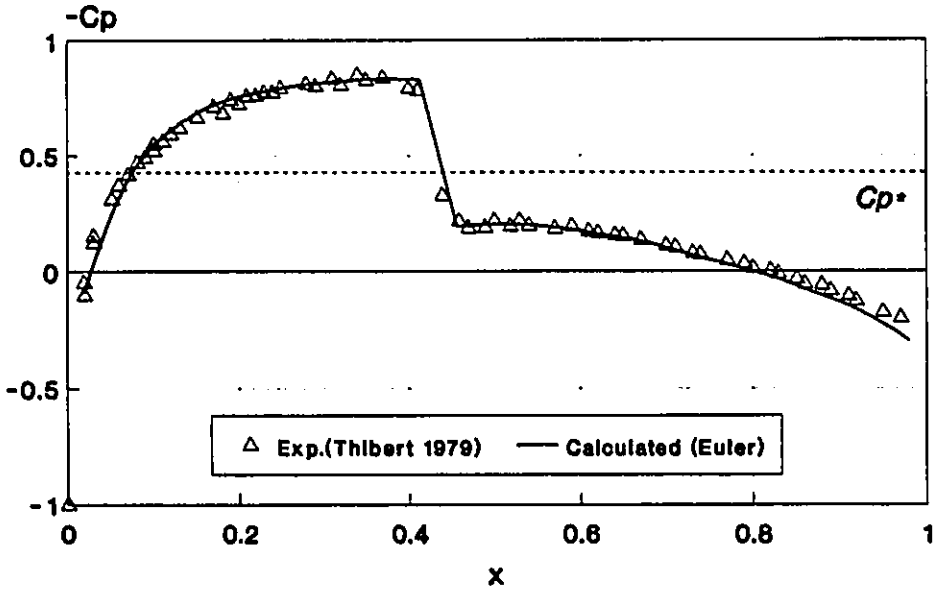

Fig. 8-5 Cp Comparison (5)

NACA 0012, α =0

M=0.814

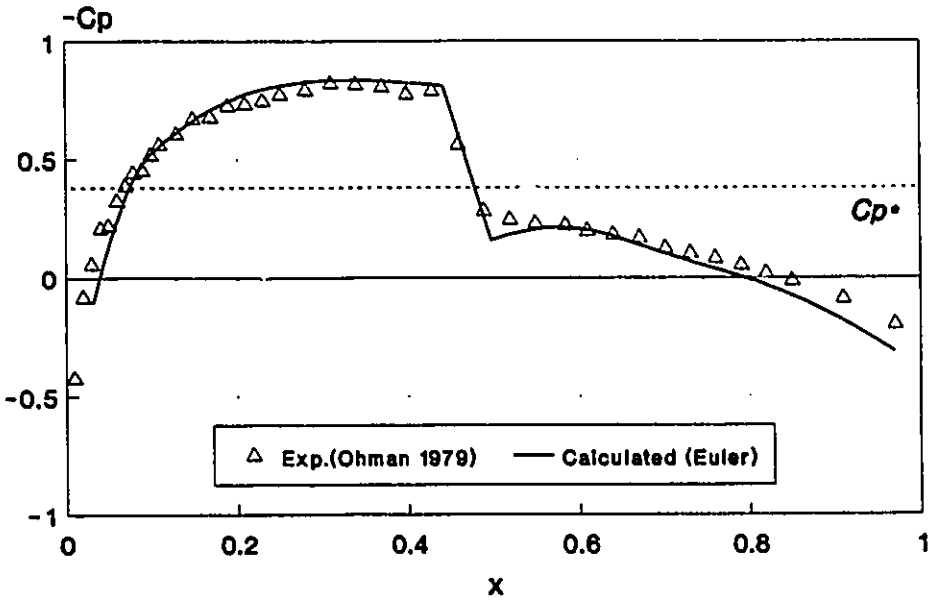

Fig. 8-6 Cp Comparison (6)
NACA 0012, α=1.25°
M=0.800

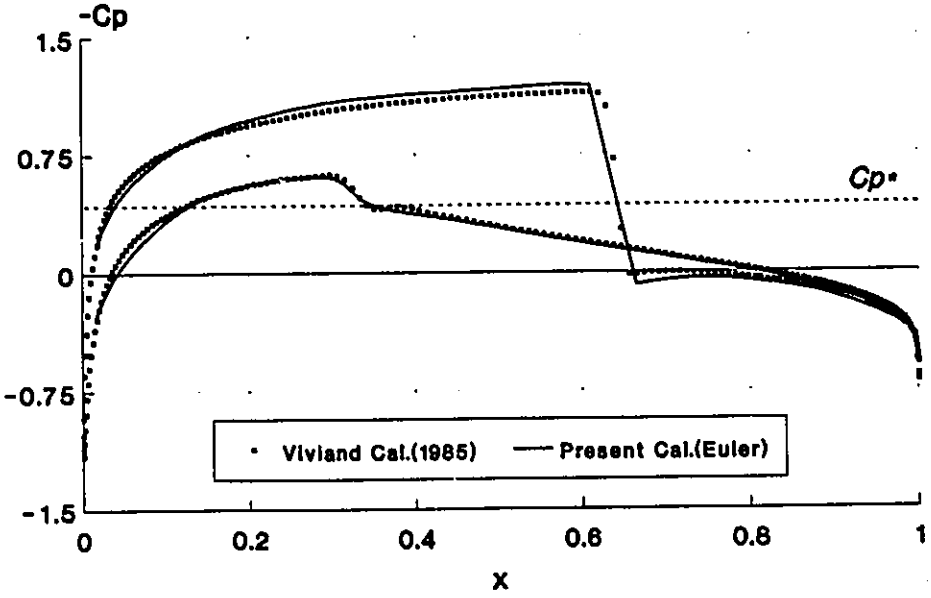

FIG. 8-7 Cp Comparison (7)
Biconvex (6%) Airfoil
M=0.840, α =0

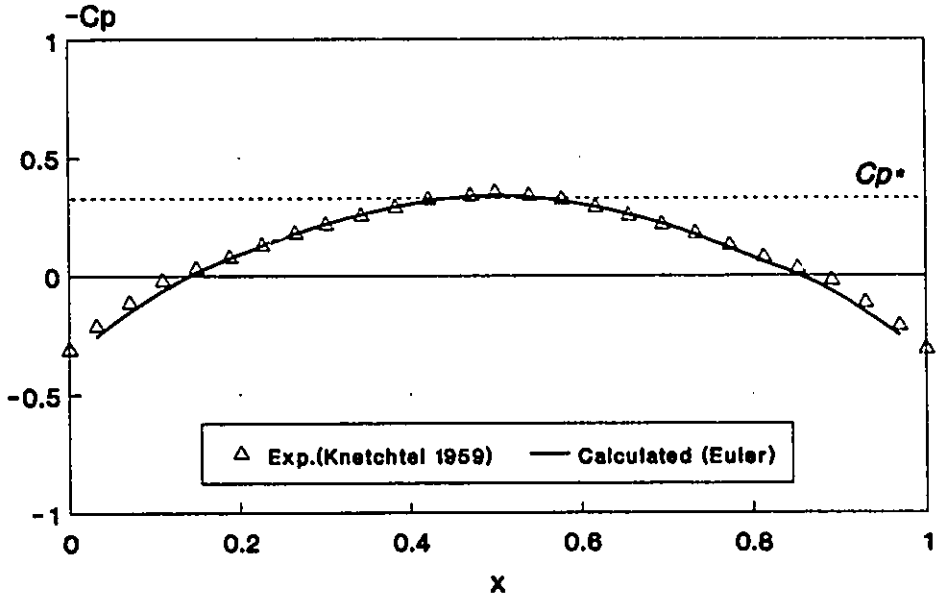

FIG. 8-8 Cp Comparison (8)
Biconvex (6%) Airfoil
M=0.909, α=0

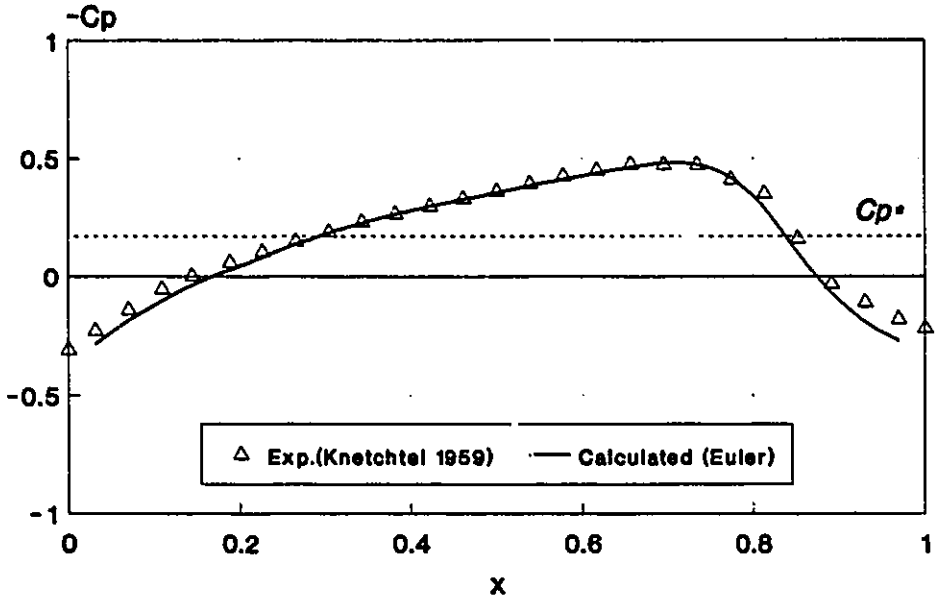

Fig. 8-9 Cp Comparison (9)
NACA 0012, M=0.5
α =0

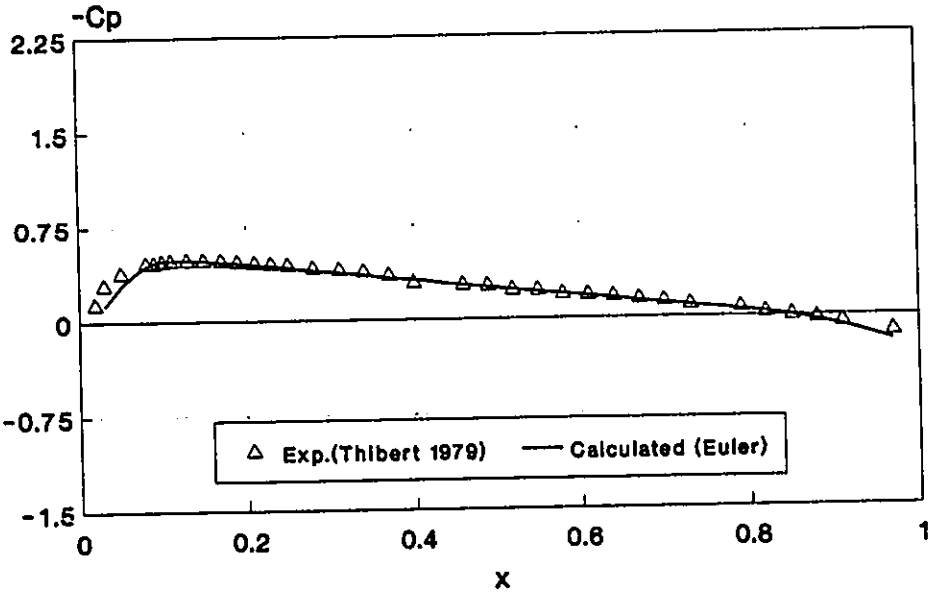

Fig. 8-10 Cp Comparison (10)

NACA 0012, M=0.502

α =2.06 °

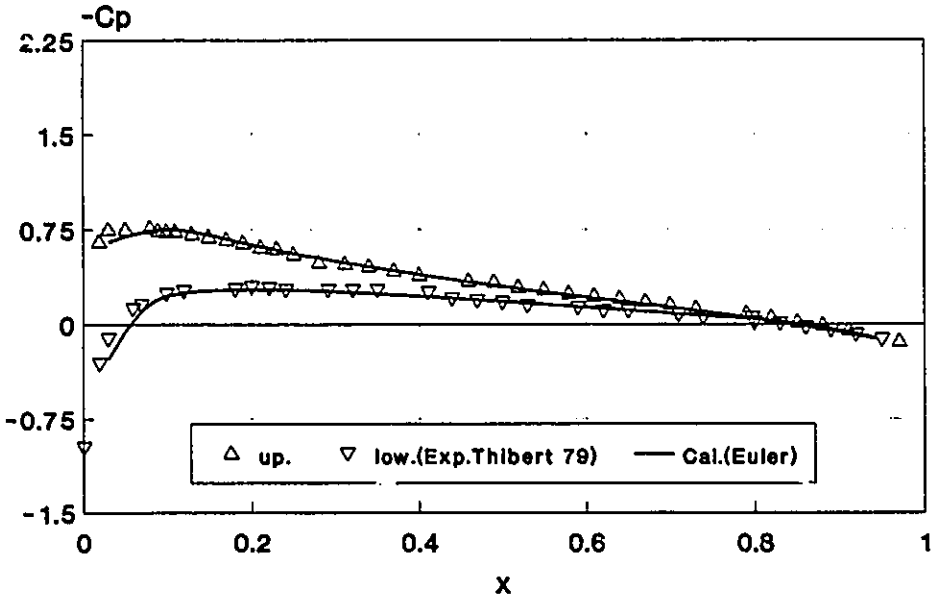

Fig. 8-11 Cp Comparison (11)
NACA 0012, M=0.504
α =4.06°

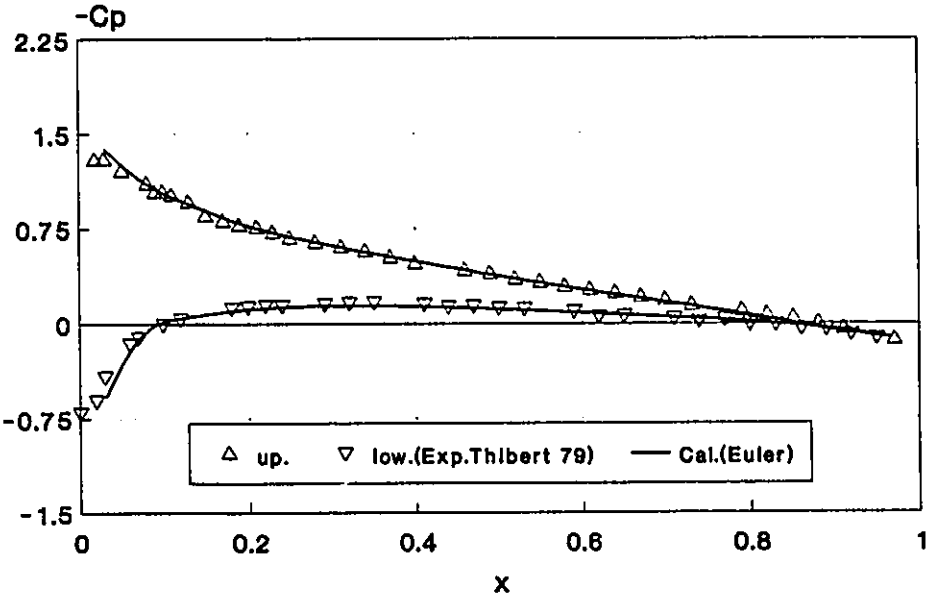

Fig. 8-12 Cp Comparison (12)
NACA 0012, M=0.503
α=6.05°

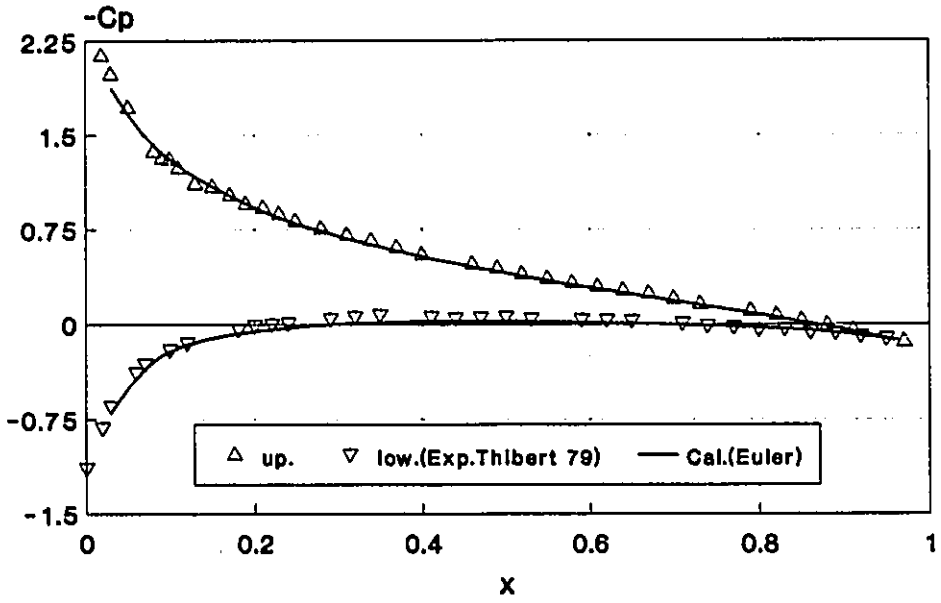

Fig. 8-13a Effect of TD and SPO (a)
NACA 0012, M=0.803, α=0
neither TD, nor SPO

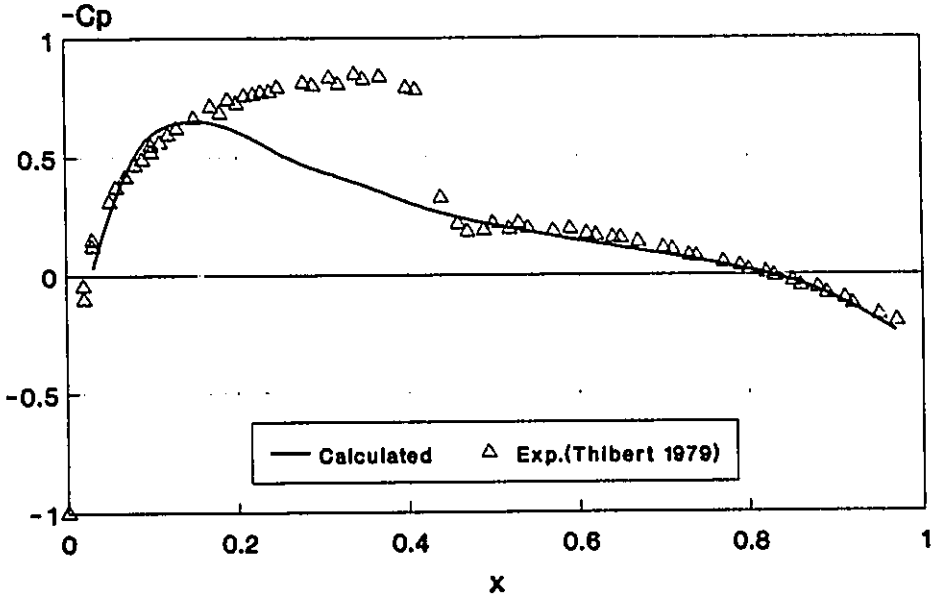

Fig. 8-13b Effect of TD and SPO (b)
NACA 0012, M=0.803, α =0
only TD, no SPO

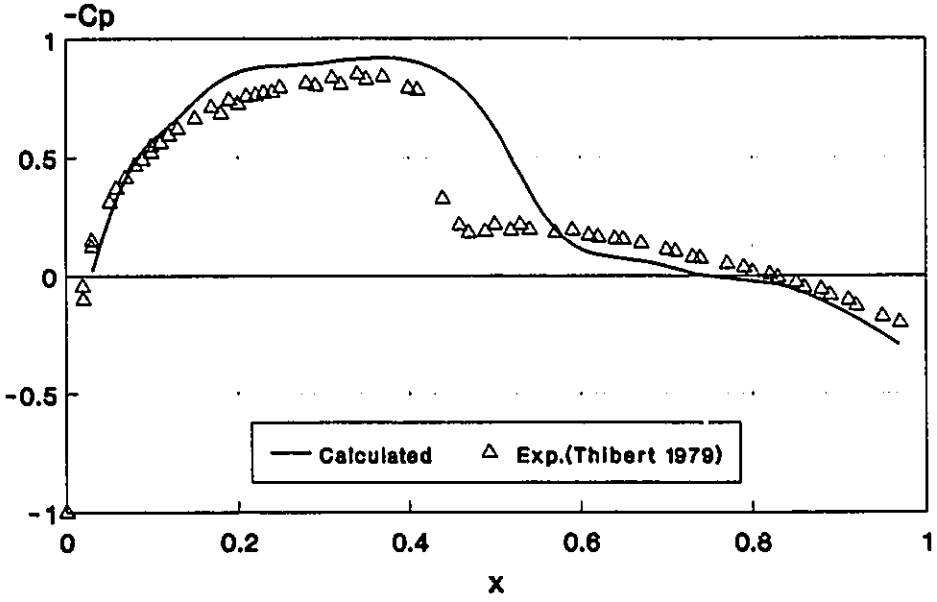

Fig. 8-13c Effect Of TD and SPO (c)

NACA 0012, M=0.803, α=0

TD + relevant SPO

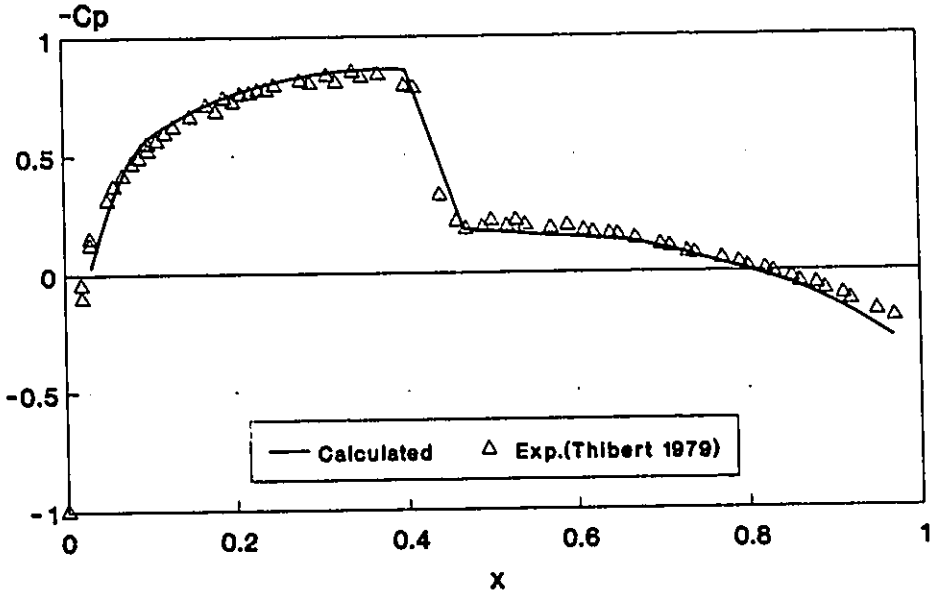

Fig. 8-13d Effect of TD and SPO (d)
NACA 0012, M=0.803, α =0
TD + too much SPO

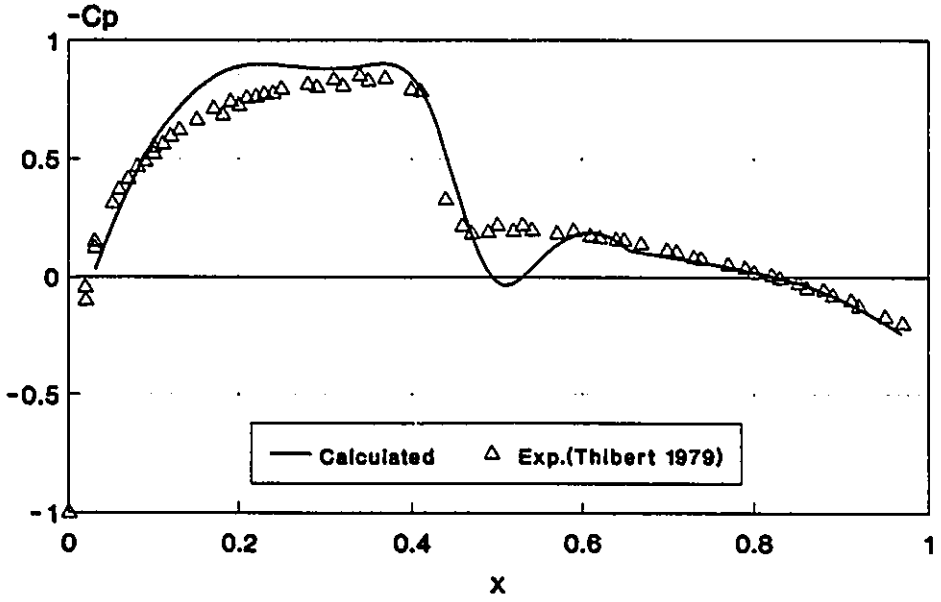

Fig. 8-14a Evolution of Iterations (a)
NACA 0012, M=0.803, α =0
N = 31

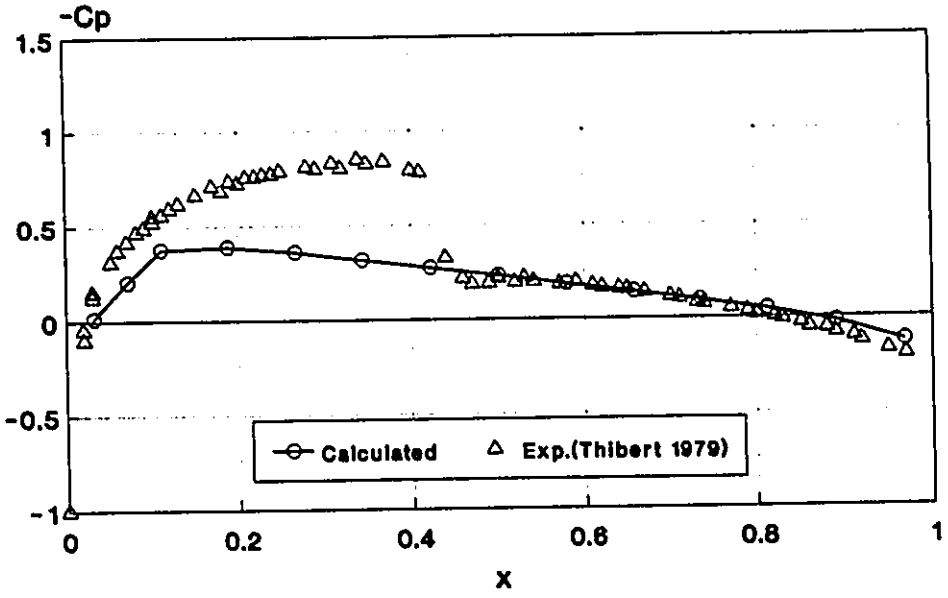

Fig. 8-14b Evolution of Iterations (b)
NACA 0012, M=0.803, α=0
N = 67

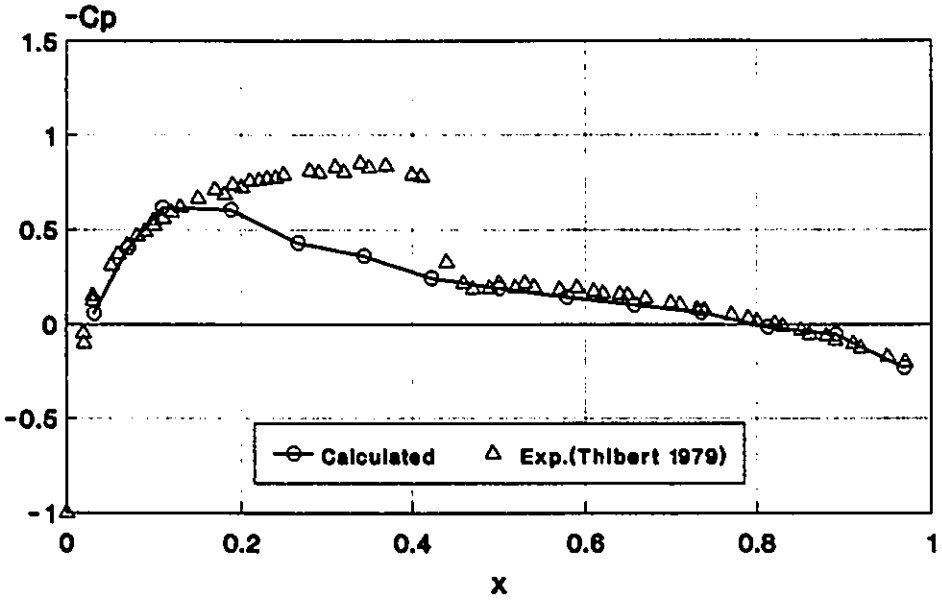

Fig. 8-14c Evolution of Iterations (c)
NACA 0012, M=0.803, α=0
N = 103

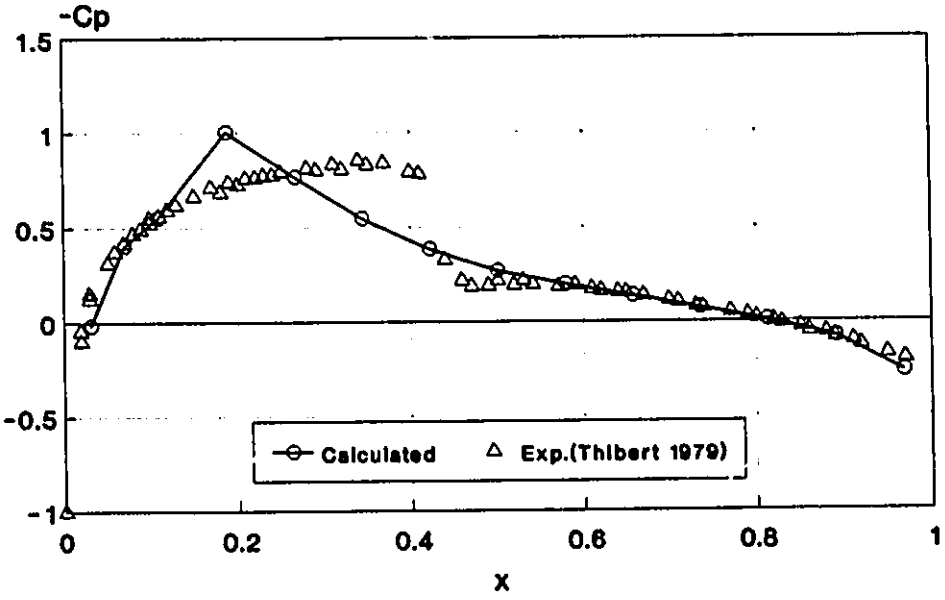

Fig. 8-14d Evolution of Iteration (d)
NACA 0012, M=0.803, α=0
N = 165

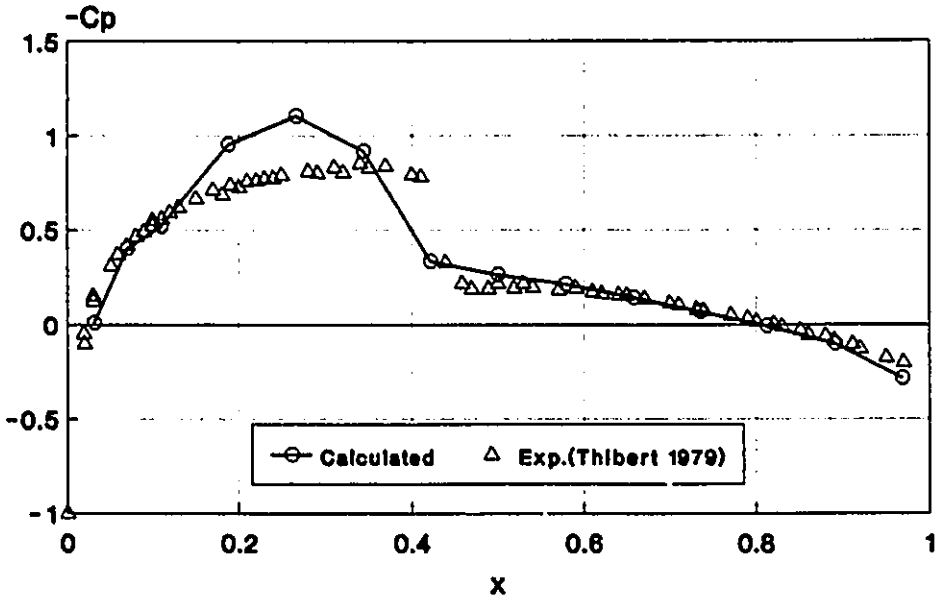

Fig. 8-14e Evolution of Iterations (e)
NACA 0012, M=0.803, α=0
N = 251

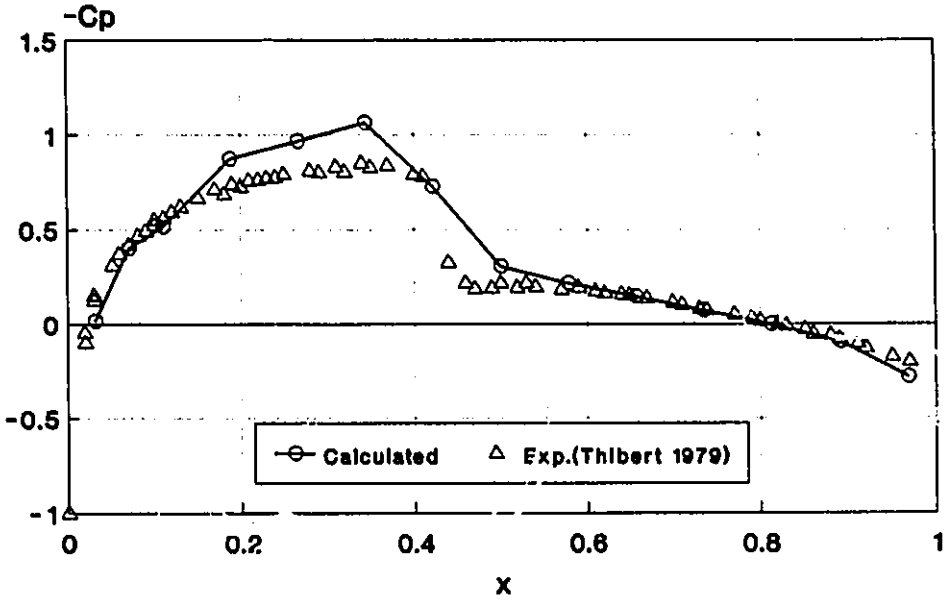

Fig. 8-14f Evolution of Iterations (f)

NACA 0012, M=0.803, α=0

N = 380

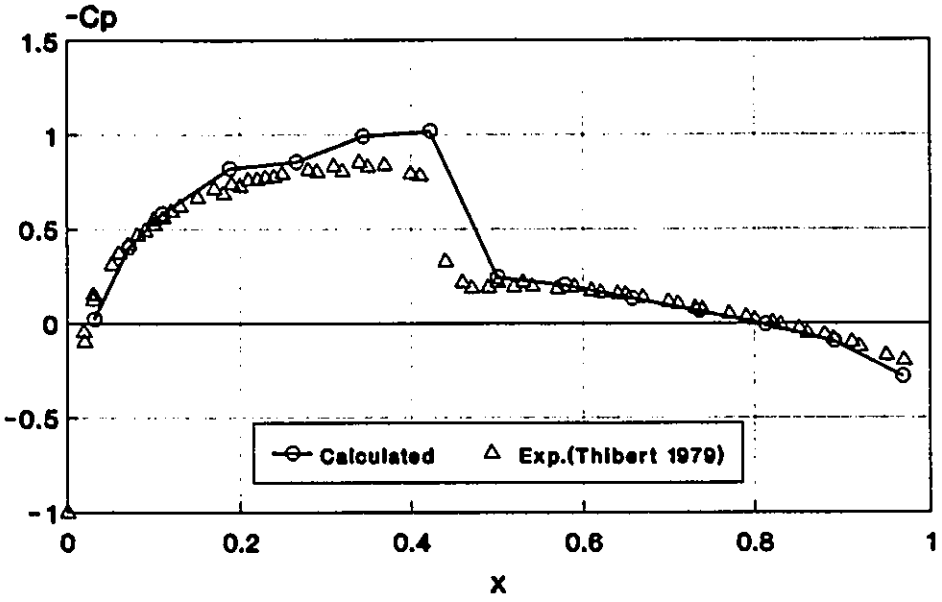

Fig. 8-14g Evolution of Iteration (g)
NACA 0012, M=0.803, α =0
N = 449

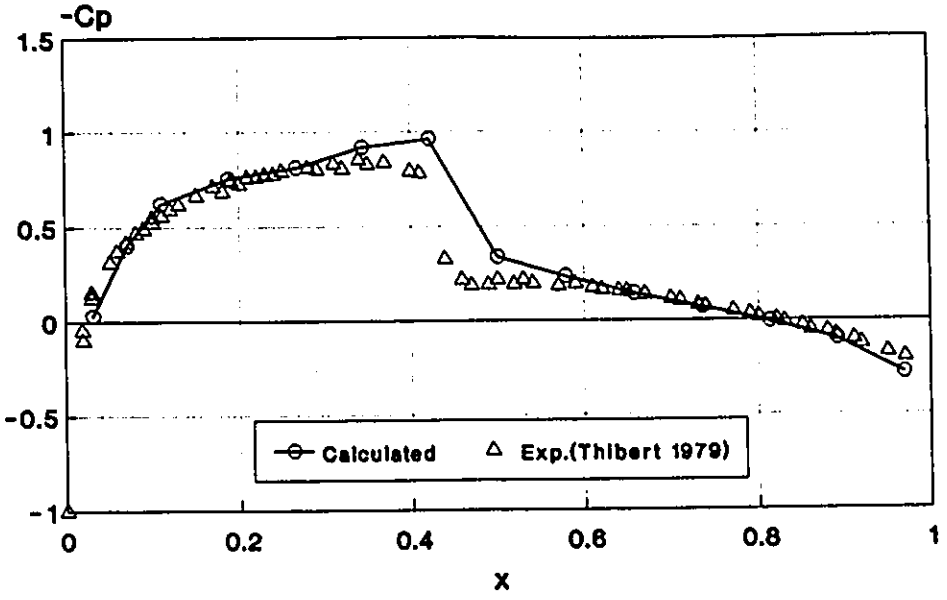

Fig. 8-14h Evolution of Iterations (h)
NACA 0012, M=0.803, α =0
N = 528

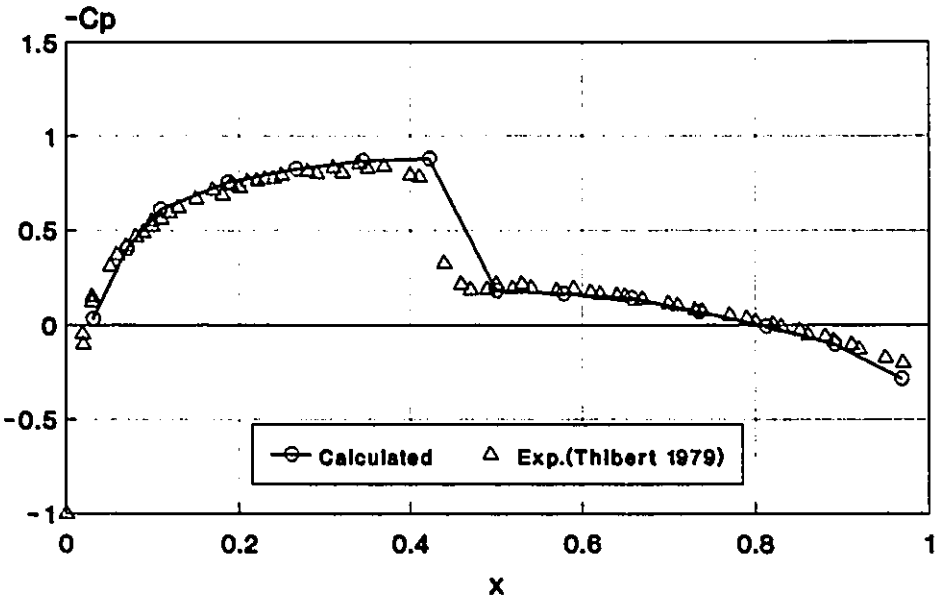

Fig. 8-15 Convergence History (2)
NACA 0012, Euler

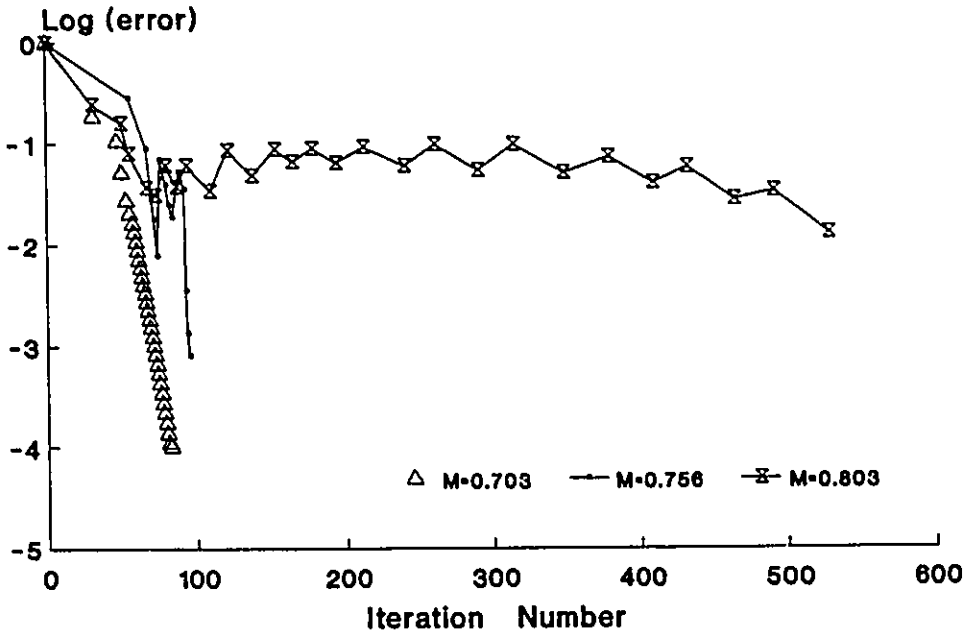

Fig. 8-16a Effect of Stretching (1)

NACA 0012, M=0.703, α =0

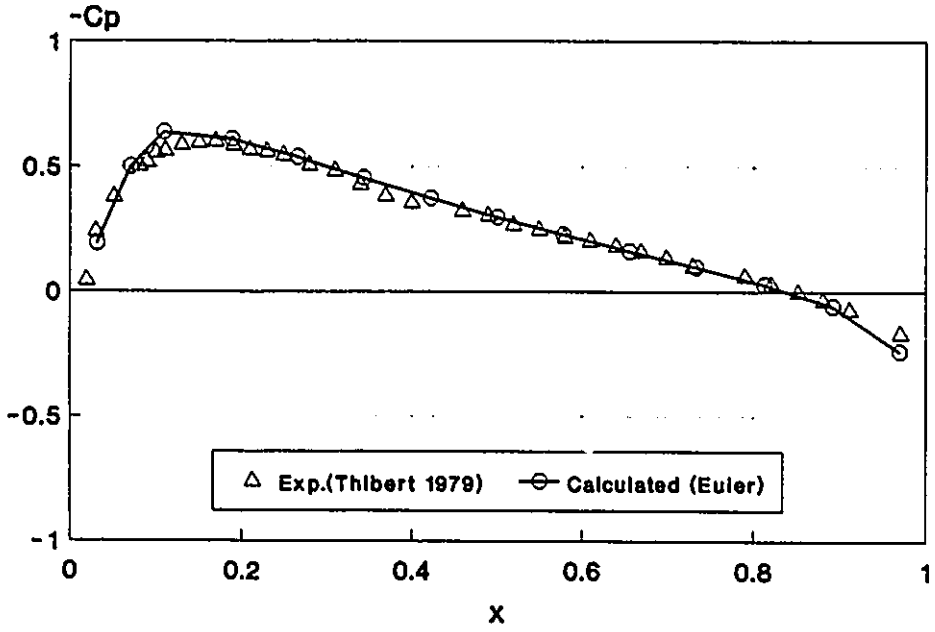

Unstretched Coordinates

Fig. 8-16b Effect of Stretching (2)
NACA 0012, M=0.703, α =0

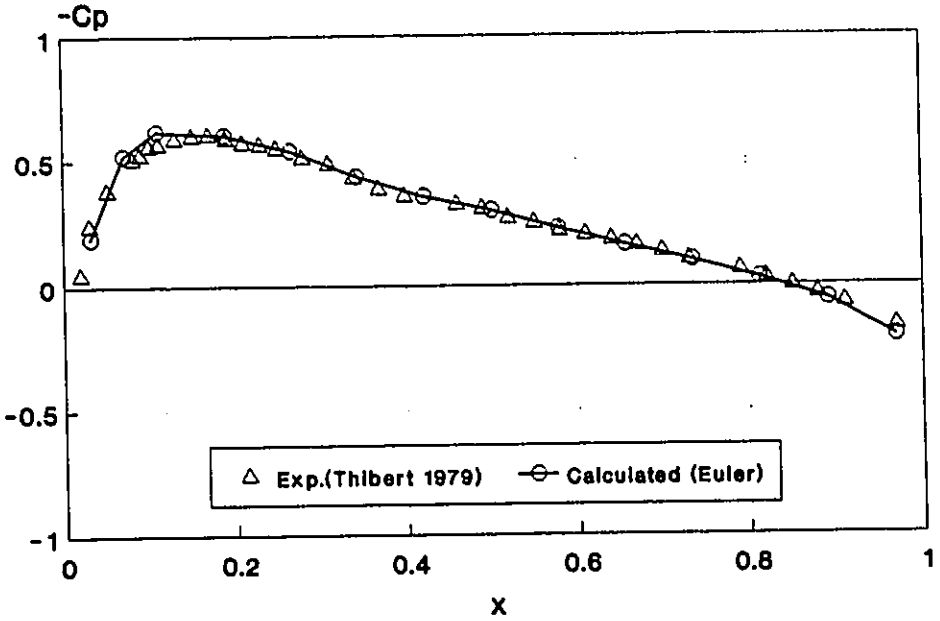

Stretched Coordinates

Fig. 8-17a Effect of Stretching (3)
NACA 0012, M=0.803, α =0

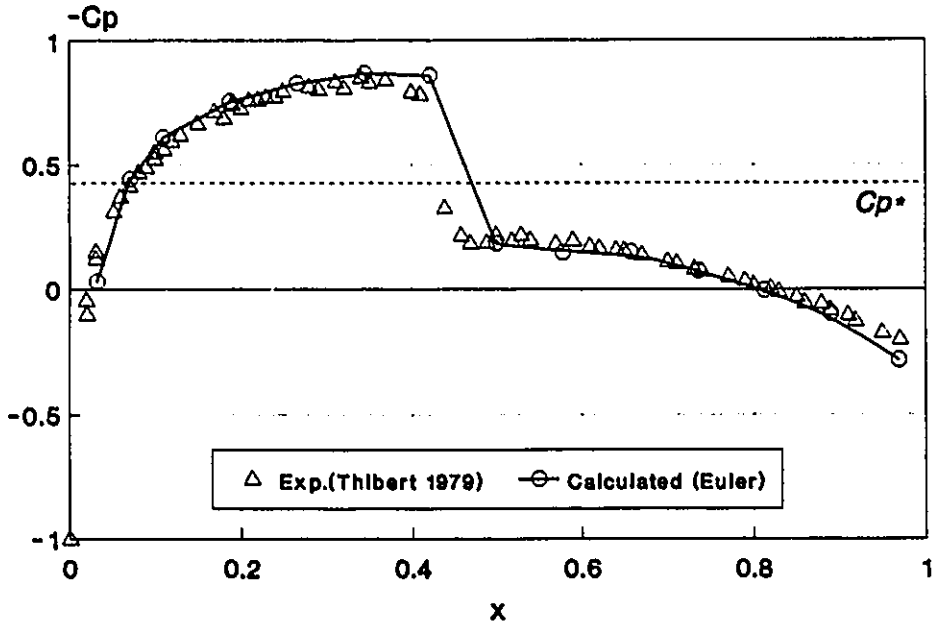

Unstretched Coordinates

Fig. 8-17b Effect of Stretching (4)
NACA 0012, M=0.803, α =0

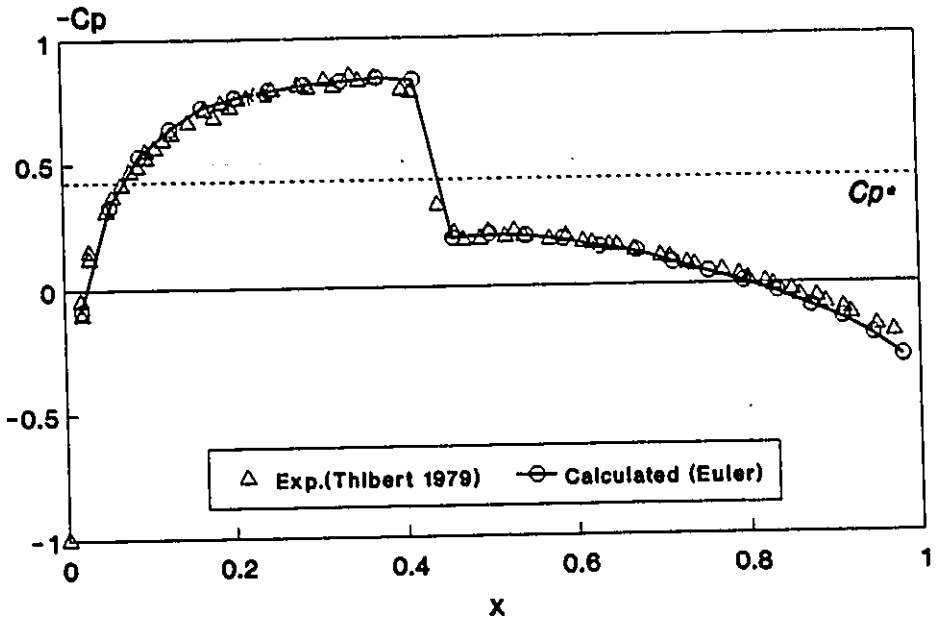

Stretched Coordinates

Fig. 9-1 Multi-Value Problem

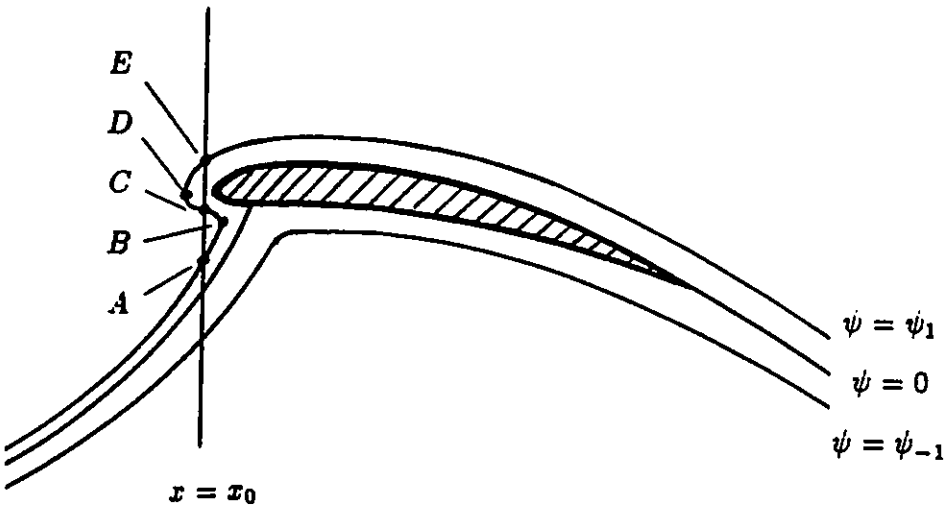

Fig. 9-2 Curvilinear Coordinates (s,ψ)

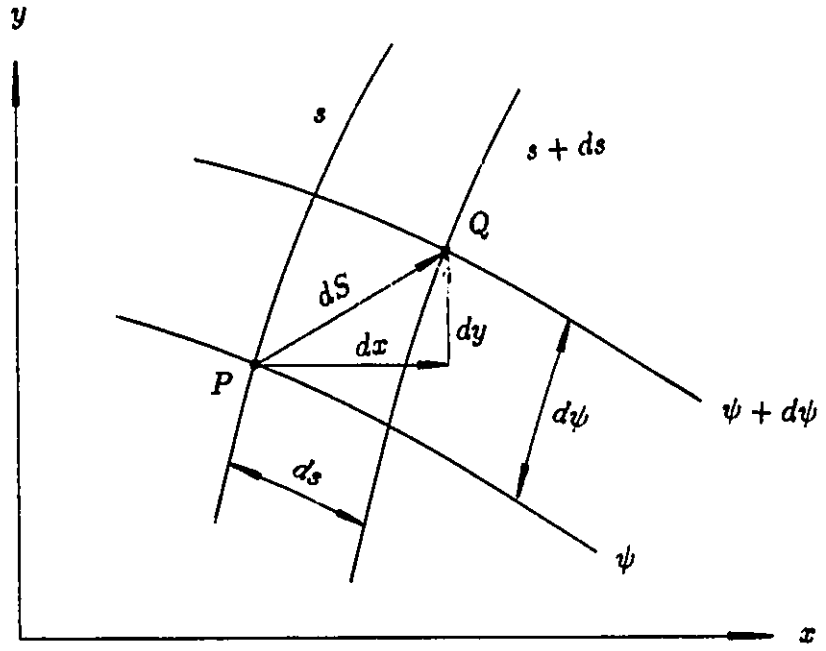

VITA AUCTORIS

Chang-Fa An was born in 1944 in Harbin, Heilongjiang, China. He received his B. Eng. in Aerospace Engineering from Harbin Institute of Technology in 1967. He had worked for 10 years as a mechanical engineer in 'Huaan' Manufacturing Company, Nianzishan, Heilongjiang, China, before he started the postgraduate study in the University of Science and Technology of China, Hefei, Anhui, China, where he obtained his M. Sc. in Fluid Mechanics in 1981. Then, he had served as an instructor in the same university for 5 years before he came to Canada in 1986. He is currently a Ph. D. candidate in the Department of Mathematics and Statistics, University of Windsor, and hopes to graduate in Fall, 1992.